IDENTIFICATION OF LOW ORDER VEHICLE HANDLING MODELS FROM
MULTIBODY VEHICLE DYNAMICS MODELS

A THESIS SUBMITTED TO
THE GRADUATE SCHOOL OF NATURAL AND APPLIED SCIENCES
OF
MIDDLE EAST TECHNICAL UNIVERSITY

BY

FERHAT SAĞLAM

IN PARTIAL FULFILLMENT OF THE REQUIREMENTS
FOR
THE DEGREE OF MASTER OF SCIENCE
IN
MECHANICAL ENGINEERING

JANUARY 2010

Approval of the thesis:

IDENTIFICATION OF LOW ORDER VEHICLE HANDLING MODELS FROM MULTIBODY VEHICLE DYNAMICS MODELS

submitted by **FERHAT SAĞLAM** in partial fulfillment of the requirements for the degree of **Master of Science in Mechanical Engineering Department, Middle East Technical University** by,

Prof. Dr. Canan Özgen
Dean, Graduate School of **Natural and Applied Sciences** ———————————

Prof. Dr. Süha Oral
Head of Department, **Mechanical Engineering** ———————————

Prof. Dr. Y. Samim Ünlüsoy
Supervisor, **Mechanical Engineering Dept., METU** ———————————

Examining Committee Members:

Prof. Dr. Mehmet Çalışkan
Mechanical Engineering Dept., METU ———————————

Prof. Dr. Y. Samim Ünlüsoy
Mechanical Engineering Dept., METU ———————————

Prof. Dr. Tuna Balkan
Mechanical Engineering Dept., METU ———————————

Asst. Prof. Dr. Gökhan Özgen
Mechanical Engineering Dept., METU ———————————

Dr. S. Çağlar Başlamışlı
Mechanical Engineering Dept., Hacettepe University ———————————

Date: 25.01.2010

I hereby declare that all information in this document has been obtained and presented in accordance with academic rules and ethical conduct. I also declare that, as required by these rules and conduct, I have fully cited and referenced all material and results that are not original to this work.

Name, Last name: Ferhat Sağlam

Signature:

ABSTRACT

IDENTIFICATION OF LOW ORDER VEHICLE HANDLING MODELS FROM MULTIBODY VEHICLE DYNAMICS MODELS

Sağlam, Ferhat

M.S., Department of Mechanical Engineering

Supervisor: Prof. Dr. Y. Samim Ünlüsoy

January 2010, 200 pages

Vehicle handling models are commonly used in the design and analysis of vehicle dynamics. Especially, with the advances in vehicle control systems need for accurate and simple vehicle handling models have increased. These models have parameters, some of which are known or easily obtainable, yet some of which are unknown or difficult to obtain. These parameters are obtained by system identification, which is the study of building model from experimental data.

In this thesis, identification of vehicle handling models is based on data obtained from the simulation of complex vehicle dynamics model from ADAMS representing the real vehicle and a general methodology has been developed. Identified vehicle handling models are the linear bicycle model and vehicle roll models with different tire models. Changes of sensitivity of the model outputs to model parameters with steering input frequency have been examined by sensitivity analysis to design the test input. To show that unknown parameters of the model can be identified uniquely, structural identifiability analysis has been performed. Minimizing the difference between the data obtained from the simulation of ADAMS vehicle model and the data obtained from the simulation of simple handling models by mathematical optimization methods, unknown parameters have

been estimated and handling models have been identified. Estimation task has been performed using MATLAB Simulink Parameter Estimation Toolbox. By model validation it has been shown that identified handling models represent the vehicle system successfully.

Keywords: Model Identification and Simplification, Parameter Estimation, Identifiability Analysis, Sensitivity Analysis, Handling Model

ÖZ

YOL ARAÇLARI BASİTLEŞTİRİLMİŞ DOĞRULTU KONTROLÜ MODELLERİNİN ÇOKLU GÖVDE DİNAMİĞİ ARAÇ MODELLERİNDEN TANILANMASI

Sağlam, Ferhat

Yüksek Lisans, Makine Mühendisliği Bölümü

Tez Yöneticisi: Prof. Dr. Y. Samim Ünlüsoy

Ocak 2010, 200 sayfa

Araç doğrultu kontrolü modelleri araçların tasarım ve dinamik analizinde kullanılmaktadır. Özellikle araç kontrol sistemlerindeki gelişmelerle birlikte doğru ve basit araç doğrultu kontrolü modellerine olan gereksinim artmıştır. Bu modellerin bazı parametreleri bilinmekte ya da kolayca elde edilebilmektedir. Ancak bazı parametrelerin elde edilmesi ya zor ya da pahalıdır. Bu parametreler, deneysel verilerden model oluşturma olarak tanımlanan sistem tanılama yoluyla elde edilebilir.

Bu tezde basitleştirilmiş araç doğrultu kontrolü modellerinin, bir çoklu gövde dinamiği programı olan ADAMS kullanılarak, karmaşık araç modellerinin simulasyonundan elde edilen simulasyon verileriyle tanılanması için genel bir metodoloji geliştirilmiştir. Değişik lastik modelleriyle oluşturulan bisiklet modeli ve yalpa modeli tanılanan araç doğrultu kontrolü modelleridir. Model çıktılarının model parametrelerine olan duyarlılıklarının tekerlek dönüş açısı frekanslarıyla değişimi incelenmiş ve test girdisi tasarlanmıştır. Bilinmeyen parametrelerin tek olarak tanılanabileceğini göstermek için yapısal tanılanabilirlik çalışması

gerçekleştirilmiştir. ADAMS araç modelinin ve basit araç modellerinin simulasyonundan elde edilen veriler arasındaki farkın, matematiksel optimizasyon yöntemleri kullanılarak en aza indirgemesiyle bilinmeyen model parametreleri kestirilmiş ve araç modelleri tanılanmıştır. Parametre kestirimi işleminde MATLAB Simulink Parametre Kestirimi Araçkutusu kullanılmıştır. Model doğrulaması yoluyla tanılanan modellerin gerçek araç dinamiğini başarılı bir şekilde izlediği gözlenmiştir.

Anahtar Kelimeler: Model Tanılama ve Basitleştirme, Parametre Kestirimi, Tanılanabilme Analizi, Duyarlılık Analizi, Doğrultu Kontrolü Modeli

Dedicated to my family

ACKNOWLEDGEMENTS

TABLE OF CONTENTS

LIST OF FIGURES

FIGURES

xiv

xix

LIST OF TABLES

TABLES

LIST OF SYMBOLS

$[H]$	Hessian matrix
$[M]$	Information matrix
$[p]$	Direction matrix
A	Amplitude
a	Distance between center of gravity and front axle
b	Distance between center of gravity and rear axle
B	Stiffness factor
BCD	Slope at the origin in Magic Formula
C	Shape factor in Magic Formula
C_α	Cornering stiffness
C_f	Front cornering stiffness
$C_{f\varphi}$	Front roll damping
C_r	Rear cornering stiffness
$C_{r\varphi}$	Rear roll damping
D	Peak factor in Magic Formula
e	Error
E	Curvature factor in Magic Formula
f	Frequency
f_0	Initial frequency
f_f	Final frequency
F_{xfl}	Front left tire longitudinal force
F_{xfr}	Front right tire longitudinal force
F_{xrl}	Rear left tire longitudinal force
F_{xrr}	Rear right tire longitudinal force
$F_{y,lag}$	Lagged tire cornering force
F_{yf}	Front axle cornering force

F_{yfl}	Front left tire cornering force
F_{yfr}	Front right tire cornering force
F_{yr}	Rear axle cornering force
F_{yrl}	Rear left tire cornering force
F_{yrr}	Rear right tire cornering force
g	Gradient of cost function
h	Center of gravity height
h_f	Front roll center height
h_r	Rear roll center height
h_s	Distance between roll center and center of gravity
I_{xx}	Vehicle roll moment of inertia about longitudinal axis
I_{zz}	Vehicle yaw moment of inertia(for roll model)
J	Cost function
J	Yaw moment of inertia(for bicycle model)
K	Lateral tire stiffness
$K_{f\varphi}$	Front roll stiffness
$K_{r\varphi}$	Rear roll stiffness
ℓ	Lagrangian
L	Wheelbase
m	Number of input
M	Total vehicle mass
M^*	Model structure
M_s	Vehicle sprung mass
M_{uf}	Front unsprung mass
M_{ur}	Rear unsprung mass
N	Number of data points
r	Yaw velocity
S_h	Vertical shift in Magic Formula
S_v	Horizontal shift in Magic Formula
T	Experiment time
t_f	Front track width

t_r	Rear track width
u	Input
U	Longitudinal velocity
v	Lateral velocity
w	Weighting factor
y	Model output
z	System output
z^N	Collected data
α_f	Front axle slip angle
α_{fl}	Front left tire slip angle
α_{fr}	Front right tire slip angle
α_r	Rear axle slip angle
α_{rl}	Rear left tire slip angle
α_{rr}	Rear right tire slip angle
δ	Steering angle
δ_w	Steering angle due to steering wheel angle
δ_f	Front steering angle
δ_r	Rear steering angle
$\delta_{\varphi f}$	Front roll steer coefficient
$\delta_{\varphi r}$	Rear roll steer coefficient
η	Step size
θ	Parameter
$\hat{\theta}$	Estimate of parameter
φ	Roll angle

LIST OF ABBREVIATIONS

ABS	Antilock Braking System
ADAMS	Automatic Dynamic Analysis of Mechanical Systems
AYC	Active Yaw Controller
DOF	Degree of Freedom
EBD	Electronic Brake Distribution
GA	Genetic Algorithm
GUI	Graphical user interface
MBD	Multibody Dynamics
s.g.i	Structurally Globally Identifiable
s.l.i	Structurally Locally Identifiable
s.u.i	Structurally Unidentifiable
SAE	Society of Automotive Engineers
SVC	Static Vehicle Characteristic
TCS	Traction Control System

CHAPTER 1

INTRODUCTION

The goal of this study is to identify low order vehicle handling models from complex Multibody Dynamics (MBD) vehicle models. MBD vehicle models in the MBD software ADAMS environment are simulated; input and output data are recorded, and a previously determined handling model structures are identified from this data. Differences between the simulation outputs of the ADAMS model and the handling model are found and minimized by optimization. As a result of this optimization, unknown parameters of the model are estimated. Some of the parameters of handling models are easily obtainable or measurable, yet some of them are difficult to obtain and so they are better estimated by means of system identification. In particular, parameters of tire model and inertial parameters of the vehicle handling models are not easily obtained or accessible so they are estimated with system identification. Identification of an entire vehicle model is of prime importance for vehicle dynamics studies. Vehicle handling models are made use of in a variety of applications including the design of control systems; on the whole in the analysis and design of vehicles, vehicle components, and subsystems. Hence, firstly an introduction to vehicle system identification will be presented and then use of vehicle handling models in vehicle dynamics studies will be clarified.

1.1. VEHICLE HANDLING MODEL IDENTIFICATION

System identification can be defined as the building models of systems from experiment. When the model used in the identification process is built, values of the parameters in model are determined from the observed data by mathematical

methods and this can be defined as parameter estimation. To be able to identify the model, data is required. This data must be informative enough to identify model accurately. Thus prior to an experiment, an optimal input for use in the test must be designed, considering previous knowledge about the system to be identified and the aim of the identification. However, in some cases the designed input may not be practical and so there is a tradeoff between optimality and practicality. After determining the model structure, parameters of this model can be estimated. Parameters are estimated by matching the data acquired from the experiment and the data taken from the model. In general, parameters are estimated by minimization of the difference between the simulation data and the test data. After the estimation of the parameters, identified model is validated by examining whether the identified model satisfies the requirements or not (model validation). Model validation is performed by using a new data set or by using the portion of current data not used in the system identification. If the identified model does not satisfy the requirements, some part or parts of the identification is revised. Thus, selected model may be changed or even experiments may be repeated to obtain new data.

Vehicle handling models are used to study vehicle handling dynamics which is complex due to the large number of parts, joints, and particularly nonlinear behavior of vehicle components. The handling model should be accurate enough to represent the handling behavior of the real vehicle in a reasonably wide range of maneuvers. Simplified low order vehicle models have certain parameters which do not directly correspond to components in the real vehicle. Even if the correspondence can be established, some of them may not be measured directly and practically, so they are better estimated through system identification. Sometimes parameters of the model and parameters of the vehicle may differ due to these simplifications even if they are physical. When the nonlinear characteristic of the parts or systems of vehicles exist, modeling becomes more intricate. By linearizing nonlinear behavior about some operating point, handling models may be simplified; yet this allows the usage of the model only within limited domains. A typical example is the cornering force characteristics of pneumatic tires which are highly nonlinear, and thus they are

difficult to model if the whole range of possible slip angles and lateral accelerations are to be considered. A characteristic can be linearized about some operating point but this limits the operating range of the tire and of the vehicle. Therefore, model parameters which cannot be measured or obtained easily and accurately are better estimated.

Vehicle handling comprises lateral (y), longitudinal (x), yaw (ψ), and roll (φ) primary motions as shown in the Figure 1.1.
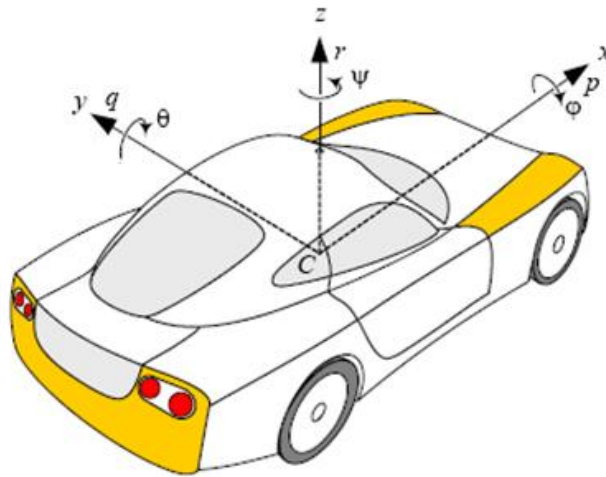
Figure 1.1: Motion associated with vehicle handling [1]

To be able to identify handling models, vehicles are tested and the data are acquired using some test hardware. Lateral, longitudinal, yaw, and, roll velocities and lateral acceleration are the commonly used test outputs and the steering wheel angle is the test input used in the identification. Longitudinal and lateral velocities are measured by velocity sensors and rotational velocities and accelerations are measured by inertial measurement units. Steering wheel input can be measured by steering wheel measurement system and by means of steering robots desired steering inputs can be applied. Also, there is need for other equipment such as data acquisition system, and

wheel speed measurement system. In this study, motion data is directly acquired from the ADAMS; yet to become the realistic, responses which are obtainable in real conditions are used. Using previously determined handling model structure, its parameters are estimated by using input-output data sets. The simplest vehicle handling model is the bicycle model which represents the in-plane dynamics of a vehicle. Generally, longitudinal velocity of the bicycle model is kept constant and treated as a model parameter, and two degree of freedom (DOF) bicycle model is obtained. Bicycle model does not include the roll motion, yet in some cases, particularly at high lateral accelerations, roll motion affects vehicle dynamics significantly and thus it should be included in the model. Another commonly used handling model is the vehicle roll model comprising the coupled in-plane and out-of-plane (roll) dynamics. Tire is an important part of the vehicle and it affects the performance of the vehicle considerably, thus it must be modeled accurately. The most simple tire model used in the vehicle handling dynamics is the linear tire model which is accurate in a limited operating region. Nonlinear tire models are used to be able to represent the nonlinear characteristic of the tire, thus increasing vehicle's operating range. Physical tire models are not used in vehicle models, since they are mathematically complicated and increase solution times considerably. Instead empirical tire models are used widely by fitting curves to test data. By combinations of the available tire and handling models, several different combinations can be obtained. Note that the model used in the identification must be simple for computational reasons and accurate enough to represent vehicle dynamics. Tire parameters and some inertial parameters like yaw moment of inertia are difficult to obtain, so they are better estimated. Other parameters like mass of the vehicle, position of center of gravity can be measured accurately, so they are assumed to be known in parameter estimation. In the estimation of parameters mathematical methods such as least square parameter estimation method and maximum likelihood parameter estimation method are commonly used. Optimization algorithms like nonlinear least square and genetic algorithm optimization are used within these methods. Each algorithm has its own advantages and disadvantages and is appropriate for a specific problem. Among these methods

genetic algorithm has become popular recently, since it is a global optimization method and it does not require differentiation. Details of these methods will be given in chapter 3. After the parameters are estimated, model validation is performed by another data set. To make the identification task easy, model may be simplified but in this case accuracy may be lost. When the complexity of the model is increased, accuracy increases but the computational cost also increases. In summary, vehicle system identification is a complex and difficult problem; in particular identification of the tire model is a very difficult problem due to nonlinear behavior of the tire.

In this study data used in the identification process is obtained from ADAMS/Chassis simulation and accordingly various simulations with different inputs can be performed, which is restricted in real tests. Steering input and the longitudinal velocity are the inputs used in the simulations. These inputs are determined according to the analysis and procedures explained in the following chapters. In ADAMS/Chassis steering input can be defined by using various mathematical functions which increases the flexibility of the simulations and by this way various virtual test scenarios can be observed. To design steering input and to determine the longitudinal velocity used in the simulation some a priori knowledge about the vehicle system and the handling model structure to be identified is necessary. The methods for generating optimal input design will be explained in detail in chapter 3. After getting the data from ADAMS, parameters of the handling models are estimated using mathematical tools by minimizing the difference between model output and ADAMS output. After the handling model is identified, it is validated by using another data set. Handling model identification algorithm is summarized in Figure 1.2.
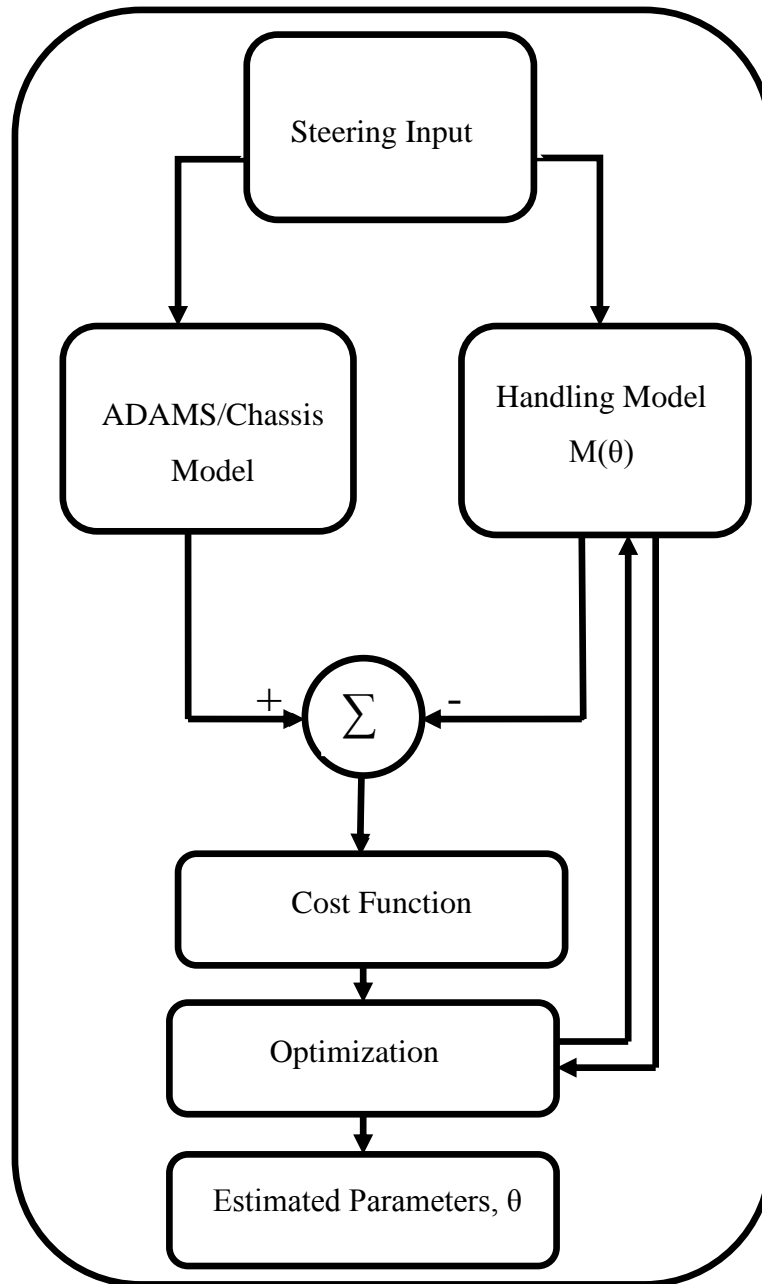
Figure 1.2: Handling model identification diagram

In this study, MATLAB Simulink Parameter Estimation Toolbox is used for parameter estimation. By this toolbox parameters of any model constructed in Simulink environment can be identified and there is no necessity about the specific

model structure. Cost function to be minimized is formed directly by Simulink. Acquired data from ADAMS is loaded in the MATLAB workspace and is called by the blocks in the Simulink. Cost function is formed as the difference between the acquired data and the simulation data by Simulink. This cost function is then minimized by some conventional and advanced optimization algorithms which are available in MATLAB. All these steps are performed in MATLAB's graphical user interface (GUI) which increases the practicality and usability of the toolbox. In summary signal processing, model construction, parameter estimation, and model validation steps are performed in this toolbox.

1.2. USAGE OF VEHICLE HANDLING MODELS

Model of a system can be defined by the relationship among the inputs and the observed response signals of the system. Mathematical models are the most commonly used model type in advanced applications of engineering and science. They describe the relationships among the system variables by means of mathematical tools, and they are used in simulation and prediction. Mathematical models may be developed via two ways. One way is first to part the system into subsystem and applying physical laws and well established relationship to these subsystems, and then combining these subsystems mathematically. The other way is building mathematical models based on the observations and experimentation which is also called system identification [2].

Vehicle models are built by the combination of the two methods explained. By using physical laws such as Newton's second law, and well established relationship such as tire force and slip angle relationships vehicle models can be built. However, all of the parameter values of the constructed model may not be accessible and accordingly they are estimated via system identification.

Mathematical vehicle handling models are used in the analysis of the vehicle handling dynamics and the design of vehicle systems and vehicle system components. They reinstate dangerous and expensive tests and experiment by easy,

flexible, and inexpensive simulations Usage of these models in the vehicle dynamics studies can be explained below shortly.

1.2.1. ANALYSIS OF VEHICLE HANDLING DYNAMICS

Analysis of the vehicle handling dynamics can be fulfilled via tests. There are some standard vehicle handling tests such as lane change test, step steer test and these tests necessitate certain specifications. These specifications can be satisfied to some extent considering the safety of the test pilot, safety of the car which is tested or the test pilot cannot perform exactly the desired operations. To illustrate, while performing step steer test, vehicle longitudinal velocity must be limited at some value for safety. Nonetheless, when the vehicle models are simulated, these tests specifications can be satisfied perfectly and extreme conditions which cannot be reached during tests can be observed. For instance in ADAMS/Chassis there are several vehicle handling tests which have certain objective to observe handling dynamics. By using these models effects of the modification in the subsystem, component, or change in the model parameters can be observed. As opposed to models, performing real tests for observing those changes and modifications on the handling are costly and sometimes unattainable.

1.2.2. DESIGN OF VEHICLE COMPONENTS AND VEHICLE SUBSYSTEMS

The other common use of the vehicle handling models is in the design and development of vehicle subsystems, vehicle components, and integration of these subsystems and components to vehicle. In particular with the developments in the electronic systems vehicle designers began to design electronic control systems to improve safety, stability and performance of the vehicles. Antilock braking system (ABS), electronic brake distribution system (EBD), traction control system (TCS), and active yaw control system (AYC) are some examples for vehicle safety systems. Vehicle handling models are used in development and design phase of these control systems. Therefore, estimation of the unknown model parameters is of primary importance for these applications.

An extensive discussion on the use of vehicle handling models in vehicle dynamics can be found in the study of Arıkan [3].

The linear bicycle model is a well known vehicle handling model and it is commonly used in the analysis of the vehicle handling dynamics. It is a simple model but it represents the planar dynamics of the vehicle successfully by providing two important variables yaw velocity and lateral velocity. Linear bicycle model is valid for low slip angle and low lateral accelerations. Validity of the bicycle model can be extended by using nonlinear tire models and the so called nonlinear bicycle model is obtained. Despite the improved accuracy of the nonlinear bicycle model with respect to the linear bicycle model, increased number of parameters of the nonlinear bicycle model is a disadvantage with respect to the linear one.

Another model commonly used in vehicle dynamics research is the vehicle roll model. Bicycle model does not consider the roll motion, yet at high lateral accelerations roll motion affects the planar motion by altering the generated tire forces and also by directly affecting the planar dynamics due to coupled roll and planar dynamics. There are various studies [4, 5] using vehicle roll model in the design and integration of vehicle control system.

In summary, vehicle handling models are crucial for analysis and design of a vehicle, vehicle subsystems, and vehicle components and thus they must be thoroughly understood.

1.3. ADAMS/CHASSIS

ADAMS is the one of the world's most widely used MBD mechanical simulation software. With ADAMS various models of systems can be built, simulated, improved, and their dynamic behavior can be examined in detail.

ADAMS/Chassis is one of the modules of ADAMS and it provides an analysis environment for automotive applications by means of standard model types and two analysis types which are full vehicle analysis and half vehicle analysis and post-processing. ADAMS Chassis has four work modes which are build mode, test mode, review mode, and improve mode. In build mode models can be edited and system configuration can be changed. Subsystem and model types can be changed, optional subsystems can be added or removed and the various parameters of the vehicle model can be changed in build mode. In test mode vehicle models can be built and simulated [6].

In test mode there are various standard vehicle tests such as [7];

- braking analysis,
- handling analysis,
- durability analysis,
- ride analysis.

In handling analysis there are also various standard simulations some of which are [7];

- constant radius,
- cross wind,
- fish hook,
- step steer
- swept sine
- lane change.

In addition to these standard vehicle tests, various vehicle tests can be built, and appropriate control algorithms can be designed. In these simulations steering input parameters which are steering frequency and steering amplitude and test variables which are velocity and accelerations can be set easily in GUI. After the model is

analyzed in test mode, analysis results can be visualized in review mode by using ADAMS/Postprocessor. Analysis plots and animation can be seen by means of ADAMS/Postprocessor. Models can be refined with the help of ADAMS/Insight in the improve mode using some advanced optimization tools [6].

In this study, data is taken from the ADAMS/Chassis simulation and this data is treated as a real test data. Full vehicle models of ADAMS/Chassis have nearly hundred of degrees of freedom and they comprise the front and rear suspension subsystems, steering subsystem, body subsystem, and tire subsystems. They have also optional subsystems like loading, brake, and power train subsystems. In ADAMS/Chassis there are various tire models with different complexity from Fiala tire model to Magic Formula tire model. Among these tire models PAC 2002 [8] tire model is one of the most complex tire model. This tire model is the extended version of the Magic Formula tire model. Therefore, ADAMS/Chassis vehicle models are the most representative model of the real vehicle and they can be used to acquire simulation data instead of making tests with the actual vehicle to acquire data. An example ADAMS/Chassis vehicle model is shown in Figure 1.3.
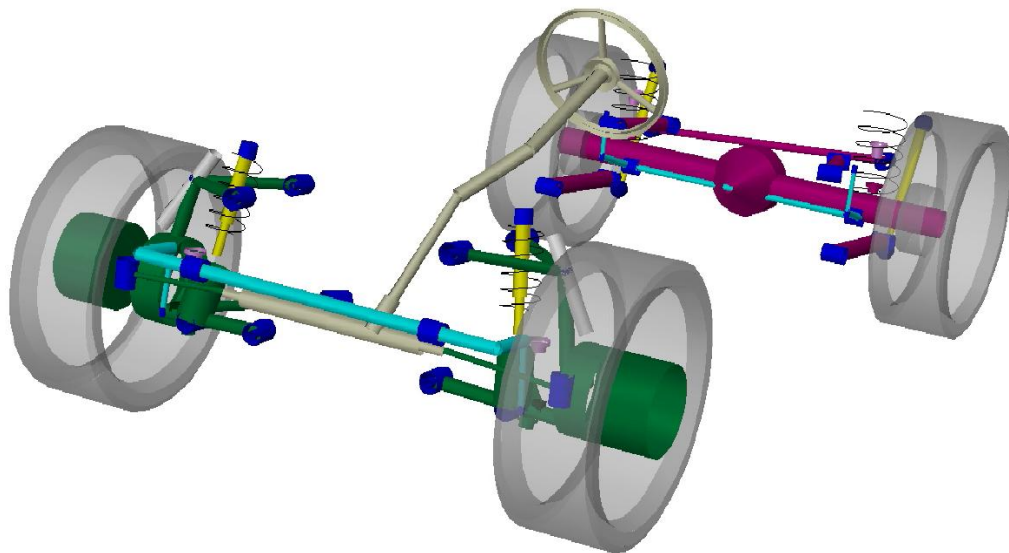
Figure 1.3: ADAMS/Chassis vehicle model [7]

1.4. OUTLINE

In chapter 2, literature survey about vehicle handling system identification is given. Types of handling models to be identified, their level of complexity, identification algorithms, data set, and model validation are steps to be examined in literature survey.

In chapter 3, system identification and its steps are explained in detail. Firstly, the design of the test input is explained and then the identification algorithms are given. Linear and nonlinear optimization methods, their algorithms, advantages and disadvantages are all explained in some detail.

In chapter 4, vehicle handling models and tire models are developed. Vehicle models include 2 DOF bicycle model, 3 DOF linear roll model, 1 DOF roll model, and finally 3 DOF nonlinear roll model. Linear tire model and Magic Formula tire models are used with the vehicle model for identification purposes. 3 DOF nonlinear roll model is used with the Magic Formula tire model.

In chapter 5, to examine how the model responses change with the unknown parameters, a detailed sensitivity analysis is performed in the frequency domain and the most appropriate frequency range of the steering input and the appropriate longitudinal velocity are found.

In chapter 6, a detailed structural identifiability study is fulfilled. Data is obtained from the simulation of the model to be identified, and the model is identified starting with the nominal model parameters. According to the results local identifiability of the model is examined. Finally, the handling models are identified and using another data set from ADAMS/Chassis, identified models are validated.

In chapter 7, discussion, conclusion, and future work are given.

CHAPTER 2

LITERATURE SURVEY

2.1. INTRODUCTION

Studies about identifications of vehicle handling models are vital in vehicle dynamics area owing to their extensive use in analysis and design of vehicle, and vehicle subsystem. Especially, with the developments in the electronic systems vehicle designers began to design electronic control systems to improve safety, stability, and performance of the vehicles and so necessity to vehicle handling models increased. Thus a large number of studies are reported in journal and conference articles and graduate thesis in literature about this topic. These studies were carried out due to a gap in handling model identification and thus those studies furnish valuable information with regard to the stages of the handling model identification starting from the data collection and ending with the model validation.

In this chapter, general steps and procedure for handling model identification performed in vehicle dynamics area will be explained. Design of optimal test or simulation input, input-output data, vehicle handling model type, estimated parameters, and parameter estimation algorithms will be explained. To start system identification a priori knowledge is required to select a model structure. After the selection of the model structure data is required and then system identification starts with experiment to observe the variation of system variables. Since the model is identified from the data acquired from the experiment, quality of the data is very important and the input and output data must be selected carefully. In handling model identification, steering input is used as the test input and thus it must be

designed before the test. Estimation of the parameters of the selected model is then performed and with the model validation using different data sets or a different part of the data used in the identification, handling model identification ends. All these part are inspected in these papers in a detailed manner.

In vehicle dynamics area there are several handling and tire models used. The simplest handling model is the bicycle model and the most simple tire model is the linear tire model. However, these models have limited use and to remove these limitations, vehicle roll models and nonlinear tire models are also used. As the complexity of the model increases, its accuracy also increases; yet computational effort to identify those models also increases. Therefore, there is a trade-off between model complexity and computational loads. The selected models should be the simple for the computational reasons and also should be complex enough to capture the real-life behavior of the vehicle.

2.2. LITERATURE SURVEY

Vehicle system identification comprises the parts which are data acquisition, model selection, parameter estimation, and model validation. In literature there are various specific methods and solutions to handling model identifications. Arikan [3] has studied the identification of bicycle model and three DOF handling model. Before making the vehicle test, a detailed structural identifiability analysis for different sensor and sensor set has been performed for the bicycle model and global identifiability of the model with certain parameter set has been determined. Then data have been acquired from the vehicle tests and unknown parameters of the bicycle model which are position of center of gravity, front and rear cornering stiffness, yaw moment of inertia, and sensor locations have been estimated with different sensor sets using genetic algorithm. Identified models have been validated by the data used in identification and also by another data set. Steering input with a wide frequency range has been used in the vehicle tests. After the identification of the bicycle model, three DOF vehicle roll model has been identified. Estimated parameters of the roll model have consisted of tire parameters, inertia parameters,

and distance parameters. Local structural identifiability of the model has been studied and the unknown parameters have been estimated from the simulated data. The main contribution of this study is that a detailed global identifiability of the bicycle model has been performed and parameter sets which can be identified uniquely from different sensor sets have been determined.

Bolhasani et al. [9] has estimated the parameters of vehicle handling model using the genetic algorithm. Data used to estimate handling model parameters have been acquired from the simulation of a complex vehicle model in ADAMS. For simulation in ADAMS environment, a combined sinusoidal and step steering angle has been used as an input to attain both the transient and steady state responses of the vehicle. Simulation has been performed at the longitudinal velocity of 50 kph with a low frequency steering input. Three vehicle responses namely the lateral velocity, yaw velocity and roll angle together with the steering angle have been used in the identification. In this paper a three DOF vehicle handling model comprising lateral, yaw, and roll degrees of freedom, with Fiala tire model which calculates the cornering force as a function of slip angle and vertical load on the tires, has been used. Front and rear cornering stiffness of Fiala tire model, yaw moment of inertia, roll moment of inertia, roll damping, and roll stiffness are the unknown parameters. Identified model has been validated by using other two data sets. Validation data has been obtained from the slalom test and single lane change maneuver in ADAMS. In slalom test, the frequency of the steering angle is taken to be 0.1 Hz. The longitudinal velocity is assumed to be 50 kph and the longitudinal velocity in single lane change maneuver is set at 60 kph. In this study the steering input has a very low frequency which does not excite the vehicle motions appropriately. Also, friction coefficients between the tire and the road have been assumed to be known even though they may not be known easily. However, tire and vehicle model used in the identification represent the vehicle handling dynamics completely for a wide operating range.

Allaum et al. [10] have identified the parameters of the nonlinear vehicle handling model by using least square methods. They have used three DOF handling model comprising the longitudinal, lateral, and the yaw motions. Data used in the identification have been taken from the vehicle test in which firstly vehicle is accelerated to 5.5 m/s longitudinal velocity and then a constant wheel steering input of 6.4^o has been applied. Inputs of the test are the traction force and the wheel steering angle, and the outputs of the test are the forward speed and the yaw velocity. The identification process is started by sensitivity analysis based on first order standard sensitivity functions in time domain which allows the determination of the effects of the parameters on system variables. After sensitivity analysis, they have performed the identifiability study to show that estimated parameters are structurally globally identifiable. Errors between the observed data and the estimated data of the longitudinal velocity and the yaw velocity have been used to construct a quadratic objective function. Estimated parameters are mass and yaw moment of inertia of the vehicle, distance between the center of mass and the front and rear track, center of gravity height, front and rear cornering stiffness, and aerodynamics and rolling resistance ratio. Some assumptions which relate the vehicle parameters to each other have been made and then identifiability study has been performed. In this paper roll motions of the vehicle has not been included in the model and also linear tire model has been used and thus the used handling model has limited to low steering angle inputs. Also some parameters such as mass and the distances between center of mass and the track width have been treated as the unknown parameters to be estimated, even though they can be measured easily. However, since the model used in the identification comprises longitudinal dynamics, vehicle tests may be performed with a greater flexibility that is there is no need to keep the longitudinal velocity at a constant value

Abdellatif et al. [11] have studied the nonlinear identification of vehicle's coupled lateral and roll dynamics in their study. Vehicle handling model coupling the lateral and roll dynamics and a linear non-stationary tire model have been used in the vehicle identification and thus conventional simplifications such as stationary tire

model and pure lateral dynamics model have been removed. Coupling the lateral and roll dynamics has been performed by adding the effects of the roll motion on the tire slip angles. However, by this way effects of the roll motion to the vertical load on the tires, and thus effect of roll motion to lateral dynamics have been disregarded to simplify the coupling. After building the model, identifiability study of the roll dynamics submodel and whole coupled model have been examined in this study. After these steps, the authors have studied the effects of the parameter and parameter changes on the response of the system by performing sensitivity analysis in the frequency domain. Accordingly, the optimal frequency range of the steering input, in which the parameter estimation has been performed, has been found as 0-2 Hz. After the sensitivity study, vehicle tests have been performed at different longitudinal vehicle speeds. A frequency sweep steering input covering frequencies up to 2.2 Hz has been used as the test input. Steering wheel angle, lateral acceleration, yaw velocity, and the roll angle have been used in the parameter estimation. Loss function have been formulated by taking the difference between the measured and the estimated data and using the nonlinear least square algorithm parameters have been estimated. In this study authors have indicated that as the interaction between vehicle's lateral and roll dynamics have been neglected, estimated parameters change with different operating points. To illustrate the authors have showed that estimated yaw moment of inertias are different for different vehicle longitudinal speeds for the non-coupled model. Conversely, those values are nearly the same for different longitudinal values for the coupled models. This observation is important for handling model identification. Moreover considering the transient effects in tire model is another contribution of the study which removes the steady state steering angle limitations.

Massel et al. [12] have studied the identification of the cornering stiffness parameters. A linear static model derived from the one track model and vehicle side slip angle model together with the linear tire model has been used for identification. Online estimation of the cornering stiffness parameters have been performed by minimizing the quadratic error functions derived by taking the difference of the

measured data and model output data by linear least square approach. The method presented in this paper has been tested with the data taken from the one track model and from the simulation of the virtual vehicle model in CARSIM, a MBD software. Slalom drive simulations with a steering frequency of 0.2 Hz for one track model, 0.5 Hz and 0.7 Hz for the CARSIM model at the longitudinal velocity of 60 kph for the one track model and 80 kph for the CARSIM model have been performed. Steering angle, yaw velocity, and lateral acceleration have been used in the identification as input-output data. The results have showed that the models which describe the lateral vehicle dynamics can be adapted by the identified cornering stiffness according to different driving conditions and the adapted model have given better response than the unadapted model. As shown in this paper, using an adaptive identification improves the estimation results.

Peng et al. [13] have studied the cornering stiffness estimation based on the vehicle lateral dynamics. Bicycle model together with linear tire model has been used in the estimation process to estimate the front and rear cornering stiffness. Estimation process has been divided into two groups; the time domain methods which have four methods and, the frequency domain (i.e. transfer function) method. In the former the bicycle model equations have been used either directly or in a various combinational forms and the later has used the transfer function between yaw velocity and steering angle to estimate cornering stiffness values. In both methods vehicle parameters mass, distance between center of gravity and front and rear axles, and yaw moment inertia have been assumed to be known even though the yaw moment inertia may not be determined so easily. In the first method vehicle measurements, namely steering wheel angle, yaw, lateral, and longitudinal velocity together with the time derivative of lateral velocity and yaw velocity are required. In the second method the transfer function between the yaw velocity and the steering input is derived. Then a least square fit is applied to obtain the transfer function parameters. After the transfer function is obtained, cornering stiffness values can be calculated from the transfer function. The performance of the methods used in this study has been tested by using the data acquired from the

bicycle model with nonlinear tires and CARSIM software, and it has been shown that two methods have better performance and thus they have been used to identify cornering stiffness values from real test data. The results have no indication with regard to indicate which of the two methods is more accurate. To sum up, in this study five methods have been used to get cornering stiffness values and the two methods have been found to shown better performance than the rest. This study has proposed methods to obtain cornering stiffness values by easy and straightforward numerical methods.

Wesemeier et al. [14] have studied the identification of vehicle parameters using stationary driving maneuvers. Using the static gain of the one track model, special combinations of the parameters have been identified. These parameter combinations include the front and rear cornering stiffness values, vehicle mass, and the distance between the center of gravity and the front and rear tracks. Firstly three static gains which are the lateral acceleration gain, yaw velocity gain, and the side slip gain have been found by using one track model and then parameters of the static gains have been estimated by using least square method from the test measurements. Certain physical parameter combinations which can be determined from these estimated static gain parameters have been determined. In this study lateral acceleration, yaw velocity, side slip velocity, longitudinal velocity, and the steering angle data have been used for identification. These data have been taken from the constant radius vehicle test which has been performed at different longitudinal vehicle speeds to be able to obtain a wider range of operating points. Then two parameter combinations have been used in the identification. One of them comprises two cornering stiffness values and the position of the center of gravity, and the other comprises only the two cornering stiffness values. One of the missing points of this study is that yaw moment of inertia cannot be estimated by the methods given in this study. However, yaw moment of inertia cannot be determined or measured easily and thus it is better estimated by parameter estimation. One of the main contributions of this study is that it does not require an excitation with

certain frequency range which is difficult in real life. However, this has the disadvantage that the input is not rich enough to identify a larger set of variables.

Abdellatif et al. [15] have studied the modeling and identification of nonlinear lateral dynamics. Conventional simplifications have been removed by coupling lateral and roll dynamics and by using nonstationary and nonlinear tire model. Lateral and roll dynamics have been coupled by adding the effects of the roll motion on the slip angles and simplified Magic Formula tire model has been used as the nonlinear tire model. After the model construction, unknown physical parameters have been estimated by using nonlinear least square formulation. Cost function has been formulated using the lateral acceleration, yaw velocity, and the roll angle measurements. This study has examined the influences of the roll motion on the lateral dynamics. These influences are important especially for vehicles with high center of gravity and for all vehicles with low speed. An important examination given in this study is that the influence of roll motion on the lateral dynamics can be neglected for velocities above nearly 60 kph for mid-size and compact vehicles. For vehicles with high center of gravity and for vehicles at low speeds ignoring roll motions leads to estimated parameters to be velocity dependent. As a result general validity and the practicability of the proposed model have been proved by making tests with several vehicles in this study.

Ryu [16] has studied the parameter estimation of the vehicle handling model in his study. Linear bicycle model and the one DOF vehicle roll models have been used in the estimation process. Vehicle states have been estimated from Global Positioning System/Inertial Navigation System method and these states have been used in the estimation. Firstly, bicycle model parameters have been estimated by using least square and total least square algorithms using the lateral velocity and yaw velocity responses together with the steering angle and then the roll model parameters have been estimated using least square algorithm using the roll rate, roll angle, and the lateral acceleration measurements. Different sets of parameters have been selected to be the unknown parameter sets of the bicycle model to be estimated. These are;

- front and rear cornering stiffness values,
- front and rear cornering stiffness values, and position of center of gravity,
- front and rear cornering stiffness, and yaw moment of inertia.

In this study it has been observed that the estimation of the parameter sets consisting position of center of gravity and yaw moment of inertia necessities a sufficiently rich excitation. When the excitation is not adequate, estimated parameters fail to converge to correct values, yet understeer gradient has been estimated correctly regardless of excitation. After the bicycle model parameters have been identified, parameters of the one DOF roll model which are the roll stiffness and roll damping have been estimated.

Bolzern et al. [17] have studied the estimation of nonlinear cornering forces from road tests. Two DOF bicycle model with the Magic Formula tire model has been used to estimate unknown parameters. To be able to use bicycle model some assumptions have been done. These are,

- longitudinal slip and camber angle have been neglected,
- roll dynamics has been neglected, and
- cornering force is only a function of the slip angle.

Unknown parameters to be estimated have been selected as the Magic Formula tire parameters like the peak value, curvature factor, and relaxation length; other parameters of the bicycle model have been treated as the known parameters. Extended Kalman filter has been used to estimate unknown parameters. Data used in the identification have been acquired from the road test performed at a longitudinal velocity of 100 kph and with 100 degree steering wheel angle which is severe enough to cover a wide range of operating points. Lateral acceleration, yaw velocity, side slip angle, and the steering wheel angle have been acquired during test. Using this data set, parameters of the tire model and the relaxation length have

been estimated. This study has used the nonlinear and transient tire model and thus wide operating points have been covered, yet it has not consider lateral load transfer which is required for proper use of Magic Formula tire model which limits the applicability of the handling model. Moreover, the yaw moment of inertia which is difficult to measure or calculate has been assumed to be known.

Yu [18] has studied the parameter identification of buses in his study. Two DOF linear bicycle model has been used in the identification. Step steer responses of the test bus at 15 mph and 20 mph have been acquired to identify unknown bus model parameters which are the front and rear cornering stiffness values, and the yaw moment of inertia. Lateral acceleration of the bus has been kept below 0.2g to ensure linearity of the bicycle model. In this study, when the responses of the model and the responses of the identified model are compared, it has been observed that responses from the model are ahead of the experimental data for some time. The author thinks that this discrepancy is most probably due to neglecting tire lag in the vehicle model.

Cabrera et al. [19] have developed a method to determine the Magic Formula tire model parameters by using genetic algorithms. The cost function has been formed as the sum of the squared difference between the tire test measurement data and the Magic Formula model data. Parameters of the Magic Formula tire model for the pure longitudinal and lateral slip conditions and for the combined slip conditions have been estimated from pure lateral and longitudinal forces and combined forces. In this study, initial value problem of the conventional optimization algorithms has been prevented by using evolutionary algorithms which has provided flexibility for parameter estimation.

Oosten and Bakker [20] have studied the determination of the Magic Formula parameters from the out of tire measurement data produced by the Delft tire measurement trailer. Tire forces acting between tire and road have been measured for different conditions. These measurements have been performed under pure

cornering with slip angle from -20 deg to 20 deg for different vertical load and camber angles, and under braking conditions from free rolling to total locking for different side slip angles. Then regression techniques have been applied to measurement data and the parameters of the Magic Formula tire model have been estimated. The authors have shown that for pure slip conditions estimation of the Magic Formula tire parameters is not difficult, yet for combined cornering and braking it becomes difficult.

Cadiou et al. [21] have proposed two methods for the identification of Magic Formula tire model parameters from vehicle tests. One of these methods is estimation based on simulation and the other is the estimation based on observation. Estimation based on simulation method uses the measured data to construct the cost function with the unknown Magic Formula basic tire parameters by simulation. By minimization of this cost function tire model parameters have been estimated. Trajectory of the vehicle is used as the data in the system identification. Estimation based on observer method uses an observer to reconstruct vehicle dynamics and hence tire side forces have been estimated. Vehicle parameters other than tire parameters have been assumed as the known. This study contributes to literature by identifying the Magic Formula tire model.

In this thesis study different types of handling models starting from the simple linear bicycle model and ending with three DOF nonlinear handling model using the Magic Formula tire model have been identified. To determine whether the handling model can be identified uniquely or not, a detailed structural identifiability analysis has been performed. To show the variation of sensitivity of the system outputs to unknown parameters with the steering frequency, a detailed sensitivity analysis has been performed and the input frequency has been specified accordingly. For the three DOF nonlinear handling model identification, sensitivity of the tire lateral force to Magic Formula tire model parameters with tire slip angle has been obtained and the practical identifiability of the Magic Formula tire model parameters has been examined. By this way the vehicle maneuver appropriate for nonlinear

23

handling model identification has been designed. Since data is taken from the simulation of the ADAMS model, different type of maneuvers can be easily acquired and maneuvers with different types of input parameters can be used and compared in the estimation process. Moreover, identified cornering force of the Magic Formula tire model has been compared with the real tire model of ADAMS model and validity of the model has been shown.

In the literature of vehicle handling model identification mostly bicycle models have been studied and focus of general consideration has been the identification of tire cornering forces. However, bicycle models have limited operating range due to assumptions made in their derivation. At higher lateral acceleration and at higher slip angles bicycle model cannot be used accurately. Lateral vehicle dynamics is coupled with the roll dynamics and at high acceleration lateral dynamics is affected by the roll motion considerably and therefore roll motion should also be modeled. As will be explained in chapter four in detail, pneumatic tire has highly nonlinear characteristic such that modeling of them is difficult. To be able to comprehend complete vehicle handling dynamics for wide operating ranges, use of nonlinear tire models is inevitable. Cornering force characteristic of the tire depends on the slip angle and vertical load on it mainly and thus vertical load on tire should also be included in the model. The identification of nonlinear tire models requires advanced test setups which are very costly. However, with road tests vehicle structural parameters and nonlinear tire parameters can be estimated to some extent using commercially available sensors and devices. In the literature there are only a limited number of studies about the identification of nonlinear roll model together with nonlinear tire model and the full potential of the approach has not yet been utilized.

In this thesis study different handling models starting from the simplest bicycle model and ending with nonlinear roll model with Magic Formula tire model have been identified. In particular identification of different nonlinear tire models with standard vehicle tests have been studied and Magic Formula tire model has been identified with reasonable success.

CHAPTER 3

SYSTEM IDENTIFICATION AND PARAMETER ESTIMATION

3.1. INTRODUCTION

The construction of model from experimental data that is system identification involves three basic elements which are data, model set, and determination of the best model. To be able to obtain data the designed experiment must be performed. By using a priori knowledge, by modeling using some physical laws or well known relationship, or by using standard model types, the model set used in the identification is determined. Then the best model is selected according to some criteria based on how the model reproduces the measured data. After these steps selected model is validated to show whether it satisfies the requirements or not that is whether it is good enough or not. A model cannot be defined as the final and true representation of the system rather it can be accepted as good enough for certain aspects one interested in. If the selected model does not satisfy validation tests some parts of the system identification process are revised. The model may not pass validation tests due to some reasons which can be summarized as: Numerical procedure may fail, criterion may not be well determined, the model set may not be appropriate to represent the system, or the data may not be informative enough to select model [2].

The system identification loop is illustrated in Figure 3.1
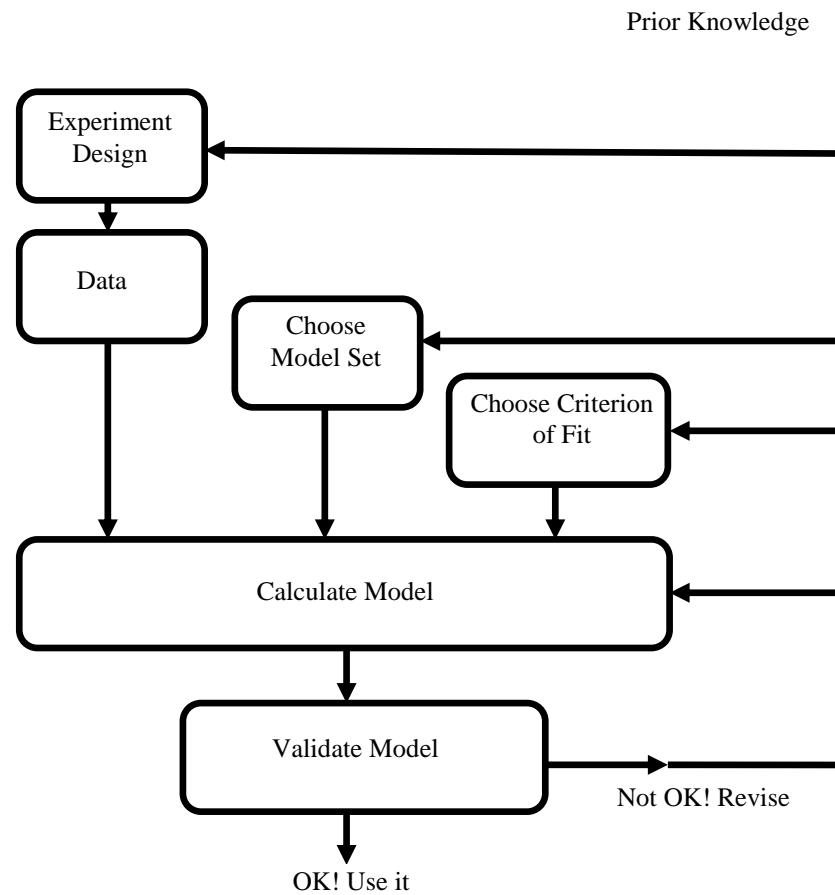
Figure 3.1: System identification loop [2]

The first step in the system identification is the experiment design performed by using a priori knowledge about the system and the aim of study. Model sets used in the identification are also selected based on the a priori knowledge, identification task, and data gathered from experiment [22]. Equivalency of the model and the system is commonly expressed in terms of a scalar cost function which quantifies equivalency of the model output y and system output z [22]:

$$J = J(y, z) \tag{3.1}$$

and this equivalency is normally expressed as a weighted sum of the squared differences between *z* and *y*. Generally, different model structures may be selected which leads to problem complexity. Instead, models M^* that have the same structure but having different values of parameters θ are selected [22]:

$$M^* = \{M(\theta)\} \tag{3.2}$$

Optimum parameters of this model minimizing the cost function can be found by optimization methods and thus system identification is reduced to parameter estimation [22]. Now details of system identification process will be given starting from the experiment design, first step of system identification.

3.2. EXPERIMENT DESIGN

Experiment design is the first task fulfilled in the system identification. It consists of several tasks some of which are the determination of input and output signals, their measurement, and designing input. Since models are identified based on the data gathered from experiment, quality of these data are very crucial for accurate identification. Therefore, experiment design should be conducted thoughtfully so as to attain the informative data.

Before making an experiment input-output signals used in identification should be determined so that required instrumentation is placed which means that sensors which measures the input and output are placed on the experimental setup. Input used in the experiment has a consequential influence on the output and thus on the identification. Operating points, parts, and the modes of the system are excited by the input and thus its characteristic such as frequency content, amplitude, shape, and duration should be well determined. Inputs used in the experiment should be informative enough that is it should excite the system modes completely. While designing experiment practical constraints should also be considered to satisfy

model assumptions. To illustrate, input amplitude and frequency may not be very high, sensors may be limited, and so on [22].

In this study, simulation data taken from ADAMS vehicle model is treated as test data and this data is used in identification, yet practical constraints faced during real vehicle test will be considered while making ADAMS simulations to become realistic.

Hardware Used in the Vehicle Handling Test

Sensors, data acquisition system, and some specialized equipment are used in the vehicle tests.

- Data acquisition system: It is used to acquire data during experiments.

Figure 3.2: Data acquisition system [23]

- Velocity Sensors: Lateral velocity and longitudinal velocity are measured by optical velocity sensors.

Figure 3.3: Optical velocity sensor [24]

- Inertial Measurement Units (IMU): Accelerations and rotational velocities are measured by inertial measurement units
- Steering Robot: Desired steering angle can be applied to the vehicle by steering robot.

Figure 3.4: Steering robot [25]

- Steering Wheel Measurement: Applied steering input is measured by steering wheel angle measurement system.

Figure 3.5: Steering wheel measurement [26]

Input Design

Input used in the experiment has a consequential influence on the output and thus on the identification. Inputs used in the experiment should be informative enough that is it should excite the system modes completely.

Input used for system identification can be classified into three categories; first of which is general purpose input, second of which is optimized input, and third of which is advanced test input. General purpose input is designed assuming that there is no a priori information about the system and so the objective is to excite the system over a broad frequency range that is general purpose input has flat power spectrum over a defined frequency range. Frequency sweeps, multisine, and impulse inputs are used for this purpose. Design of optimized input is performed by

using a priori information about the system. Square wave input used to excite the system at its natural frequency is in this category. In advanced test input, not only the test input is optimized but also its first and second derivative are also taken into consideration [27].

Data information content of the input signals can be quantified by signal to noise ratio, and for good identification signal to noise ratio must be high. Moreover, data information content of the input signals can be determined by quantifying the sensitivities of the model outputs to model parameters. The input that maximizes these sensitivies is selected as the best input. When the sensitivities are high, small changes in the model parameters bring about large changes in the outputs, and thus correct parameter values can be estimated that minimizes the difference between the model outputs and the measurement data. On the other hand, when the sensitivity values are small, changes in the parameters will not cause considerable effects in the outputs and thus different parameter values minimizing the difference between the model outputs and the measured outputs can be estimated. For a multiple output system the information content in the data can be quantified by a matrix which is called the information matrix [22]. For a parameter vector $\vec{\theta}$ the information matrix $[M]$ is [22],

$$\left[M\right] = \sum_{i=1}^{N} \left[\frac{\partial \vec{y_i}}{\partial \vec{\theta}}\right]^{T} \left[R\right]^{-1} \left[\frac{\partial \vec{y_i}}{\partial \vec{\theta}}\right] \tag{3.3}$$

When $[R]$ is the diagonal matrix, diagonal elements of $[R]^{-1}$ scales the output sensitivities according to the inverse of the individual output measurement noise variances and N is the number of data samples and y is the output. If the sensitivities are large and are uncorrelated with each other, then outputs are strongly dependent on each parameter distinctly and thus parameter values can be estimated accurately by minimizing the difference between the model output and measured output. The information matrix gives valuable information about the parameters [22]. Inverse of

the information matrix is the theoretical lower limit which is also called Cramer-Rao lower limit or the dispersion matrix for the estimated parameter covariance and is given by [22],

$$[M]^{-1} = \left\{ \sum_{i=1}^{N} \left[\frac{\partial \vec{y}_i}{\partial \vec{\theta}} \right]^{T} [R]^{-1} \left[\frac{\partial \vec{y}_i}{\partial \vec{\theta}} \right] \right\}^{-1} \leq Cov\left(\vec{\theta} \right)$$

(3.4)

Calculations of the information matrix and dispersion matrix require a priori knowledge about the system and model. There are also some practical constraints on input design. Normally experiment with a longer time and large amplitude produces more information yet due to practical reasons experiment time and input amplitude are limited [22].

Swept sine input also called chirp sine input is a sine input frequency of which increases or decreases with time. Mathematical representation of the linear swept sine input is [22],

$$u(t) = A\sin(f\,t) = A\sin\left(\left(f_0 + \left(f_f - f_0 \right) \frac{t}{2T} \right) t \right)$$

(3.5)

where

A: amplitude,

f_0: initial frequency

f_f: final frequency

T: experiment duration

The main advantage of the frequency sweep input is that it covers a frequency band so that data taken by this input is informative [22]. Figure 3.6 and Figure 3.7 show frequency sweep input and its power spectrum respectively.
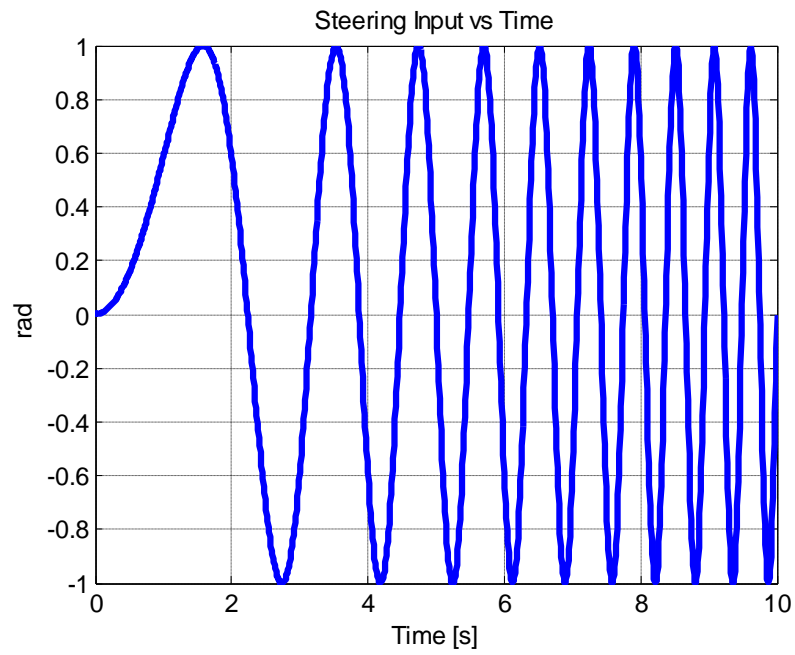
32

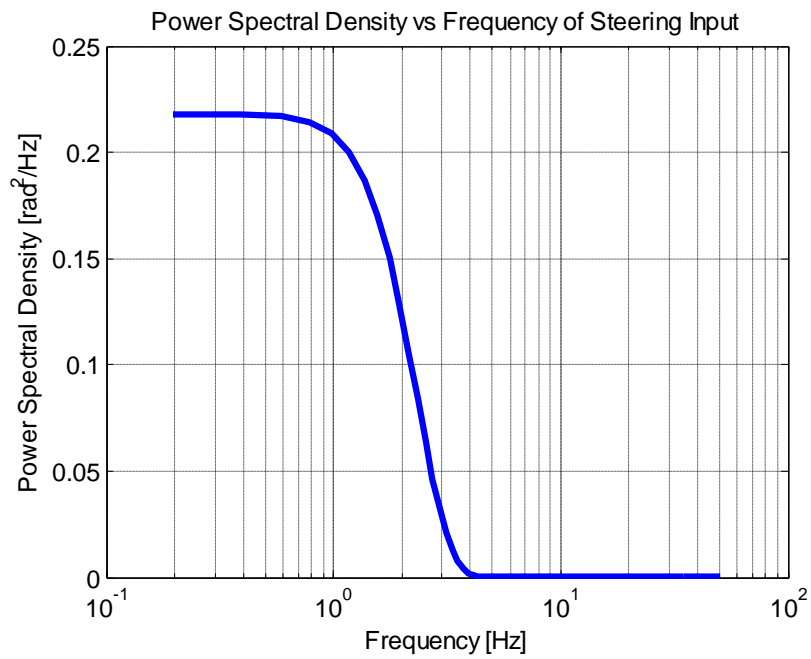**Figure 3.6: Frequency sweep input**

Figure 3.7: Power spectral density of frequency sweep input

33

Another general purpose input is the multisine input which covers a set of sine waves. Mathematical representation of this input is,

$$u(t) = \sum_{i=1}^{m} A_i \sin(f_i t + \phi_i) \qquad (3.6)$$

where m is the number of inputs, f is the frequency, ϕ is the phase, and A is the amplitude. Similar to sweep sine input multisine input can excite the system over a frequency band by determining the appropriate frequencies and amplitudes of the sine wave according to a desired power spectral density [22].

In vehicle handling identification sinusoidal inputs are commonly used. However, pure sinusoidal input cannot excite the system accurately when the frequency of it is not close to natural frequency of the system. Using a priori information about the system and the model, test input can be optimized such that the dispersion matrix is minimum. While optimizing these parameters there are some constraints like limited input and output amplitudes for validity of the model such as validity of the linear tire model. However, for multiple parameters and multiple outputs system this process is quite complex and difficult. Chirp and multisine inputs can excite the system over a broad frequency range and desired power spectral densities can be obtained. Therefore, these inputs can be used in vehicle handling identification. In addition to designing the chirp input according to modes of the system, sensitivity study can also give valuable information about the frequencies at which sensitivity values are high. In this study detailed sensitivity analysis are performed to be able to obtain the most appropriate frequency range of the input.

3.3. PARAMETER ESTIMATION

After the experiment is performed and the input output data is collected, the next step is the parameter estimation. The parameters of the selected model structure is determined in such a way that the selected model represents the system successfully that is the data acquired from experiment is used to select proper parameter values

of the determined model structure according to some criteria. One of them can be selected as the model's prediction aspect. The prediction error is given as [2],

$$e(t,\theta) = y(t) - \hat{y}(t|\theta) \tag{3.7}$$

where

$z^N = [y(1),u(1),y(2),u(2)...,y(N),u(N)]$: collected data,

N: number of data samples,

$y(t)$: output data at time t,

u: input data

$\hat{y}(t|\theta)$: predicted output at time t using the model with parameter θ .

According to this criterion a model is good when its prediction errors are small when applied to the observed data; that is the model is good in terms of its prediction performance. Therefore, prediction error is computed and the parameter vector is selected at time $t=N$ such that the prediction errors are as small as possible. The criteria on prediction error can be qualified by two approaches. One of them is to quantify the size of prediction error by using a scalar function of e and the other one is to estimate the parameters such that the error is uncorrelated with the data [2]. The scalar valued function of the model parameter θ can be formed as [2],

$$V\left(\theta, Z^N\right) = \sum f\left(e(t,\theta)\right) \tag{3.8}$$

where f is the scalar valued function.

Thus, the function $V\left(\theta, Z^N\right)$ for a given data Z^N is a function of the parameter vector θ and it is a measure of how the model represent the collected data. The estimate of the parameter vector, $\hat{\theta}_N$ is then determined by the minimization of the V.

35

Parameter estimation by this way is named as prediction error identification methods. Special cases of this method are built and named by changing some properties of this method like the error function and the optimization methods. Least square parameter estimation, the maximum likelihood estimation are some special cases of prediction error system identification method [2].

In this study least square parameter estimation with different optimization algorithms are used for parameter estimation and thus that topic will be explained in more detail.

3.3.1. LEAST SQUARE ESTIMATION

Parameters of the model can be estimated by quantifying the error between the model output and the collected data. This quantification is performed by constructing the appropriate function of error. By using this error function, optimal parameter set can be estimated; that is the parameter vector is selected such that the model output approximates the measured output successfully. In other words parameters are selected such that error is minimum. Error between the model and the measured output is shown in Figure 3.8 and is given as,
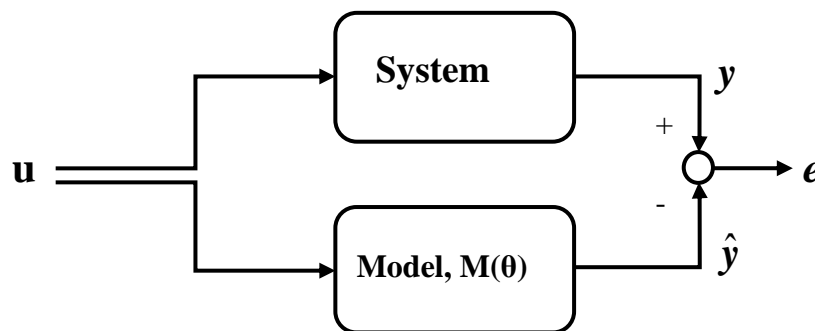
$$e = y - \hat{y} \tag{3.9}$$

Figure 3.8: Error between model and system outputs

where y is the system output and the $\hat{y}$ is the model output.

Error function in least square problem may be formed as the square of the function of the difference between measured and the model outputs as [28],

$$J(\vec{\theta}) = \sum_{i=1}^{N} f^2(i,\vec{\theta})$$ (3.10)

When the error function is linear in parameters, linear least square problem is formed; when the error function is nonlinear in parameters, nonlinear least square problem is formed. In linear least square problem global solution is found in one computation [28].

Derivation of the minimization algorithm for least square minimization given here is taken from reference [28] and the details which are not given here can be found in the same reference:

The cost function can be written in vector form as,

$$J\left(\vec{\theta}\right) = \vec{f}^T \vec{f}$$ (3.11)

j^{th} component of gradient of the cost function is,

$$g_j = \frac{\partial J(\vec{\theta})}{\partial \theta_j} = 2 \sum_{i=1}^{N} f(i) \frac{\partial f(i)}{\partial \theta_j}$$ (3.12)

The gradient of cost function can be written as,

$$[g] = 2[J]^T \vec{f}$$ (3.13)

where the Jacobian is,

$$[J] = \begin{bmatrix} \dfrac{\partial f(1)}{\partial \theta_1} & .. & \dfrac{\partial f(1)}{\partial \theta_n} \\ \vdots & .. & .. \\ \dfrac{\partial f(N)}{\partial \theta_1} & .. & \dfrac{\partial f(N)}{\partial \theta_n} \end{bmatrix}$$
(3.14)

The entries of Hessian of loss function is calculated as the derivative of the gradient,

$$H_{lj} = \frac{\partial^2 J(\vec{\theta})}{\partial \theta_j \partial \theta_l} = 2\sum_{i=1}^{N}\left(\frac{\partial f(i)}{\partial \theta_l}\frac{\partial f(i)}{\partial \theta_l} + f(i)\frac{\partial^2 f(i)}{\partial \theta_l \partial \theta_j} \right)$$
(3.15)

Hessian of cost function is;

$$[H] = 2[J]^T[J] + 2\sum_{i=1}^{N} f(i)\big[T(i)\big]$$
(3.16)

where $T(i)$ represents the entries of Hessian of the error function $f(i)$.

Nonlinear least square problems are based on the Hessian to derive an algorithm, and can be divided into two approaches according to calculation of the second term of the Hessian matrix [28],

$$\sum_{i=1}^{N} f(i)\big[T(i)\big]$$
(3.17)

First approach assumes that this second term is small and so it may be neglected. This assumption is true for small *f(i)*. According to the second approach that term is not neglected and it is computed [28].

The first approach is the Gauss-Newton Method. In this approach Hessian is approximated as,

$$[H] = 2[J]^T[J] \qquad (3.18)$$

and so Gauss-Newton algorithm becomes,

$$\vec{\theta}_k = \vec{\theta}_{k-1} - \eta_{k-1}[H_{k-1}]^{-1}\vec{g}_{k-1} = \vec{\theta}_{k-1} - \eta_{k-1}[J_{k-1}^T J_{k-1}]^{-1}J_{k-1}^T\vec{f}_{k-1} \qquad (3.19)$$

The second approach is the use of Levenberg-Marquardt Method. Parameters are calculated according to,

$$\vec{\theta}_k = \vec{\theta}_{k-1} - \eta_{k-1}[J_{k-1}^T J_{k-1} + \alpha_{k-1}I]^{-1}J_{k-1}^T\vec{f}_{k-1} \qquad (3.20)$$

where α is selected in different ways.

Difference between the estimated output and the measured output is called residual. Investigation of the residuals gives valuable information about the model and the estimation. When the residuals are random, model and the estimation process are good; yet the residuals having deterministic components shows model deficiency [22, 28].

3.3.2. NONLINEAR LOCAL OPTIMIZATION

When the loss function is nonlinear in parameters, the optimal parameters minimizing the error can be found by nonlinear optimization methods. Nonlinear

optimization problems have different local optimal points and as contrast to linear optimization problem there is no analytical solution, an iterative algorithm is used to find optimal points. Nonlinear optimization problem is difficult to solve since there are many local optimal points. When the search is started at the initial point, optimal solution is found generally at the neighborhood of initial point thus, global optimum solution may not be obtained. To be able to find global optimal solution a local search from many initial points should be started and then the best solution among them may be taken or some global optimization algorithms can be used. Also, selection of the initial values are very important since when the initial values are selected well global optimal points can be obtained and also converge to that solution may be fast. To select good initial points, a priori knowledge about the parameters can be used. Especially, when the parameters are physical their initial values can be selected properly. Nonlinear local optimization can be grouped into two classes as indirect search methods and direct search methods. Indirect search methods use derivative knowledge of the loss function to optimize loss function, whilst direct search methods use only loss function to optimize it. In nonlinear local optimization an initial point is selected and the optimal solution is found in the neighborhood of this point. Nonlinear local optimization methods are classified as direct search methods and general gradient-based methods [28].

Gradient-Based Methods

The most common and important nonlinear local optimization methods are the gradient-based methods. In gradient based methods, gradient of the optimized function with respect to parameters is required [28]. Derivation of the gradient based methods given here is taken from reference [28] and more details can be found in the same reference.

In all gradient-based methods, the aim is to change the parameter vector using gradient knowledge as,

$$\vec{\theta}_k = \vec{\theta}_{k-1} - \eta_{k-1}\vec{p}_{k-1} \quad \text{with} \quad \vec{p}_{k-1} = [R_{k-1}]\vec{g}_{k-1} \tag{3.21}$$

where,

$g = \dfrac{\partial J(\theta)}{\partial \theta}$: gradient of the loss function with respect to parameters,

η_{k-1} : step size,

$\vec{p}_{k-1}$: direction vector

$[R]$: direction matrix

Gradient based algorithms can be classified according to different selection of direction matrix and step size. When the direction matrix is set to identity matrix $[I]$, steepest descent method is obtained as [28],

$$\vec{\theta}_k = \vec{\theta}_{k-1} - \eta_{k-1} \vec{g}_{k-1} \tag{3.22}$$

Steepest descent algorithm does not require the second order derivatives and it has very slow convergence [28].

When the direction matrix is set to inverse of the Hessian matrix, $[H_{k-1}]^{-1}$ at $\vec{\theta}_{k-1}$, the Newton's method is formed as [28],

$$\vec{\theta}_k = \vec{\theta}_{k-1} - \eta_{k-1} [H_{k-1}]^{-1} \vec{g}_{k-1} \tag{3.23}$$

where the Hessian is the second derivative of the loss function with respect to parameters, that is,

$$[H] = \dfrac{\partial^2 J(\vec{\theta})}{\partial \theta^2} \tag{3.24}$$

Thus in Newton's method second order derivatives of the loss function has to be found by analytically or by finite difference techniques and has to be inverted which increases computational cost. The main advantage of the Newton's method is that its rate of convergence is very fast [28].

The main drawback of the Newton's method is that it requires the Hessian matrix and the inverse of the Hessian matrix. Even if the Hessian matrix is calculated analytically or by finite difference techniques inverse of it increases the computational load. This drawback can be eliminated by Quasi-Newton Methods which replaces the Hessian matrix or inverse of it as [28];

$$\vec{\theta}_k = \vec{\theta}_{k-1} - \eta_{k-1} \left[\hat{H}_{k-1} \right]^{-1} \vec{g}_{k-1} \qquad (3.25)$$

where,

$$\left[\hat{H}_k \right]^{-1} = \left[\hat{H}_{k-1} \right]^{-1} + \left[\tilde{Q}_{k-1} \right] \qquad (3.26)$$

or

$$\left[\hat{H}_k \right] = \left[\hat{H}_{k-1} \right] + \left[Q_{k-1} \right] \qquad (3.27)$$

Approximating the inverse of the Hessian directly is very advantageous since there is no need to inverse it. In addition similar to Newton's Method converge is very fast [28].

Conjugate gradient methods are like Quasi-Newton methods yet it avoids a direct approximation of the Hessian. These algorithms can be described by,

$$\vec{\theta}_k = \vec{\theta}_{k-1} - \eta_{k-1}\vec{p}_{k-1} \qquad (3.28)$$

with

$$\vec{p}_{k-1} = \vec{g}_{k-1} - \vec{\beta}_{k-1}\vec{p}_{k-2} \qquad (3.29)$$

where $\vec{\beta}_{k-1}$ is scalar and it distinguishes different conjugate gradient methods. Conjugate gradient methods will require more iterations for converge as compared with the Quasi-Newton methods. However, overall computation will be smaller and so it is suitable for large problems [28].

Direct Search Methods

The optimization algorithms explained so far are the indirect search algorithms which require derivatives of the loss function for the optimization. Direct search algorithms do not require the derivative of loss function to optimize it; they only use loss function for optimization. Especially when the calculation of the derivative of the loss function is difficult or impossible direct search algorithms are used. Moreover these methods can be used for smooth functions. These methods are easy to implement yet their convergence is slow [28].

Some of these methods are [29]:

- Random Search Methods: In these methods random numbers are generated and used in the optimization.
- Grid Search Methods: In this methods grid points are generated in the design space and the functions are evaluated at these grid points. The point which generates the minimum function value is selected as the optimal points. Grid points can be generated by dividing the distance between maximum and minimum design values into equal ranges and setting the grid points in these

ranges. These methods require large number of function evaluations, yet they can be used together with the other methods while selecting initial points.

- Simplex Methods: In simplex methods, a simplex, that is, a geometric figure which is formed by $n+1$ points in a n dimensional space is generated. The value of the loss function at $n+1$ vertices are calculated and then compared with each other and so simplex moves according to this comparison to find optimal value. Simplex moves by three operations, reflection, contraction, and expansion. The vertex with the largest loss function value is reflected at the opposite face. If this new vertex generated by reflection yields a minimum value, simplex is expanded. On the other hand, if this new vertex generated by reflection yields a value which is higher than values of other vertices except maximum value, simplex is contracted. This procedure is continued until the minimum is found. At the minimum the centroid of the latest vertex is taken as the optimal points

3.3.3. CONSTRAINED NONLINEAR OPTIMIZATION

In constrained nonlinear optimization, in addition to the loss function there are constraints. Constraints help to optimization by minimizing the parameter space in which the optimal solution is found. However they result in problem complexity since constraints may not be incorporated into problem easily. The general constrained optimization problem is given as [28],

Minimize $J(\vec{\theta})$

subject to

$$g_i\left(\vec{\theta}\right) \leq 0 \quad i = 1,....,m$$
$$h_j\left(\vec{\theta}\right) = 0 \quad j = 1,....,l$$

This constraint optimization problem can be solved by constructing Lagrangian [28],

$$\ell\left(\vec{\theta},\vec{\lambda}\right) = J\left(\vec{\theta}\right) + \sum_{i=1}^{m} \lambda_i g_i\left(\vec{\theta}\right) + \sum_{j=1}^{l} \lambda_{j+m} h_j\left(\vec{\theta}\right) \qquad (3.30)$$

One of the most commonly used algorithm for constrained nonlinear optimization problem is the *Sequential Quadratic Programming (SQP).*

3.3.4. NONLINEAR GLOBAL OPTIMIZATION

In the previous part nonlinear local optimization methods have been examined. Solutions of the nonlinear local optimization problems start from an initial point and search within the neighborhoods of the initial point in the design space and thus these approaches result in solutions which are close to initial point and the optimal solution is generally local, not the global. In this part, global nonlinear optimization methods are examined. One of the basic strategies for nonlinear global optimization is to start local optimization from many points. In this method the solution is started with many different initial points and local optimization method is applied for each initial point. The best solution among these local optimizations is selected. One of these solutions may be the global solution since global solution may not be known. Moreover there are some specific global optimization methods. These methods are applied when there is a need to find a global optimum or a satisfactory local optimum and when the function to be minimized is non-smooth or the computational loads for taking the derivative of the function is high. The main drawback of the global optimization is that the computational loads are very high since the entire design space must be searched for global solution and thus the convergence to solution is very slow. Global optimization methods are used to eliminate the drawback of the local optimization methods which is the selection of the initial points. Evolutionary algorithms are inspired from the natural evolution process. These types of algorithms start with the population of individuals which evolves in generations. These evolutions are due to mutation and crossover and new

45

individuals are created after them. These individuals are evaluated and the ones showing better performance that is having more fitness are selected. Evolutionary algorithms are classified according to type of selection procedure, type of genetic operation etc. as evolution strategies, genetic algorithms, genetic programming etc [28].

Genetic algorithms are the most popular one of the evolutionary algorithms. Firstly, initial populations are selected. Then, fitness of the individuals is evaluated and according to this fitness selection of individuals are performed. After that crossover and mutation operations are applied on these selected individuals and the new generations are formed. These subsequent genetic operations continue until some termination criteria are reached and the final generations are the optimal solution [28, 30].

Genetic algorithm can be summarized as [30],

1) Form the initial population P_0;

2) Evaluate P_k;

3) If stopping criterion is satisfied then stop otherwise go to step 4;

4) Perform selection P_{sel} from P_k;

5) Apply genetic operations(crossover and mutation) to evolve P_{k+1} from P_{sel};

6) Continue iterations, $k=k+1$.

In this thesis study different methods of optimization which are simplex search, nonlinear least square method, grid search method, and genetic algorithm method are used according to the aim of study and problem complexity. Sometimes hybrid

algorithms are used to get rid of the disadvantages and to exploit advantage of the specific algorithm.

3.4. SIMULINK PARAMETER ESTIMATION SOFTWARE

Simulink Parameter Estimation Software is a Simulink-based product of MATLAB which is used for estimation of model parameters from experimental data. It supports the estimation of model parameters, estimation of the initial conditions of the states and the estimation of the values in the adaptive lookup tables from experimental data. This software works with the MATLAB technical computing software, Simulink software and Optimization Toolbox and thus they are required softwares. To be able to use this software firstly model is built on the Simulink environment and the parameters to be estimated are specified. After that experimental data is imported and it is processed if necessary that is input-output data can be filtered, outliers can be removed etc. Then the parameters and the initial state to be estimated are selected and the estimation process is started. Trajectory of the estimated parameters and the plots of the simulated and the experimental data can be seen during estimation. After the estimation model validation can be performed by acquiring another data set and comparing this with the estimated models. To estimate the parameters, experimental data is imported into this software. If there is multiple output data, they can be weighted according to their importance or order of magnitude. Parameters to be estimated are selected and their initial values, typical values, upper and lower bounds are determined. Typical values of the parameters are the average order of magnitude of them. Specifying the upper and lower bounds for parameters simplify the estimation progress since the search space can be decreased. In particular if the parameters have physical meaning these bounds should be used. Estimation process can be performed by different user selected cost functions and different solvers. Estimation results can be seen from plots of the cost function, measured and simulated output, parameter trajectory, and sensitivity of cost function to parameters In Simulink Parameter

Optimization Software different optimization methods and different cost functions are available [31].

Optimization algorithms: [31];

- Gradient Descent: This choice uses gradient type optimization methods and MATLAB optimization function 'fmincon' is used.

- Nonlinear Least Squares: This choice uses nonlinear least square optimization methods and MATLAB optimization function 'lsqnonlin'.

- Pattern Search: This choice uses advanced pattern search algorithms and it requires Genetic Algorithms and Direct Search Toolbox.

- Simplex Search: This choice uses one of the derivative free optimization methods, simplex methods, and it uses MATLAB optimization function, 'fminsearch'.

Furthermore, there are two options for cost functions which are [31];

- SSE(sum of squared error)

- SAE(sum of absolute error)

- Use robust cost: Optimizer is more robust to cost function especially when the experimental data is noisy.

CHAPTER 4

VEHICLE HANDLING MODELS

4.1. INTRODUCTION

In this chapter, vehicle and tire models will be derived and built in Simulink environment.

Some parameters of ADAMS/Chassis vehicle model corresponding to handling model are known previously, and so estimated parameters will be simply compared with parameters of ADAMS model, that is, estimated parameters will be compared with their nominal values. Also cornering force data is taken from ADAMS to be able to compare it with the estimated cornering force characteristic of Magic Formula tire model.

Parameters of the ADAMS/Chassis vehicle model can be obtained either directly from model or from some specific simulations. Static Vehicle Characteristic (SVC) is a set of ADAMS subroutines and it computes vehicle characteristic at static equilibrium. By SVC both half and full vehicles can be analyzed, suspension parameters like roll center position and full vehicle parameters like mass and inertias of vehicle can be obtained [6]. Some of these parameters can be measured easily from the real vehicle like mass and wheelbase, yet some of them, as in the case of moment of inertias of the vehicle body, cannot be calculated accurately or difficult to measure. Parameters of ADAMS/Chassis vehicle model is given in Table 4.1.

Table 4.1: Parameters of ADAMS/Chassis vehicle model

Parameter	Value	Unit
Total Mass, m	1040	kg
Front Ground Reaction	6036	N
Rear Ground Reaction	4179	N
Total Roll Inertia	365	kgm^2
Total Yaw Inertia	1724	kgm^2
Sprung Mass	926	kg
Sprung Roll Inertia	297	kgm^2
Sprung Yaw Inertia	1472	kgm^2
Total Center of Gravity Height	546	mm
Sprung Mass Center of Gravity Height	576	mm
Wheelbase	2611	mm
Front Unsprung Mass	62	kg
Front Roll Center Height	114	mm
Front Track Width	1489	mm
Axle Distance from Center of Gravity	1068	mm
Rear Unsprung Mass	53	kg
Front Roll Center Height	197	mm
Front Track Width	1483	mm
Axle Distance from Center of Gravity	1543	mm

4.2. TIRE AND VEHICLE HANDLING MODELS

In this part various handling and tire models used in the identification are constructed. The simplest vehicle handling model is the bicycle model. The bicycle model represents the vehicle planar dynamics successfully, yet it has limited range

of validity around operating points. Vehicle roll model comprises the coupling between the vehicle planar and roll motion and thus is a more accurate model.

Tires are the most important parts of the vehicle handling since the vehicle interacts with road by means of tires. Therefore, modeling of the tire is important for an accurate vehicle handling model. However, characteristics of tires are highly nonlinear and difficult to model. Even if they are modeled adequately, determining the parameter values is extremely difficult. The simplest tire model is the linear tire model in which the lateral force changes linearly with the slip angle. There are other models such as Magic Formula tire model which explain lateral force of tires as a function of several variables such as normal load on tires, lateral slip, and several other parameters. In this study, linear tire model is used only for identification purposes, and Magic Formula tire models are used for both identification and ADAMS/Chassis simulation.

4.2.1. BICYCLE MODEL

Bicycle model is a vehicle handling model commonly used in vehicle handling studies. Bicycle model is a simple model, yet it comprises important vehicle handling dynamics; lateral dynamics and yaw dynamics. Equation of motion for the bicycle model can be derived by using the Newton's second law as shown in Figure 4.1.
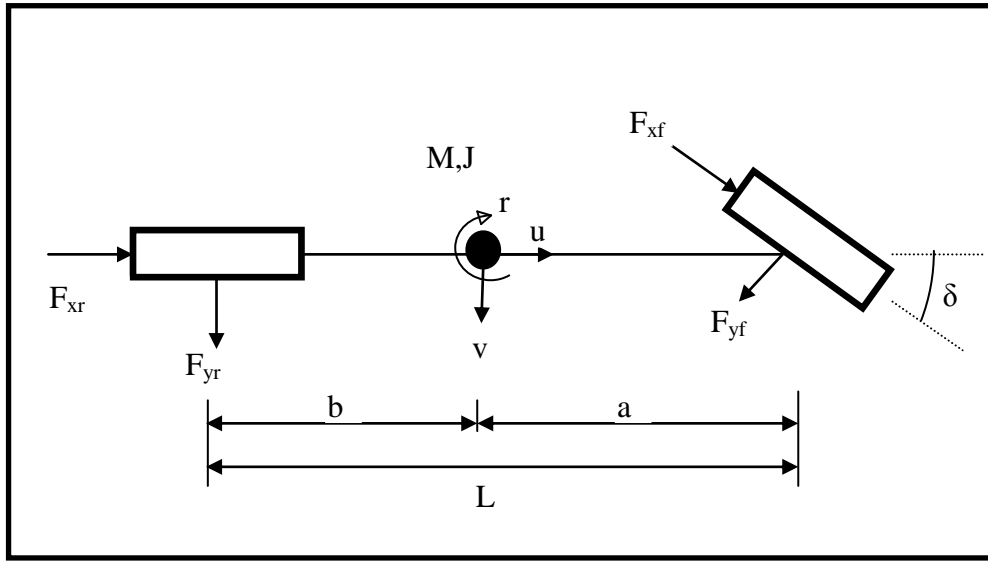
Figure 4.1: Bicycle model

Equation of Motion

Equation of motion for longitudinal direction is obtained by summing forces in longitudinal direction:

$$M \cdot a_x = \sum F_x = F_{xr} + F_{xf} \cos(\delta) - F_{yf} \cdot \sin(\delta) \tag{4.1}$$

where longitudinal acceleration is;

$$a_x = \dot{U} - v \cdot r \tag{4.2}$$

Equation of motion for lateral direction is obtained by summing forces in lateral direction:

$$M \cdot a_y = \sum F_y = F_{yr} + F_{yf} \cos(\delta) + F_{xf} \sin(\delta) \tag{4.3}$$

where lateral acceleration is;

$$a_y = \dot{v} + U \cdot r \tag{4.4}$$

Equation of motion for yaw direction is obtained by summing moment of forces about center of gravity:

$$J \cdot \dot{r} = \sum M_z = a \left[F_{yf} \cos(\delta) + F_{xf} \sin(\delta) \right] - b \cdot F_{yr} \tag{4.5}$$

where,

M: vehicle mass

J: yaw moment of inertia

a: distance between center of gravity and front axle

b: distance between center of gravity and rear axle

F_{yf}: Front axle cornering force

F_{yr}: Rear axle cornering force

U: longitudinal velocity

v: lateral velocity

r: yaw velocity

δ: steering angle

While deriving bicycle model some assumptions are done: Since steer angle is small, *cos(δ)~1* and *sin(δ)~0* and the term '*vr*' is small so it can be neglected. Moreover, longitudinal velocity can be kept constant so it becomes a parameter rather than state. Therefore, lateral and yaw motions can be uncoupled from longitudinal motion and two DOF bicycle model is obtained.

With this assumption equations of motion become:

$$M \cdot a_y = \sum F_y = F_{yr} + F_{yf} \tag{4.6}$$

$$J \cdot \dot{r} = \sum M_z = a \cdot F_{yf} - b \cdot F_{yr} \tag{4.7}$$

Cornering force can be calculated according to selected tire model. When the linear tire model is used cornering force becomes,

$$F_c = C_\alpha \cdot \alpha \tag{4.8}$$

where C_α is the cornering stiffness and the α is the slip angle which is defined for front and rear axles as,

$$\alpha_f = \frac{v + a \cdot r}{U} - \delta \tag{4.9}$$

$$\alpha_r = \frac{v - b \cdot r}{U} \tag{4.10}$$

By combining linear tire model with bicycle model equations, two DOF linear bicycle model can be obtained as,

$$M(\dot{v} + U \cdot r) = C_f \left(\frac{v + a \cdot r}{U} - \delta \right) + C_r \left(\frac{v - b \cdot r}{U} \right) \tag{4.11}$$

$$I_{zz} \cdot \dot{r} = a \cdot C_f \left(\frac{v + a \cdot r}{U} - \delta \right) - b \cdot C_r \left(\frac{v - b \cdot r}{U} \right) \tag{4.12}$$

Then state space form of linear bicycle model is obtained as,

$$\{\dot{x}\} = [A]\{x\} + [B]\{u\} \tag{4.13}$$

$$\{y\} = [C]\{x\} + [D]\{u\} \tag{4.14}$$

where $\{x\}$ is the state vector, $\{u\}$ is the input vector, $\{y\}$ is the output vector; $[A]$ is the system matrix, $[B]$ is the input matrix and $[C]$ is the output matrix. In bicycle model lateral velocity v and yaw velocity r are the state variables, δ is the steering input at the front tires. Output vector of the model can be constructed according to the variables to be selected as outputs Therefore;

$$\{x\} = \begin{Bmatrix} v \\ r \end{Bmatrix} \tag{4.15}$$

$$[A] = \begin{bmatrix} \dfrac{C_f + C_r}{M \cdot U} & \dfrac{a \cdot C_f - b \cdot C_r}{M \cdot U} - U \\ \dfrac{a \cdot C_f - b \cdot C_r}{J \cdot U} & \dfrac{a^2 \cdot C_f + b^2 \cdot C_r}{J \cdot U} \end{bmatrix} \tag{4.16}$$

$$[B] = \begin{Bmatrix} -\dfrac{C_f}{M} \\ -\dfrac{a \cdot C_f}{J} \end{Bmatrix} \tag{4.17}$$

$$\{u\} = \delta \tag{4.18}$$

When the lateral velocity and yaw velocity are the outputs $[C]$ and $[D]$ matrices become,

$$[C] = \begin{bmatrix} 1 & 0 \\ 0 & 1 \end{bmatrix} \tag{4.19}$$

$$[D] = \begin{bmatrix} 0 \\ 0 \end{bmatrix} \tag{4.20}$$

Note that linear bicycle model is valid for small slip angle nearly below 4 degree and for low lateral acceleration nearly below 0.3g. These limitations are due to the linear tire model which states that cornering force is linearly dependent on slip angle for low slip angles. However, when the slip angles increase, this linear

relationship becomes nonlinear and linear tire model is no longer valid. Also cornering force characteristic of the tires changes with the vertical load on it. When the lateral acceleration is below nearly 0.3g, lateral load transfer is small and thus vertical load on the tire does not change much. However, when the lateral acceleration increases above 0.3g lateral load transfer changes the vertical load on the tires and so cornering force changes. These limitations can be removed by using more complex tire models. In this study, Magic Formula tire model which considers the nonlinear changes of cornering force with slip angle and vertical load are used and thus vehicle model having wider operating points is obtained.

4.2.2. THREE DEGREE OF FREEDOM ROLL MODEL

Three degree of freedom vehicle roll model considers the plane motion of the vehicle together with the roll motion. Roll motion is coupled with the plane motion of the vehicle directly and also it is coupled indirectly by means of tire dynamics. In other words roll motion affects the load transfer and so the normal loads on the tires, and in turn the tire forces change. Therefore, a more accurate model is obtained. Since the bicycle model does not include the roll motion, lateral load transfer cannot be included in the model. Especially, for high lateral acceleration, load transfer becomes important and the tire dynamics are affected considerably.

In the roll model, masses of the parts of the vehicles can be lumped as the sprung mass and the front and rear unsprung masses. Sprung mass and unsprung masses are connected via the suspension. Sprung mass rolls about the roll axis defined by the front and the rear roll centers which are the characteristics of the suspensions. Moments of the spring and the damper of the suspension about the roll axis form the roll stiffness and the roll damping which are assumed to be constant during the roll motion. Further, since roll centers are defined by the geometry of the suspensions and since the suspension geometry may change with the roll motion, position of the front and rear roll centers may also change during the roll motion. However, in here roll centers and so the roll axis is assumed to be stationary. Vertical motion and the pitch motion of the vehicle are not included in the model.

In the derivation of the equation of the motion of the model Newton's second law is used. The body fixed coordinate frame located at the mass center is used and for this coordinate system SAE (Society of Automotive Engineering) convention is used. SAE reference frame is shown in the Figure 4.2.
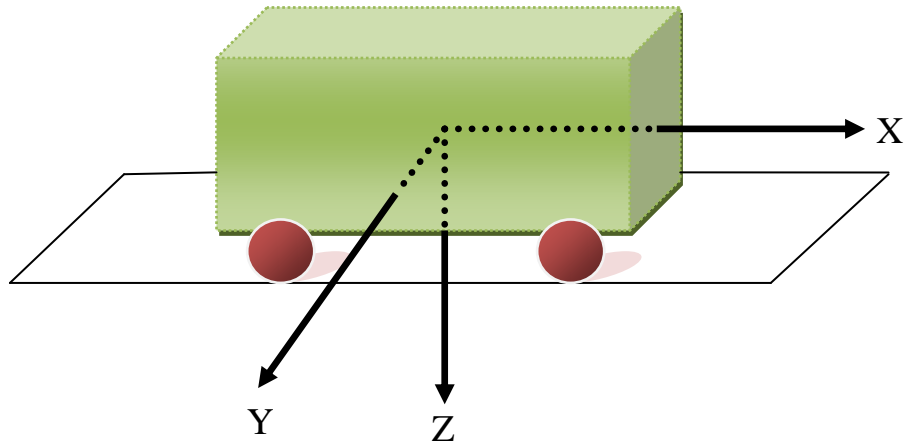
Figure 4.2: SAE reference frame
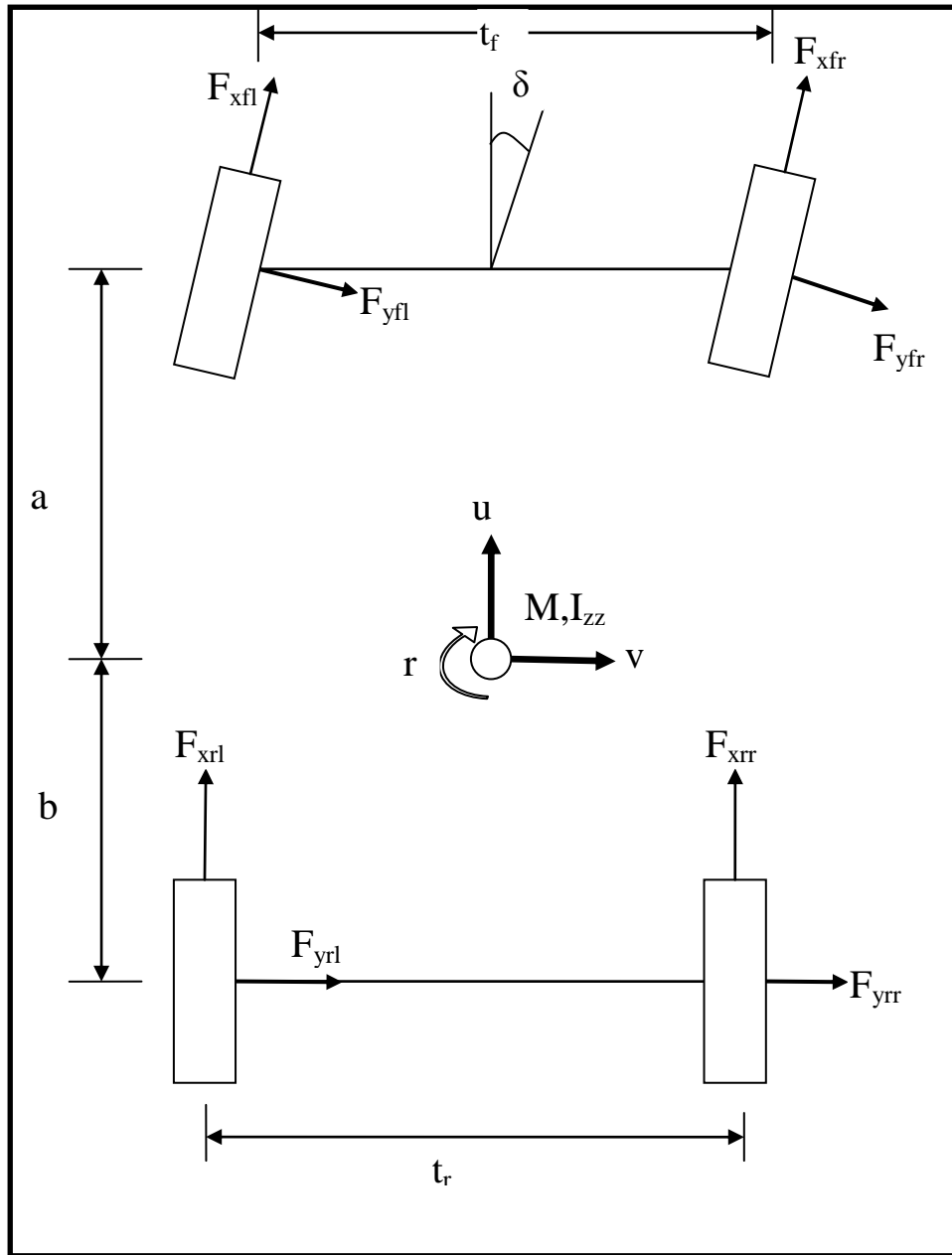
Figure 4.3: Vehicle plane model
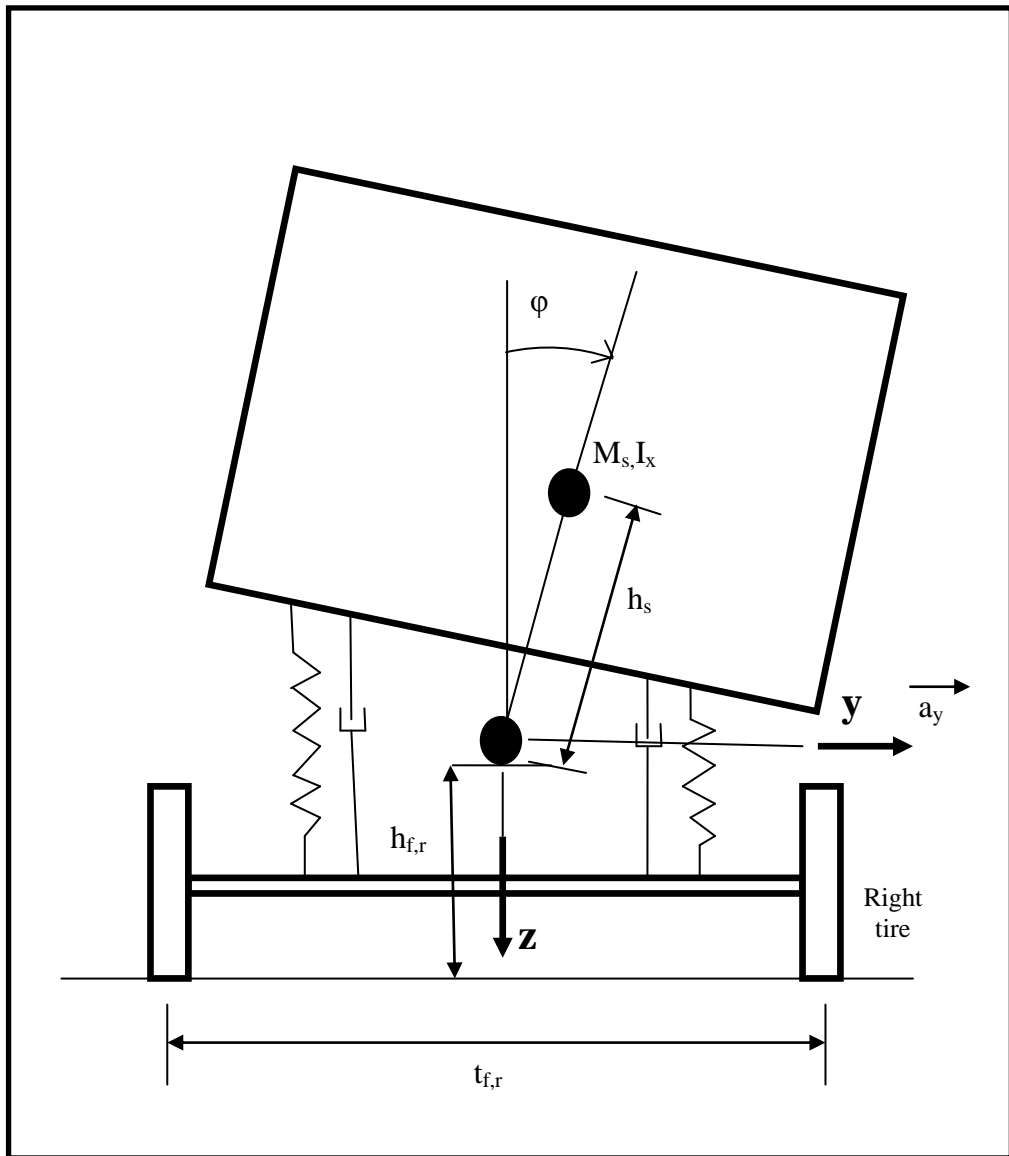
Figure 4.4: Vehicle roll model

Equations of motion

Vehicle roll model comprises degrees of freedom which are lateral, yaw, roll, and longitudinal motion. Schematic of the vehicle plane motion and vehicle roll motion are shown in Figure 4.3 and Figure 4.4 respectively.

Equation of motion for longitudinal direction:

Equation of motion for longitudinal direction is obtained by summing forces in longitudinal direction:

$$M \cdot a_x = \sum F_x = F_{xrl} + F_{xrr} + \left(F_{xfl} + F_{xfr}\right)\cos\left(\delta\right) - \left(F_{yfl} + F_{yfr}\right)\sin\left(\delta\right) \qquad (4.21)$$

where longitudinal acceleration a_x is given in (4.2)

Equation of motion for lateral direction:

Equation of motion for lateral direction is obtained by summing forces in lateral direction:

$$M \cdot a_y + M_s \cdot h_s \cdot \ddot{\phi} \cdot \cos\left(\phi\right) - M_s \cdot h_s \cdot \dot{\phi}^2 \cdot \sin\left(\phi\right) = \sum F_y \qquad (4.22)$$

$$\sum F_y = \left(F_{yfl} + F_{yfr}\right) \cdot \cos\left(\delta\right) + F_{yrl} + F_{yrr} + \left(F_{xfl} + F_{xfr}\right) \cdot \sin\left(\delta\right) \qquad (4.23)$$

where lateral acceleration a_y is given in (4.4)

Equation of motion for yaw motion:

Equation of motion for yaw direction is obtained by summing moment of forces about center of gravity:

$$I_{zz} \cdot \dot{r} = \sum M_z \qquad (4.24)$$

$$\sum M_z = a\left[\left(F_{yfl} + F_{yfr}\right)\cos\left(\delta\right) + \left(F_{xfl} + F_{xfr}\right)\sin\left(\delta\right)\right] - b\left(F_{yrl} + F_{yrr}\right)$$
$$+ \frac{t_f}{2}\left[\left(F_{xfl} - F_{xfr}\right)\cos\left(\delta\right) + \left(-F_{yfl} + F_{yfr}\right)\sin\left(\delta\right)\right] + \frac{t_r}{2}\left(F_{xrl} - F_{xrr}\right) \qquad (4.25)$$

Equation of motion for roll motion:

Equation of motion for roll direction is obtained by summing moment of forces about roll axis:

$$I_{xx} \cdot \ddot{\phi} + M_s \cdot h_s (\dot{v} + r \cdot U) \cdot \cos(\phi) = M_s \cdot g \cdot h_s \cdot \sin(\phi) - K_\phi \cdot \phi - C_\phi \cdot \dot{\phi} \qquad (4.26)$$

$$K_\phi = K_f + K_r \qquad (4.27)$$

$$C_\phi = C_{f\phi} + C_{r\phi} \qquad (4.28)$$

where,

M: total vehicle mass,

M_s: sprung mass

M_{uf}: front unsprung mass

M_{ur}: rear unsprung mass

F_{xfl}: front left longitudinal tire force

F_{xfr}: front right longitudinal tire force

F_{xrl}: rear left longitudinal tire force

F_{xrr}: rear right longitudinal tire force

F_{yfl}: front left lateral tire force

F_{yfr}: front right lateral tire force

F_{yrl}: rear left lateral tire force

F_{yrr}: rear right lateral tire force

h_f: front roll center height

h_r: rear roll center height

h_s: vertical distance between roll axis and center of gravity

K_φ: total roll stiffness

K_f: front roll stiffness

K_r: rear roll stiffness

C_φ: total roll damping

$C_{f\varphi}$: front roll damping

$C_{r\varphi}$: rear roll damping

I_{xx}: roll moment of inertia about x axis

I_{zz}: yaw moment of inertia about z axis

φ: roll angle

t_f: front track width

t_r: rear track width

Longitudinal velocity is assumed as a parameter rather than variable by keeping it at a constant value. Moreover since in this study aim is to identify handling models without longitudinal dynamics, longitudinal motion is not included in the roll model. Note that the term 'vr' in the longitudinal acceleration expression is very small so it can be neglected. By this way longitudinal motion can be decoupled from roll model. Similarly, in the lateral equation of motion the term $M_s \cdot h_s \cdot \dot{\phi}^2 \cdot \sin(\phi)$ is small so it can be neglected. Also when the mass symmetry in x-y plane is considered product inertia term I_{xz} are relatively small as compared to I_{xx} and I_{zz} and so it is neglected in the derivation of equation of motion. With all these assumptions roll model is simplified to three degree of freedom roll model as:

$$M(\dot{v}+r\cdot U)+M_s \cdot h_s \cdot \ddot{\phi}\cdot\cos(\phi) = \sum F_y = \left(F_{yfl}+F_{yfr}\right)\cos(\delta)+F_{yrl}+F_{yrr} \qquad (4.29)$$

$$I_{zz}\cdot\dot{r} = \sum M_z = a\left(F_{yfl}+F_{yfr}\right)\cos(\delta)-b\left(F_{yrl}+F_{yrr}\right) \qquad (4.30)$$

$$I_{xx}\cdot\ddot{\phi}+M_s \cdot h_s(\dot{v}+r\cdot U)\cdot\cos(\phi) = M_s \cdot g \cdot h_s \cdot \sin(\phi) - K_\phi\cdot\phi - C_\phi\cdot\dot{\phi} \qquad (4.31)$$

Lateral Load Transfer

Lateral load transfer is calculated since vertical load in each tire is used for the calculation of the lateral force produced by the tire. Lateral load on each tire is calculated as follows:

$$F_{zfl} = \frac{M \cdot g \cdot b}{2(a+b)} + \frac{M_s \cdot \left(a_y + h_s \cdot \ddot{\phi}\right) \cdot h_f \cdot b}{t_f(a+b)} - F_{\phi,f} \tag{4.32}$$

$$F_{zfr} = \frac{M \cdot g \cdot b}{2(a+b)} - \frac{M_s \cdot \left(a_y + h_s \cdot \ddot{\phi}\right) \cdot h_f \cdot b}{t_f(a+b)} + F_{\phi,f} \tag{4.33}$$

$$F_{zrl} = \frac{M \cdot g \cdot a}{2(a+b)} + \frac{M_s \cdot \left(a_y + h_s \cdot \ddot{\phi}\right) \cdot h_r \cdot a}{t_r(a+b)} - F_{\phi,r} \tag{4.34}$$

$$F_{zrr} = \frac{M \cdot g \cdot a}{2(a+b)} - \frac{M_s \cdot \left(a_y + h_s \cdot \ddot{\phi}\right) \cdot h_r \cdot a}{t_r(a+b)} + F_{\phi,r} \tag{4.35}$$

where,

$$F_{\phi,f} = \frac{K_f \cdot \phi + C_{f\phi} \cdot \dot{\phi}}{t_f} \tag{4.36}$$

$$F_{\phi,r} = \frac{K_r \cdot \phi + C_{r\phi} \cdot \dot{\phi}}{t_r} \tag{4.37}$$

The first term on the vertical load equations accounts for the static load distribution for each tire. The second term accounts for the load transfer due to lateral acceleration and the third term accounts for the load transfer due to roll motion. Note that while calculating vertical loads on the tires, load transfer due to unsprung masses are not taken into account due to the fact that they are small as compared with the other effects.

Tire Slip Angle

To be able to calculate the lateral tire forces, tire slip angles are also needed. Tire slip angles are,

$$\alpha_{fl} = \tan^{-1}\left(\frac{v + ar}{U + {}^{t_f}\!/_2\, r}\right) - \delta \tag{4.38}$$

$$\alpha_{fr} = \tan^{-1}\left(\frac{v + ar}{U - {}^{t_f}\!/_2\, r}\right) - \delta \tag{4.39}$$

$$\alpha_{rl} = \tan^{-1}\left(\frac{v - br}{U + {}^{t_r}\!/_2\, r}\right) \tag{4.40}$$

$$\alpha_{rr} = \tan^{-1}\left(\frac{v - br}{U - {}^{t_r}\!/_2\, r}\right) \tag{4.41}$$

Now the effect of the suspension on the steering characteristic of the vehicle is also taken into account. When the suspension deflects tires are steered, which is called roll steer effect.

$$\delta_f = \delta_{f\phi} \cdot \phi + \delta_w \tag{4.42}$$

$$\delta_r = \delta_{r\phi} \cdot \phi \tag{4.43}$$

where,

δ_f :front steering angle,

δ_r : rear steering angle,

δ_w : steering angle due to steering wheel rotation

$\delta_{f\phi}$: front roll steer coefficient

$\delta_{r\phi}$: rear roll steer coefficient

Three DOF roll model may be linear and nonlinear depending on the tire model. According to nonlinear tire model such as Magic Formula tire models cornering force depends on vertical load on the tire and the slip angle nonlinearly. On the other hand according to linear tire model there is a linear relationship between cornering force and slip angle. Therefore, nonlinear tire models are more accurate and have a wider operating range as compared to the linear tire model. However the more accurate roll model has more computational load than the linear roll model. In this study both linear and nonlinear roll models are used.

4.2.3. ONE DEGREE OF FREEDOM ROLL MODEL

One DOF roll model is a simple roll model and it can be used in vehicle roll dynamics studies. Using this model basic roll dynamics parameters may be estimated easily. One DOF roll model considers only the roll motion of vehicle. Vehicle roll motion is caused by the lateral acceleration and so lateral acceleration is considered as the input, and the roll velocity is considered as the output.

Equation of motion:

Equation of motion for one DOF roll model can be obtained from equation (4.31) by assuming that $cos(\varphi)\sim 1$ and $sin(\varphi)\sim\varphi$ for small φ.

$$I_{xx}\cdot\ddot{\phi}+M_s\cdot h_s(\dot{v}+r\cdot U)=M_s\cdot g\cdot h_s\cdot\phi - K_\phi\cdot\phi - C_\phi\cdot\dot{\phi} \tag{4.44}$$

In state space form equation of motion becomes,

$$\begin{Bmatrix}\dot{\psi}_1\\\dot{\psi}_2\end{Bmatrix}=\begin{bmatrix}-\dfrac{C_\phi}{I_{xx}} & -\dfrac{K_\phi - M_s\cdot g\cdot h_s}{I_{xx}}\\1 & 0\end{bmatrix}\begin{Bmatrix}\psi_1\\\psi_2\end{Bmatrix}+\begin{Bmatrix}-\dfrac{M_s\cdot h_s}{I_{xx}}\\0\end{Bmatrix}a_y \tag{4.45}$$

where,

$$\psi_1 = \dot{\phi} \tag{4.46}$$

$$\psi_2 = \phi \tag{4.47}$$

Transfer function representation of the one DOF roll model is obtained to study the identifiability of this model as,

$$\frac{\Phi(s)}{a_y(s)} = \frac{-\dfrac{M_s \cdot h_s}{I_{xx}}}{s^2 + \dfrac{C_\phi}{I_{xx}}s + \dfrac{K_\phi - M_s \cdot h_s \cdot g}{I_{xx}}} \tag{4.48}$$

4.2.4. THREE DEGREE OF FREEDOM LINEAR ROLL MODEL

For small steering angle δ and roll angle φ, $cos(\delta)\sim 1$; $cos(\varphi)\sim 1$ and $sin(\varphi)\sim\varphi$, With this assumptions equations of motion for linear three DOF linear roll model can be derived from the roll model equations and linear tire model equation. With these assumptions equations of motion for roll become;

$$M(\dot{v} + r \cdot U) + M_s \cdot h_s \cdot \ddot{\phi} = \sum F_y = F_{yfl} + F_{yfr} + F_{yrl} + F_{yrr} \tag{4.49}$$

$$I_{zz} \cdot \dot{r} = \sum M_z = a\left(F_{yfl} + F_{yfr}\right) - b\left(F_{yrl} + F_{yrr}\right) \tag{4.50}$$

$$I_{xx} \cdot \ddot{\phi} + M_s \cdot h_s(\dot{v} + r \cdot U) = M_s \cdot g \cdot h_s \cdot \phi - K_\phi \cdot \phi - C_\phi \cdot \dot{\phi} \tag{4.51}$$

Then equations of motions for linear three DOF roll model are derived by inserting (4.8), (4.9), and (4.10) into (4.49), (4.50), and (4.51) as:

$$M(\dot{v}+r\cdot U)+M_s\cdot h_s\cdot\ddot{\phi}=\sum F_y=C_f\cdot\alpha_f+C_r\cdot\alpha_r \tag{4.52}$$

$$I_{zz}\cdot\dot{r}=\sum M_z=a\cdot C_f\cdot\alpha_f-b\cdot C_r\cdot\alpha_r \tag{4.53}$$

$$I_{xx}\cdot\ddot{\phi}+M_s\cdot h_s(\dot{v}+r\cdot U)=M_s\cdot g\cdot h_s\cdot\phi-K_\phi\cdot\phi-C_\phi\cdot\dot{\phi} \tag{4.54}$$

State space representation of the three DOF linear roll model is,

$$\begin{Bmatrix}\dot{v}\\\dot{r}\\\dot{\psi}_1\\\dot{\psi}_2\end{Bmatrix}=\begin{bmatrix}a_{11}&a_{12}&a_{13}&a_{14}\\a_{21}&a_{22}&a_{23}&a_{24}\\a_{31}&a_{32}&a_{33}&a_{34}\\a_{41}&a_{42}&a_{43}&a_{44}\end{bmatrix}\begin{Bmatrix}v\\r\\\psi_1\\\psi_2\end{Bmatrix}+\begin{Bmatrix}b_1\\b_2\\b_3\\b_4\end{Bmatrix}\delta \tag{4.55}$$

where, ψ_1 and ψ_2 are given in (4.46) and (4.47).

and,

$$a_{11}=\frac{I_{xx}}{A\cdot U}\left(C_f+C_r\right) \tag{4.56}$$

$$a_{12}=\frac{I_{xx}}{A\cdot U}\left(a\cdot Cf-b\cdot Cr\right)-U \tag{4.57}$$

$$a_{13}=\frac{M_s\cdot h_s\cdot C_\phi}{A} \tag{4.58}$$

$$a_{14}=-\frac{M_s^2\cdot h_s^2\cdot g}{A}+\frac{M_s\cdot h_s\cdot K_\phi}{A} \tag{4.59}$$

$$a_{21}=\frac{a\cdot C_f-b\cdot C_r}{U\cdot I_{zz}} \tag{4.60}$$

$$a_{22}=\frac{a^2\cdot C_f+b^2\cdot C_r}{U\cdot I_{zz}} \tag{4.61}$$

$$a_{23}=0 \tag{4.62}$$

$$a_{24} = 0 \tag{4.63}$$

$$a_{31} = -\frac{M_s \cdot h_s}{A \cdot U}\left(C_f + C_r\right) \tag{4.64}$$

$$a_{32} = \frac{M_s \cdot h_s}{A \cdot U}\left(-a \cdot C_f + b \cdot C_r\right) \tag{4.65}$$

$$a_{33} = -\frac{M \cdot C_\phi}{A} \tag{4.66}$$

$$a_{34} = \frac{M\left(M_s \cdot g \cdot h_s - K_\phi\right)}{A} \tag{4.67}$$

$$a_{41} = 0 \tag{4.68}$$

$$a_{42} = 0 \tag{4.69}$$

$$a_{43} = 1 \tag{4.70}$$

$$a_{44} = 0 \tag{4.71}$$

$$b_1 = -\frac{I_{xx} \cdot C_f}{A} \tag{4.72}$$

$$b_2 = -\frac{a \cdot C_f}{I_{zz}} \tag{4.73}$$

$$b_3 = \frac{M_s \cdot h_s \cdot C_f}{A} \tag{4.74}$$

$$b_4 = 0 \tag{4.75}$$

and

$$A = M \cdot I_{xx} - M_s^2 \cdot h_s^2 \tag{4.76}$$

4.2.5. TIRE MODELING

Modeling of the tire accurately is important for vehicle dynamics studies since it provides the connection of vehicle with the road. Dynamics of the tire is very complex, and thus modeling of the dynamics of the tire is difficult. In the literature

there are plenty of studies about modeling of the tire some of which are physical and some of them are empirical.

At small slip angle cornering forces produced by the tire are linearly related to slip angles and a linear tire model can be used. However, when the slip angle increases the linear tire characteristics start to saturate and the tire forces depend on various parameters and slip angle nonlinearly. In this case, nonlinear tire models are used and operating range of the tires widens. In this study two tire models which are linear tire model and Magic Formula tire model are used for identification purposes, and an advanced version of the Magic Formula tire model in ADAMS tire models (PAC 2002 [8]) is used for simulations in ADAMS/Chassis.

Linear tire model is the most simple tire model. This tire does not consider the effects of the variation of cornering force with the load on the tire and this model assumes linear relationship between slip angle and cornering force. This model is valid for small slip angle.

4.2.5.1. MAGIC FORMULA TIRE MODEL

Magic Formula tire model is a semi empirical tire model which is used to generate steady state tire force and moment characteristic. Magic formula tire model produces force and moment characteristic at pure slip conditions; that is pure cornering and pure traction or braking. By an extension to pure slip conditions, combined force characteristic can be obtained. According to Magic Formula tire model the cornering force is given by the expression [32],

$$y(x) = D \cdot \sin[C \cdot \arctan\{B \cdot x - E(B \cdot x - \arctan(B \cdot x))\}] \qquad (4.77)$$

where,

$$Y(X) = y(x) + S_v \qquad (4.78)$$

$$x = X + S_h \tag{4.79}$$

The formula produces characteristic of the tire for cornering force F_y, longitudinal force F_x and aligning force M_z as a function of the longitudinal slip and lateral slip.

Meaning of the some factors used in formula for lateral tire force can be explained as:

D: peak factor,

E: curvature factor,

BCD: slope at the origin,

C: shape factor,

B: stiffness factor,

S_v: horizontal shift,

S_h: vertical shift,

These parameters are dependent on the vertical force F_z and the camber angle γ. For lateral force and slip angles these parameters are,

$$C = a_0 \tag{4.80}$$

$$D = a_1 \cdot F_z^2 + a_2 \cdot F_z \tag{4.81}$$

$$BCD = a_3 \cdot \sin(2 \cdot \arctan(F_z / a_4))(1 - a_5 \cdot |\gamma|) \tag{4.82}$$

$$E = a_6 \cdot F_z + a_7 \tag{4.83}$$

$$S_h = a_9 \cdot F_z + a_{10} + a_8 \cdot \gamma \tag{4.84}$$

$$S_v = a_{11} \cdot F_z \cdot \gamma + a_{12} \cdot F_z + a_{13} \tag{4.85}$$

4.2.5.2. DYNAMIC TIRE MODEL

Magic Formula tire model and linear tire model explained in previous sections are valid for steady state conditions. However, when the maneuver is transient or when the steering input is transient, transient properties of the tire has important effect on the outputs of the tire and static tire model cannot produce the correct force characteristic of the tire. Therefore, transient properties of the tire must be modeled. A typical dynamic model for lateral tire force dynamics is first order and is given as [33], [34];

$$\tau \cdot \dot{F}_{y,lag} + F_{y,lag} = F_y \tag{4.86}$$

where, F_y is the tire lateral force obtained from the steady state tire model, $F_{y,lag}$ is the dynamic force and τ is the relaxation time constant. Relaxation time constant can be approximated as,

$$\tau = \frac{C_\alpha}{U \cdot K} \tag{4.87}$$

where K is the tire lateral stiffness, C_α is the cornering stiffness and U is the longitudinal velocity and this tire model is not valid for low longitudinal velocities [35].

CHAPTER 5

SENSITIVITY ANALYSIS

To determine the effects of the parameters on the vehicle dynamics system response, sensitivity analysis should be performed. By sensitivity analysis, synthesis and the identification of the mechanical system can be improved [36]. Information related to where and how the parameters affect the system response is crucial for identification studies since the domain of the identification can be determined by sensitivity analysis. Therefore sensitivity analysis must be performed prior to identification.

Sensitivity analysis can be performed in time and in frequency domain. In time domain, sensitivity of the state variables to parameters is the aim and in the frequency domain sensitivity of the transfer function to parameters is aimed. Generally in the frequency domain sensitivity of the amplitude and phase of the transfer function to parameters are examined instead of complex valued transfer function directly. Sensitivity analysis in time domain is difficult since it depends on the type and the shape of the excitation [36].

In this study sensitivity analysis is performed in frequency domain to be able to determine the frequencies or frequency ranges at which the system responses are most sensitive. In this study, sensitivities of the amplitudes of the lateral velocity transfer function and yaw velocity transfer function to bicycle model parameters are obtained. Then sensitivity analysis will be performed for three DOF linear roll

model. Sensitivities of the yaw, lateral, and the roll velocities to roll model parameters are calculated.

Logarithmic sensitivity of the variable v to parameter θ can be calculated as [36],

$$S_{v,p} = \frac{\partial v}{\partial \theta} \frac{\theta}{v} \tag{5.1}$$

Logarithmic sensitivity function is dimensionless and thus influence of various parameters on the variables can be found easily. However, it gives the sensitivity of the absolute value of the variable to parameter rather than the real value. That is when the sensitivity value is negative, an increase in the parameter value results in a decrease in the absolute value of the variable. When the sensitivity value is positive, an increase in the parameter value results in an increase in the absolute value of the variables. Also as can be understood from Equation 5.1, when value v approaches zero, sensitivity value may become too large [36].

In this study sensitivities of the amplitude of the transfer function with respect to parameters are examined and sensitivity analysis is performed for bicycle model and three DOF linear roll model in frequency domain. Transfer function of this model can be obtained from their state space model as,

$$[T(s)] = [C]\left(s[I]-[A]\right)^{-1}[B]+[D] \tag{5.2}$$

Explicit form of the bicycle model and roll model transfer function are obtained from the MATLAB Symbolic Toolbox using (5.2).

5.1. BICYCLE MODEL SENSITIVITY ANALYSIS

In the two DOF bicycle model, there are two states which are lateral velocity and yaw velocity. Sensitivities of the lateral and yaw velocities to bicycle model

parameters are calculated as a function of the frequency and longitudinal velocity and the results are given in Figure 5.1 to Figure 5.6. Sensitivity of lateral and yaw velocity to other bicycle model parameters are given in Appendix A.

Sensitivity of Lateral Velocity to Cf vs Frequency, Longitudinal Velocity
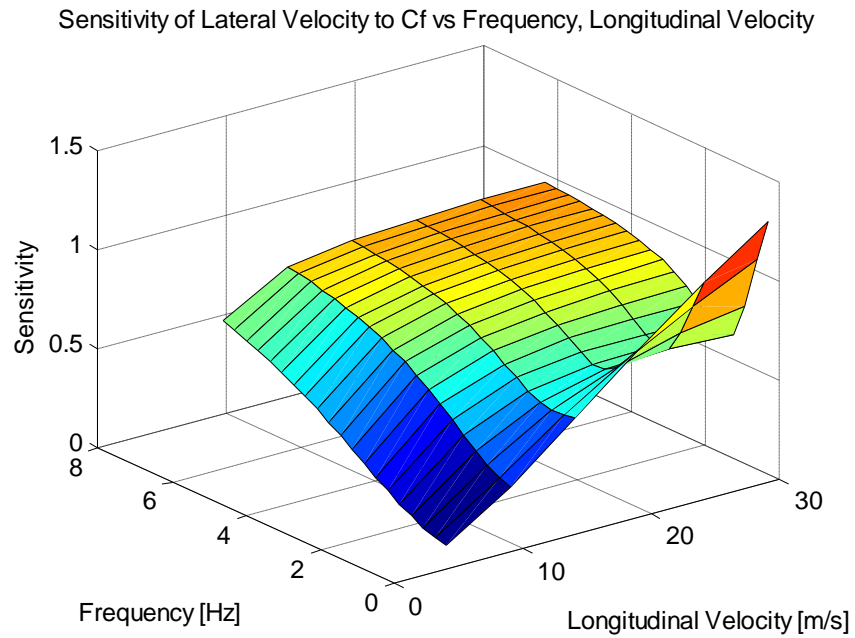
Figure 5.1: Sensitivity of lateral velocity to C_f
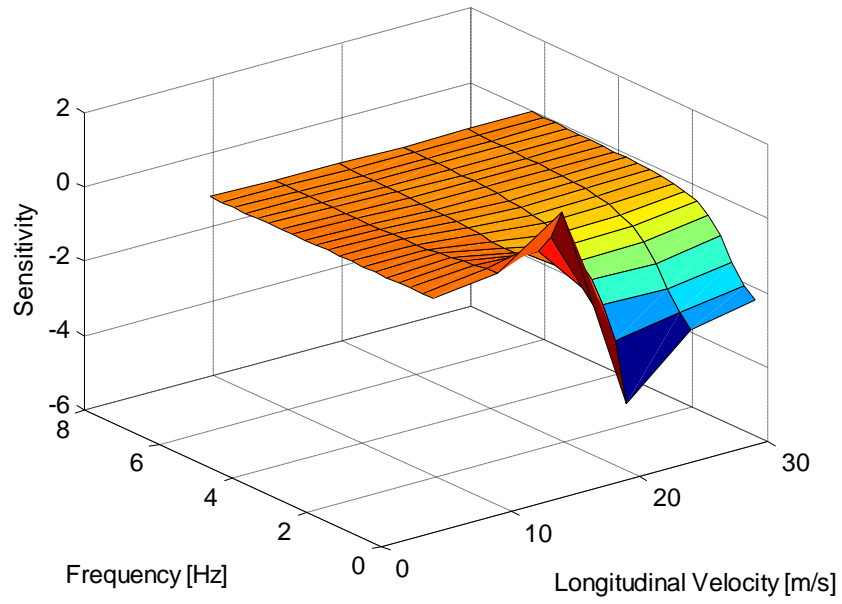
Figure 5.2: Sensitivity of lateral velocity to C$_r$

Figure 5.3: Sensitivity of lateral velocity to J

As observed from Figure 5.3 sensitivity of the lateral velocity to yaw moment of inertia increases starting from 0 Hz and decreases after nearly 2 Hz, and it reaches a peak around 1 Hz. Sensitivity of the lateral velocity to front cornering stiffness is high nearly at all frequencies and slightly decreases around 1 Hz. Sensitivity of lateral velocity to rear cornering stiffness is high between 0 and 1 Hz. Moreover, as observed from Figure 5.7 amplitude of the lateral velocity has a peak value between 0 and 2 Hz. Also longitudinal velocity has an important effect on the sensitivity values and lateral velocity amplitude and when it is increased, amplitude of the lateral velocity increases.
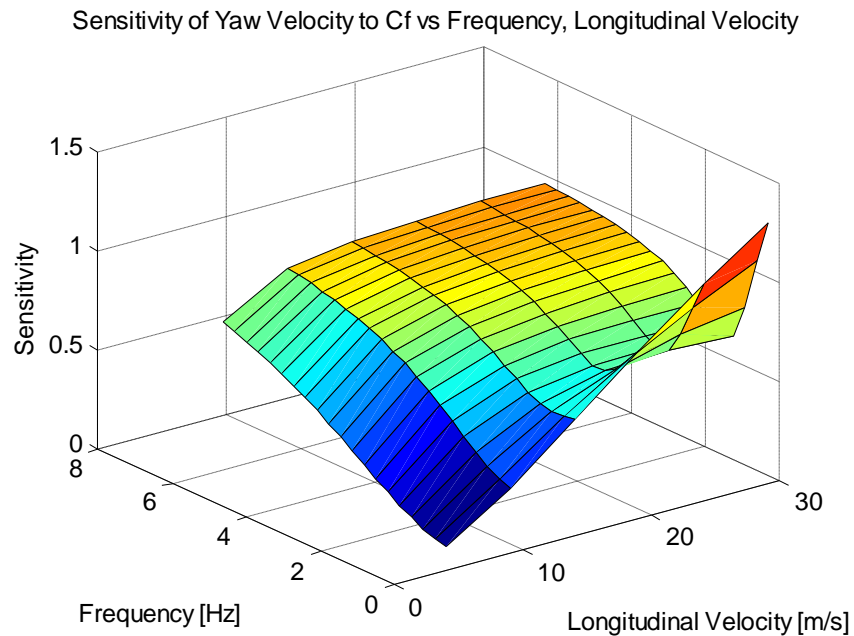
Figure 5.4: Sensitivity of yaw velocity to C_f

Sensitivity of Yaw Velocity to Cr vs Frequency, Longitudinal Velocity
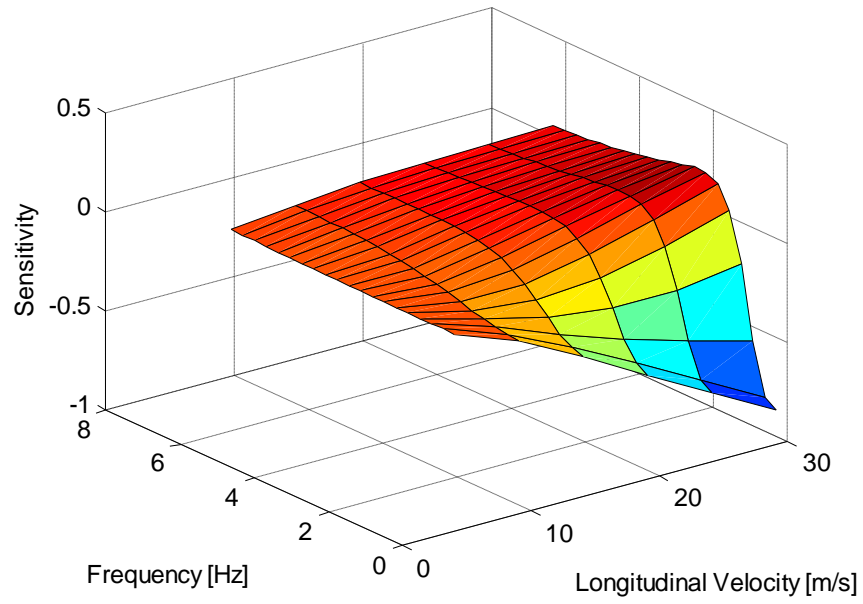
Figure 5.5: Sensitivity of yaw velocity to C_r

Sensitivity of Yaw Velocity to J vs Frequency, Longitudinal Velocity
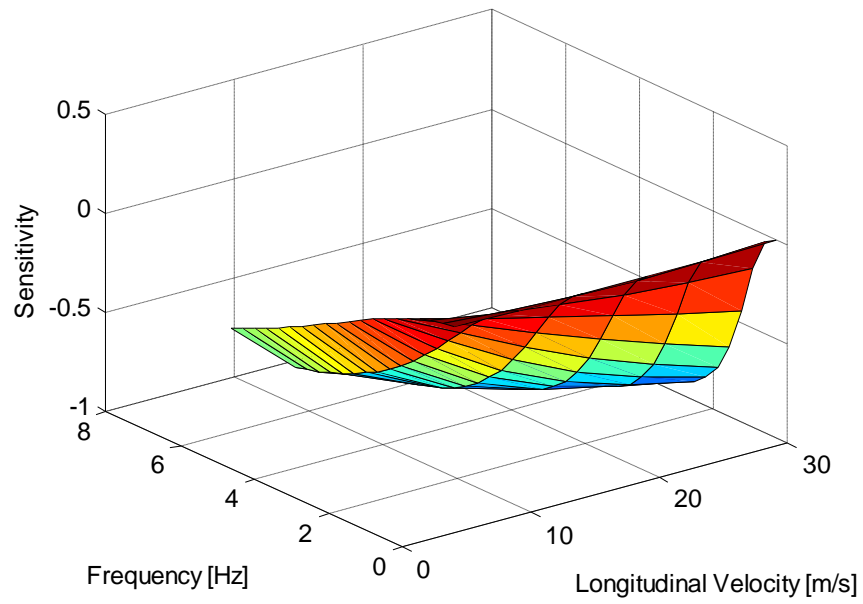
Figure 5.6: Sensitivity of yaw velocity to J

When Figure 5.4 is examined it is seen that yaw velocity is sensitive to front cornering stiffness nearly at all frequencies. When Figure 5.5 is examined, it can be seen that again yaw velocity is more sensitive to rear cornering stiffness below nearly 2 Hz. However, sensitivity of the yaw velocity to yaw moment of inertia increases starting from the 1 Hz. Also, similar to lateral velocity data, amplitude of the yaw velocity increases with increasing longitudinal velocity and is high between 0 and 2 Hz as can be seen from Figure 5.8.
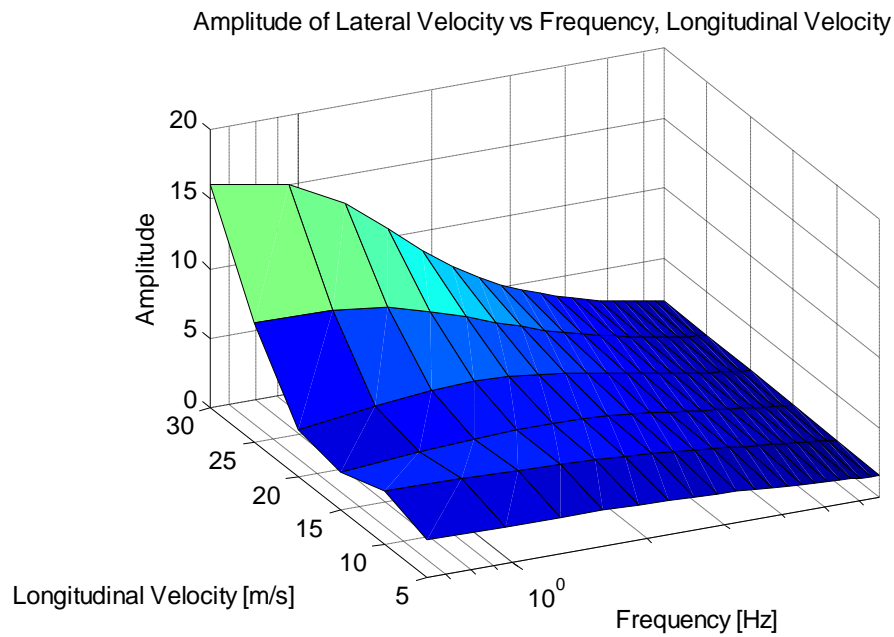
Figure 5.7: Amplitude of the lateral velocity
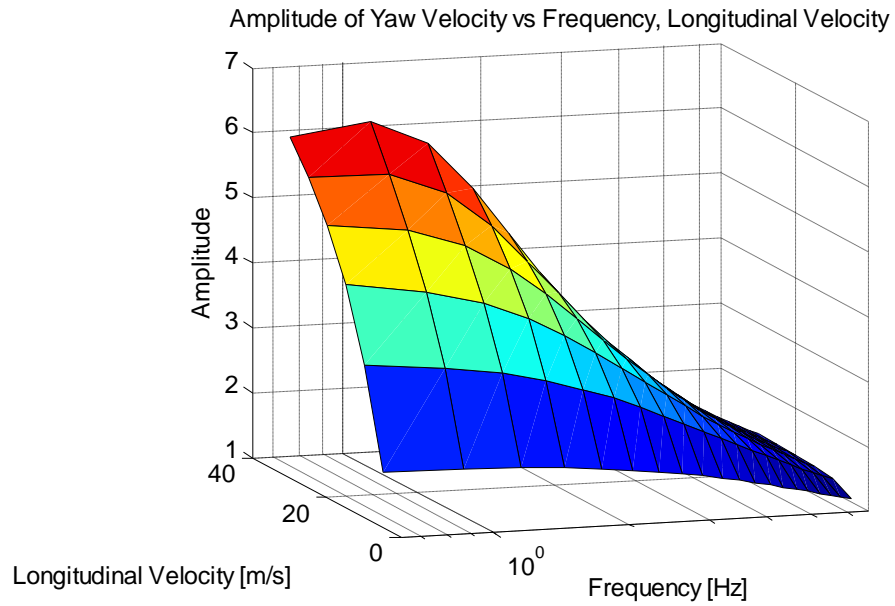
Figure 5.8: Amplitude of the yaw velocity

5.2. THREE DEGREE OF FREEDOM ROLL MODEL SENSITIVITY ANALYSIS

In the three DOF roll model sensitivities of the lateral, yaw, and the roll velocities to roll model parameters are calculated as a function of the frequency and longitudinal velocity and the results are given in Figure 5.9 to Figure 5.26. Sensitivity of lateral, yaw and roll velocity to other roll model parameters are given in Appendix A.
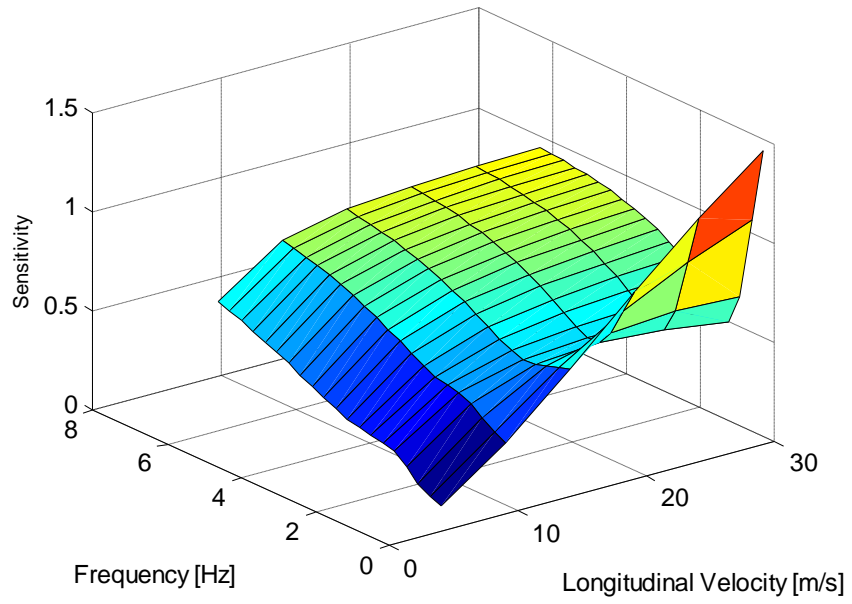
Figure 5.9: Sensitivity of lateral velocity to C_f
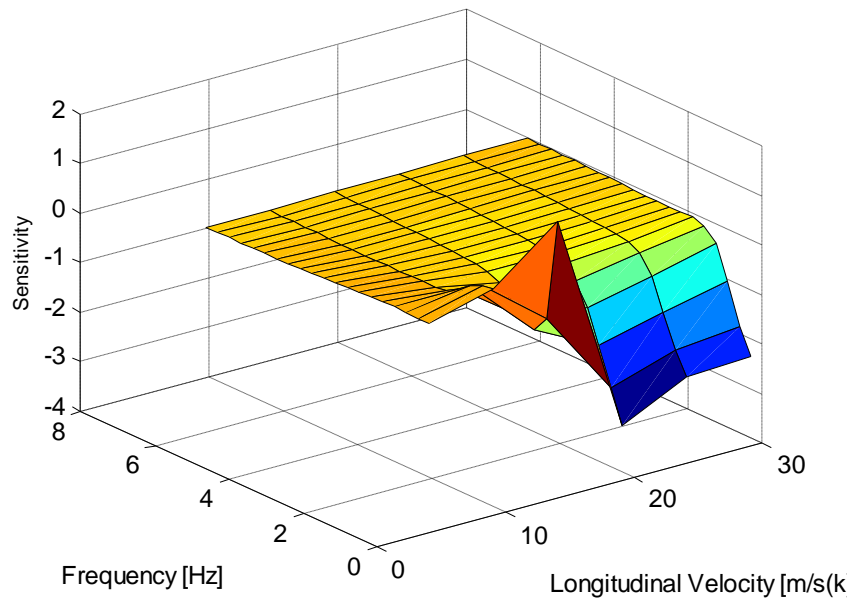
Figure 5.10: Sensitivity of lateral velocity to C_r

Sensitivity of Lateral Velocity to Izz vs Frequency, Longitudinal Velocity
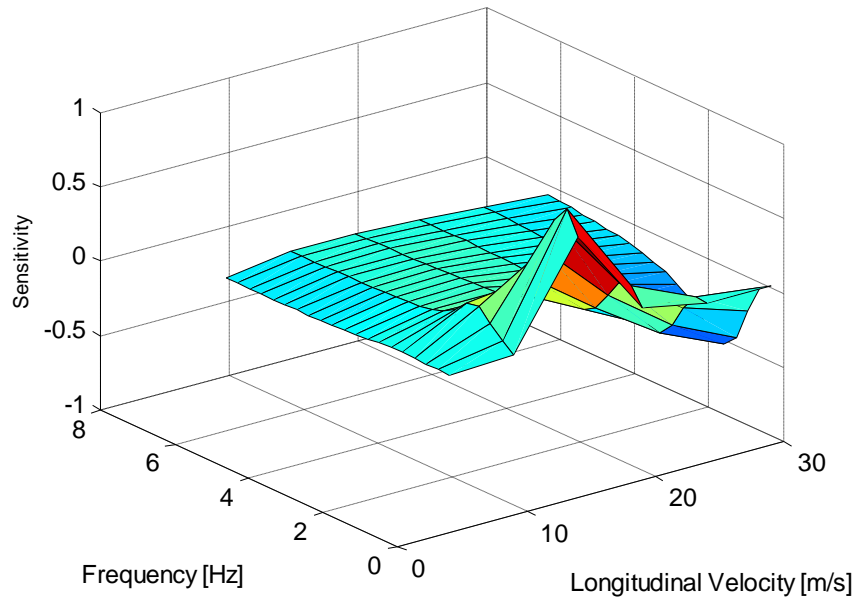
Figure 5.11: Sensitivity of lateral velocity to I$_{zz}$

Sensitivity of Lateral Velocity to Ixx vs Frequency, Longitudinal Velocity
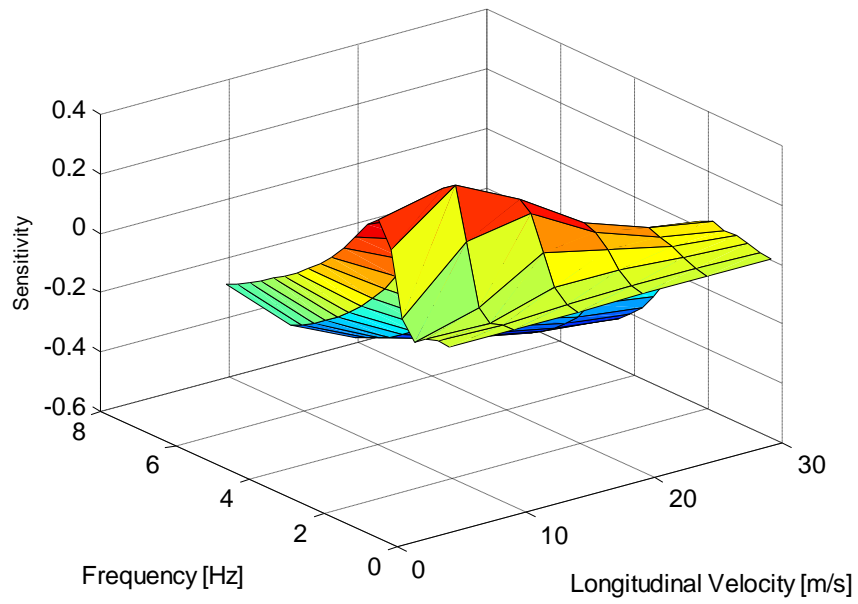
Figure 5.12: Sensitivity of lateral velocity I$_{xx}$

Sensitivity of Lateral Velocity to Kphi vs Frequency, Longitudinal Velocity
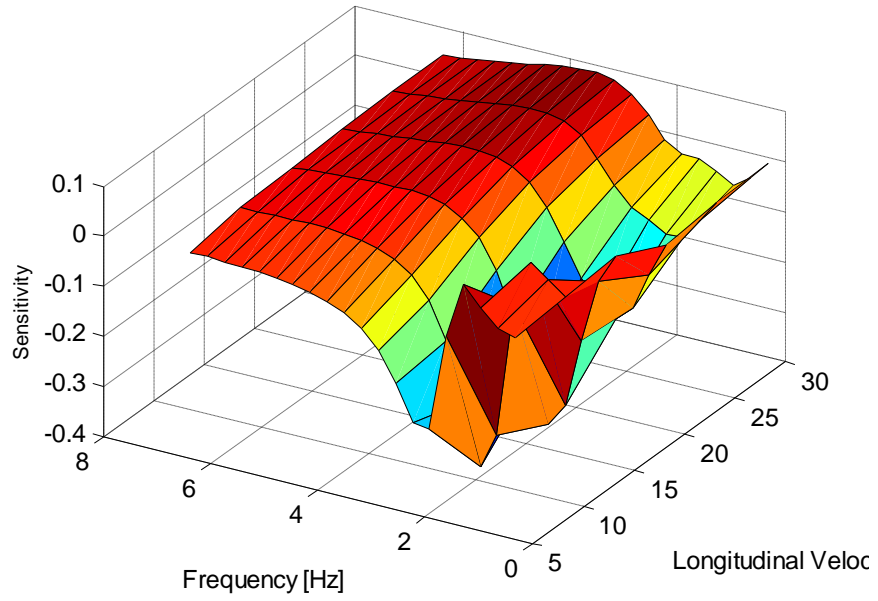
Figure 5.13: Sensitivity of lateral velocity to K$_\varphi$

Sensitivity of Lateral Velocity to Cphi vs Frequency, Longitudinal Velocity
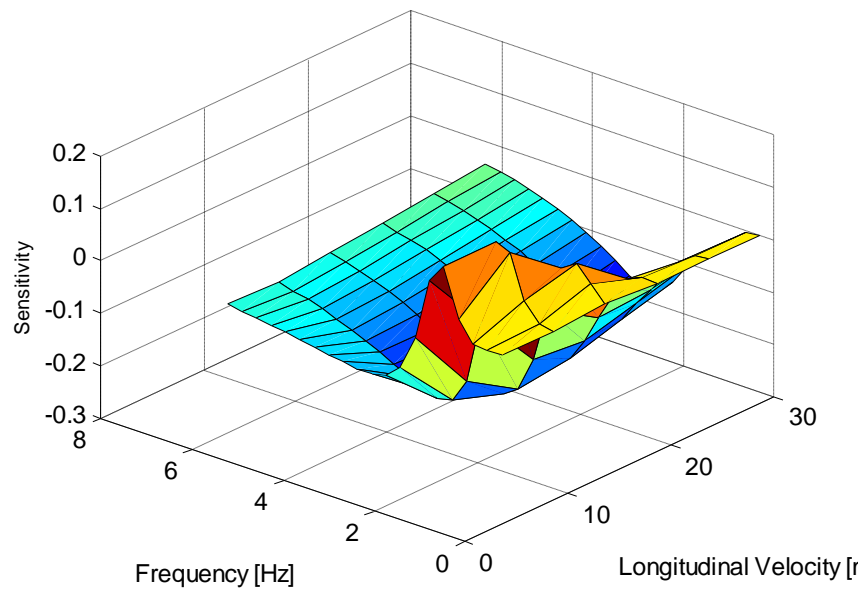
Figure 5.14: Sensitivity of lateral velocity to C$_\varphi$

82

Sensitivity of Yaw Velocity to Cf vs Frequency, Longitudinal Velocity
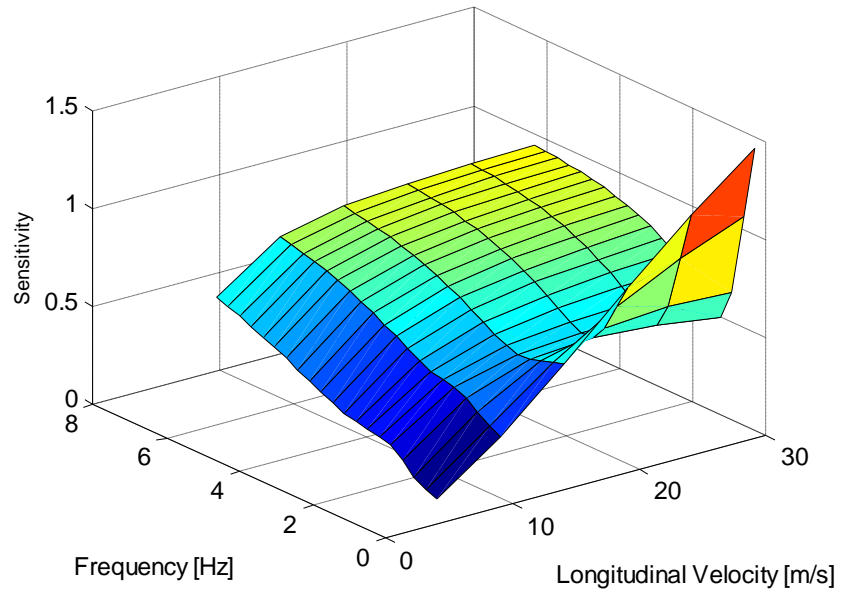
Figure 5.15: Sensitivity of yaw velocity to C$_f$,

Sensitivity of Yaw Velocity to Cr vs Frequency, Longitudinal Velocity
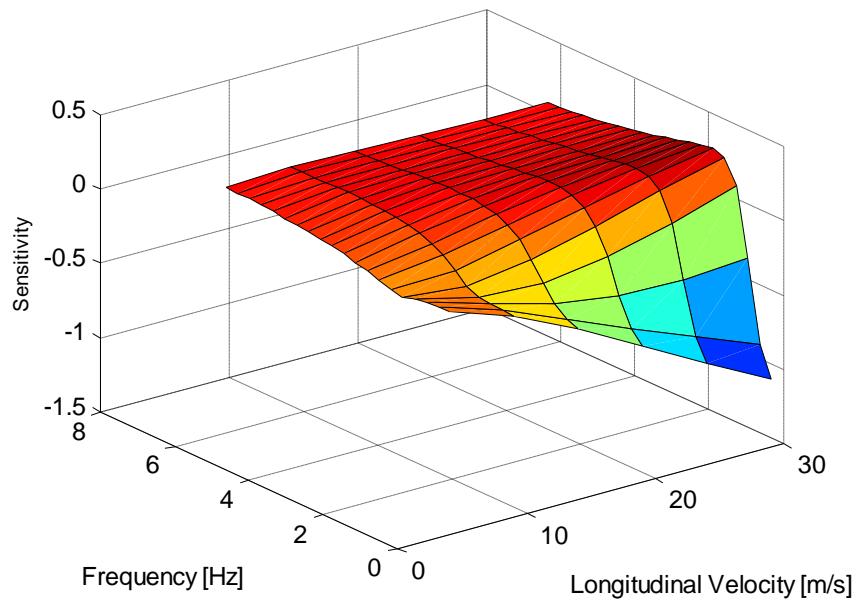
Figure 5.16: Sensitivity of yaw velocity to C$_r$

Figure 5.17: Sensitivity of yaw velocity to I$_{zz}$

Figure 5.18: Sensitivity of yaw velocity I$_{xx}$

84

Sensitivity of Yaw Velocity to Kphi vs Frequency, Longitudinal Velocity

Figure 5.19: Sensitivity of yaw velocity to K$_\varphi$

Sensitivity of Yaw Velocity to Cphi vs Frequency, Longitudinal Velocity
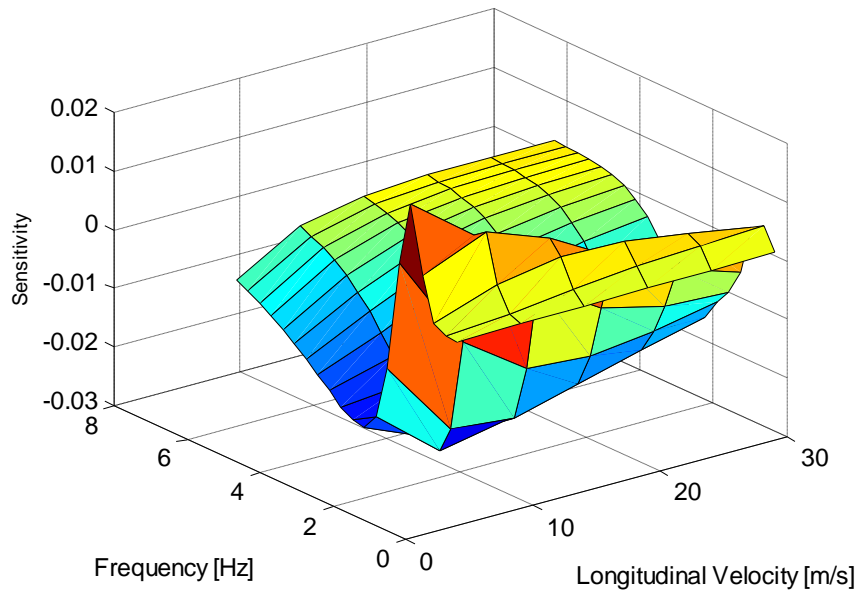
Figure 5.20: Sensitivity of yaw velocity to C$_\varphi$

Sensitivity of Roll Velocity to Cf vs Frequency, Longitudinal Velocity
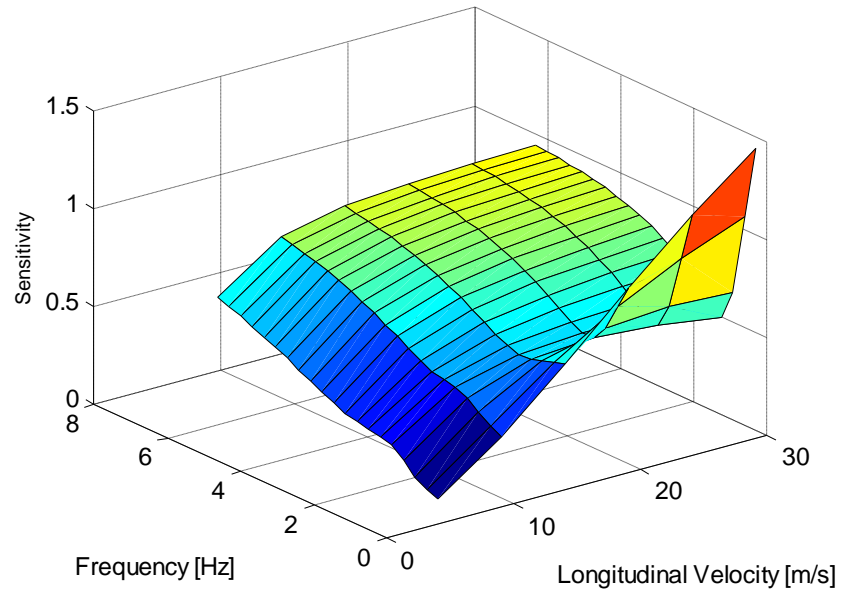
Figure 5.21: Sensitivity of roll velocity to C$_f$

Sensitivity of Roll Velocity to Cr vs Frequency, Longitudinal Velocity
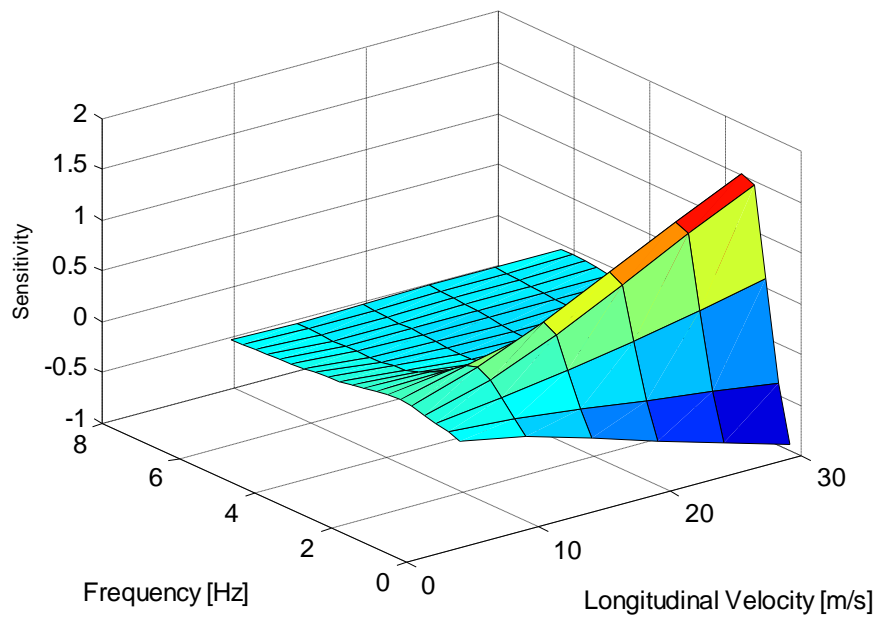
Figure 5.22: Sensitivity of roll velocity to C$_r$

Figure 5.23: Sensitivity of roll velocity to I$_{zz}$

Figure 5.24: Sensitivity of roll velocity I$_{xx}$

87

Figure 5.25: Sensitivity of roll velocity to K_φ

Figure 5.26: Sensitivity of roll velocity to C_φ

Figure 5.27: Amplitude of lateral velocity

Figure 5.28: Amplitude of yaw velocity

89
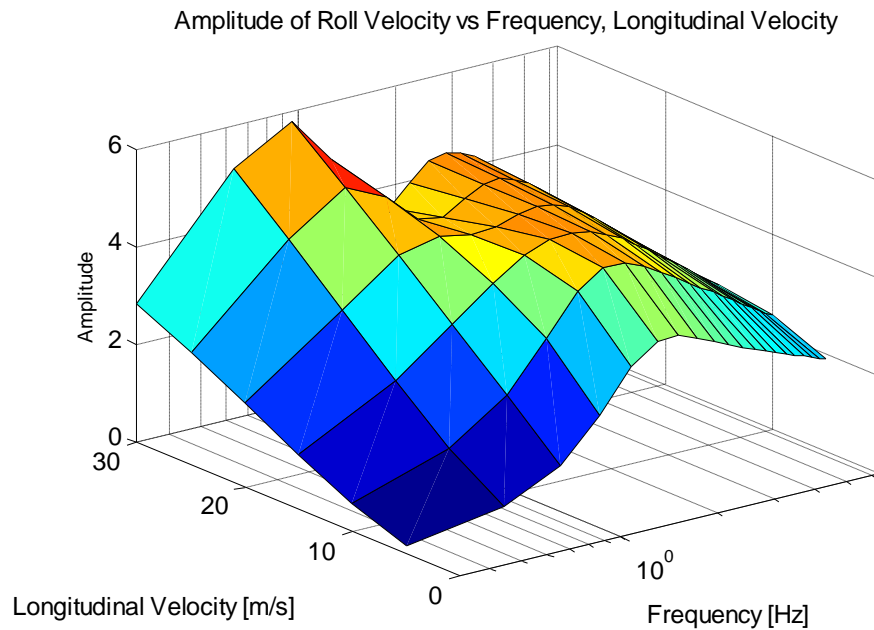
Figure 5.29: Amplitude of roll velocity

For the three DOF roll model, sensitivity of lateral velocity to rear cornering stiffness is high below 1 Hz. As opposed to lateral velocity and yaw velocity, roll velocity are highly sensitive to nearly all parameters. Sensitivities of the roll velocity to cornering stiffness values, roll stiffness, roll damping, and yaw moment of inertia and roll moment of inertia are high between nearly 0 and 3 Hz and. Also, amplitude of the lateral, yaw and roll velocities decrease after 2 Hz and increase with longitudinal velocity. As can be seen from the sensitivity plots, longitudinal velocity is highly effective on the sensitivities and generally an increase in velocity results in an increase in the sensitivity values.

In addition to specifying appropriate steering input frequency and vehicle longitudinal velocity, practical aspects of the identifiability can be interpreted. That is to say some responses may become insensitive to parameters and thus this parameter may not be identified from that response accurately. As can be observed from Figure 5.18, Figure 5.19, and Figure 5.20 sensitivity of the yaw velocity to roll

stiffness, roll damping, and roll moment of inertia are very low, which means that the dependence of yaw velocity to those parameters is not significant.

In summary, it is possible to specify the parameter set which can be estimated, and the appropriate frequency or frequency interval and longitudinal velocity are selected. For instance in the three DOF linear roll model, roll stiffness cannot be estimated from yaw velocity data accurately since sensitivities of the yaw velocity to roll stiffness is low. As another example, in the bicycle model sensitivity of the lateral velocity to rear cornering stiffness is high for the frequency range of 0-2 Hz nearly and thus input should cover this frequency interval for accurate estimation. In this study, frequency range of the steering input is taken as the 0-2 Hz and the longitudinal velocity of the vehicle is taken as 20 m/s. For the nonlinear roll model, ADAMS model is simulated at 15 m/s longitudinal velocity to obtain appropriate slip angle characteristic. These values change with the nominal values of the test vehicle, yet the general shape of the sensitivity curves and the approximate sensitivity values give valuable information. As a result, it is possible to specify handling model parameters which can be identified practically and the characteristics of the test input can be determined.

CHAPTER 6

IDENTIFIABILITY STUDY AND VEHICLE IDENTIFICATION

Identifiability problem is related to the model structure and it investigates whether the model parameters can be estimated uniquely from the noise free data. It is important for system identification and it should be performed prior to experiments and according to the result of the identifiability study, experiment design and model selection processes are performed. For model structures that cannot be identified, experiments can be redesigned and extra data can be acquired to make the model identifiable. Additional inputs and/or outputs can be acquired or places of the sensors can be changed. Structural identifiability method used in this study is adapted from the study of Walter and Pronzato [37] and can be summarized as:

- Parameter θ_i is structurally globally identifiable (s.g.i) if,

$$M(\hat{\vec{\theta}}) = M(\vec{\theta}^*) \Rightarrow \hat{\theta}_i = \theta^*_i \tag{6.1}$$

If all parameters of the model structure are s.g.i, then the model structure M is s.g.i.

- The parameter θ_i is structurally locally identifiable (s.l.i) if there is a neighborhood such that $M(\hat{\vec{\theta}}) = M(\vec{\theta}^*) \Rightarrow \hat{\theta}_i = \theta^*_i$

If all parameters of the model structure are s.l.i, then the model structure is s.l.i

- The parameter θ_i is structurally unidentifiable (s.u.i) if there is no neighborhood of θ^* such that $M(\hat{\vec{\theta}}) = M(\vec{\theta}^*) \Rightarrow \hat{\theta}_i = \theta^*_i$

If at least one parameter of the model structure is s.u.i, then the model structure is s.u.i.

where $\hat{\theta}$ is the estimate of parameter θ, θ^* is the true value of parameter θ and M is the model structure.

Identifiability study must be performed prior to experiment and the experiment should be designed according to result of it. Model identifiability is a prerequisite for system identification, yet it does not guarantee accurate parameter estimation. However, even if the model is unidentifiable, error between acquired and estimated data may become small and in different identification different parameter sets may be identified.

There are various methods for checking model identifiability and some of these methods are specified for certain types of model structures. Analytical identifiability techniques are difficult to perform when the model is nonlinear and it contains a large number of parameters. In this study, identifiability of the handling models are examined by Numerical Local Approach adapted from [37]. Moreover, identifiability of the model can also be examined as stated in [38]: Firstly model to be identified is simulated with nominal parameters and the simulation data is treated as actual test data. Then model is identified by using initial parameter values which are slightly different than nominal values. If the model is identifiable convergence is achieved in a few iterations. If the convergence is not satisfied or if the number of iterations is high, model may be unidentifiable. Numerical Local Approach was also used in the study [11] to examine the coupled roll and lateral dynamics.

Numerical Local Approach [37]

There are various approaches [37] for checking structural identifiability. In these approaches, algebraic ones require high computational power and so they are difficult. Numerical Local Approach can be used to check model identifiability at least locally. Application steps of this method are [37];

- Produce fictitious data by simulating model $M(\theta_0)$ with nominal parameter value θ_0.

- Estimate parameter θ from simulated fictitious data by minimizing the quadratic cost function between acquired simulation data and output of model to be identified. This minimization is performed by second order optimization methods such as Gauss-Newton method. Set initial parameter values used in estimation to nominal parameter values, θ_0.

- If the estimated parameters remains stable at θ_0 then model M is s.l.i, if estimator remains unstable then model M is s.u.i. or θ_0 is close to a hyper surface so the matrices inverted during the optimization is singular. For this another parameter θ_0 is used to generate fictitious data and the other steps are repeated and a conclusion about identifiability of the model is reached.

Note that as specified in [37] Levenberg-Marquardt approach cannot be used for this method since it includes regularization.

In this study identifiability of the model structure is examined by these two approaches. Schematic of the Numerical Local Approach for handling model identification is shown in Figure 6.1.
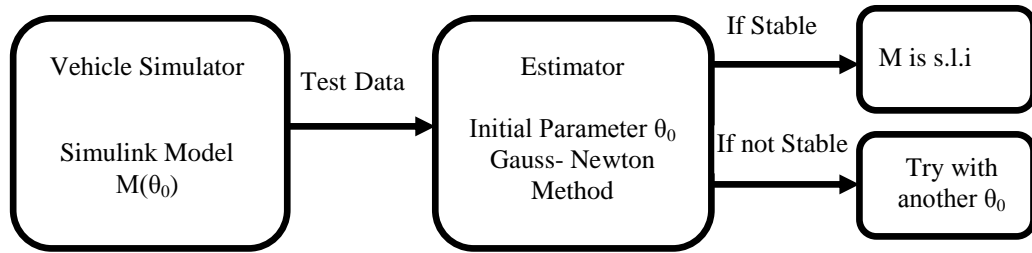
Figure 6.1: Numerical Local Approach for handling model identification

In this study test data is obtained from the simulation of the Simulink vehicle models $M(\theta_0)$ with nominal parameters θ_0. Cost function for the estimation process is obtained from the Simulink. Optimization process is performed by MATLAB function 'lsqnonlin' with Gauss-Newton algorithm nested in MATLAB M-File. Therefore, optimization is performed by interaction of Simulink model and MATLAB M-File.

Simulation data for the bicycle model, one DOF roll model, and the three DOF linear roll model are acquired with the nominal parameters listed in Table 6.1. Nominal parameter values used in the simulation for nonlinear roll model are given in Table 6.2.

Table 6.1: Nominal parameter values used in the simulation of linear models for structural identifiability study

C_f=-80000 N/rad	C_r=-70000 N/rad	I_{zz}=1700 kgm^2	I_{xx}=400 kgm^2
C_φ=3000 Nms	K_φ=40000 Nm	τ=0.025 s	

Table 6.2: Nominal parameter values used in the simulation of nonlinear models for structural identifiability study

I_{zz}=1700 kgm^2	I_{xx}=400 kgm^2	C_φ=3000 Nms	K_φ=40000 Nm	τ=0.025s
a_0=1.3	a_1=-50	a_2=900	a_3=40000	a_4=3
a_6=-0.70	a_7=-0.30	$\delta_{f\varphi}$= 0.1	$\delta_{r\varphi}$=0.1	

6.1. IDENTIFIABILITY OF THE BICYCLE MODEL WITH A STEADY STATE TIRE MODEL

Identifiability of the bicycle model with a steady state tire model is examined separately for different output sets; namely lateral velocity, yaw velocity, and both lateral and yaw velocity.

- *Identifiability with lateral velocity*

According to result of Numerical Local Approach, bicycle model with parameters C_f, C_r, and I_{zz} is s.l.i with the lateral velocity output. Estimated parameters converge to their nominal values. Output of the estimation is given in Figure 6.2.

```
                                                      Directional
 Iteration  Func-count     Residual      Step-size     derivative
     0             4     1.27785e-006
     1            11        1.24e-006            1        2.2e-016
Optimization terminated: directional derivative along
 search direction less than TolFun and infinity-norm of
 gradient less than 10*(TolFun+TolX).

Cf =

 -7.9993e+004


Cr =

 -6.9998e+004


Izz =

  1.7001e+003

>>
```

Figure 6.2: Output of the bicycle model identifiability study with parameters
C_f, C_r, and I_{zz} with lateral velocity

- *Identifiability with yaw velocity*

Similar to identifiability of the bicycle model with lateral velocity bicycle model with parameters C_f, C_r, and I_{zz} is s.l.i with yaw velocity output.

- *Identifiability with lateral and yaw velocity*

The bicycle model with parameters C_f, C_r, and I_{zz} is s.l.i with lateral velocity and yaw velocity separately; it is also s.l.i with both outputs. That is analytically one of the output can be used to identify three parameter (C_f, C_r, and I_{zz}). However, this does not guarantee accurate parameter estimation as will be shown in parameter estimation section.

When the mass of the vehicle is also assumed to be among the unknown parameters to be estimated, estimator is unstable and estimated parameters converge to other

97

values. Instability of the estimator is specified with the term 'ill-conditioned'. In other words matrix cannot be inverted in the Gauss-Newton algorithm. Thus, optimization algorithm is automatically changed to Levenberg Marquardt algorithm which regularizes ill-conditioned matrix. Identifiability result is given in Figure 6.3. Therefore, bicycle model with parameters C_f, C_r, I_{zz}, and M is structurally unidentifiable (s.u.i).

```
                                                    Directional
  Iteration   Func-count      Residual      Step-size      derivative
      0            5         0.00115456
      1           14         0.00113962            81        4.46e-015
Iteration matrix ill-conditioned - Switching to LM method.
      2           50         0.00113948      1.49e+007      -1.24e-008
Optimization terminated: directional derivative along
 search direction less than TolFun and infinity-norm of
 gradient less than 10*(TolFun+TolX).

Cf =

 -9.1862e+013


Cr =

 -8.0379e+013


Izz =

  1.9521e+012


M =

  1.1965e+012

>>
```

Figure 6.3: Output of the bicycle model identifiability study with parameters C_f, C_r, I_{zz}, and M with lateral velocity and yaw velocity data.

6.2. IDENTIFIABILITY OF THE BICYCLE MODEL WITH TRANSIENT TIRE MODEL

Similar to the bicycle model with the steady state tire model, identifiability of the bicycle model with the transient tire model with parameters C_f, C_r, I_{zz}, and τ can be

examined by using output lateral velocity, yaw velocity, and both lateral and yaw velocity.

The bicycle model with parameters C_f, C_r, I_{zz}, and τ is s.l.i with lateral velocity, yaw velocity and both lateral and yaw velocity.

6.3. IDENTIFIABILITY OF THE ONE DEGREE OF FREEDOM ROLL MODEL

One DOF roll model has three parameters to be identified which are K_φ, C_φ, and I_{xx}. According to the result of the identifiability analysis, one DOF linear roll model is s.l.i. Result is given in Figure 6.4.

```
                                                Directional
  Iteration   Func-count      Residual      Step-size      derivative
      0            4        0.0977398
      1           11        0.0122843          0.999      -2.69e-008
      2           18        0.0122843          0.999      -6.31e-013
      3           25        0.0122843          0.0579     -4.66e-016
Optimization terminated: directional derivative along
 search direction less than TolFun and infinity-norm of
 gradient less than 10*(TolFun+TolX).

Ixx =

  399.7829


Cphi =

  2.9978e+003


Kphi =

  3.9981e+004

>>
```

Figure 6.4: Output of the one DOF roll model identifiability study with parameters I_{xx}, C_φ, and K_φ.

When parameters h_s is also assumed to be unknown, estimator is unstable and estimated parameters converge to values other than nominal values and thus one DOF roll model with parameters I_{xx}, C_φ, K_φ, and h_s is s.u.i. Result of the identifiability is shown in Figure 6.5. The same result for this identifiability study can also be obtained by Laplace Transform Approach [37]:

$$\frac{\Phi(s)}{a_y(s)} = \frac{-\dfrac{M_s h_s}{I_{xx}}}{s^2 + \dfrac{C_\phi}{I_{xx}} s + \dfrac{K_\phi - M_s h_s g}{I_{xx}}} = \frac{a_1}{s^2 + a_2 s + a_3} \tag{6.2}$$

where

$$-\frac{M_s h_s}{I_{xx}} = a_1 \tag{6.3}$$

$$\frac{C_\phi}{I_{xx}} = a_2 \tag{6.4}$$

$$\frac{K_\phi - M_s h_s g}{I_{xx}} = a_3 \tag{6.5}$$

From equations (6.5), (6.6), and (6.7) parameters C_φ, K_φ, and I_{xx} can be identified uniquely.

In study [11] it was shown that one DOF roll model with unknown parameters, C_φ, K_φ, and I_{xx} is structurally globally identifiable.

```
                                                  Directional
  Iteration  Func-count    Residual     Step-size   derivative
      0           5        0.0977398
      1          13        0.0166842            1     1.28e-010
Iteration matrix ill-conditioned - Switching to LM method.
      2          42        0.0166772    3.23e+005     4.24e-006
Optimization terminated: directional derivative along
 search direction less than TolFun and infinity-norm of
 gradient less than 10*(TolFun+TolX).

Ixx =

  2.0854e+011


Cphi =

  1.5641e+012


Kphi =

  2.0854e+013


hs =

  2.1760e+008

>>
```

Figure 6.5: Output of the one DOF roll model identifiability study with parameters I_{xx}, C_φ, K_φ, and h_s

As shown in Figure 6.5, iteration matrix is ill-conditioned and the optimization algorithm is switched to Levenberg Marquardt algorithm and estimated parameters converge to values different than nominal parameters.

6.4. IDENTIFIABILITY OF THE THREE DEGREE OF FREEDOM LINEAR ROLL MODEL

In the three DOF linear roll model the unknown parameters are C_f, C_r, I_{zz}, I_{xx}, C_φ, K_φ, and τ. Identifiability of this model is examined with lateral velocity, yaw velocity and roll velocity outputs. According to result of identifiability study which is shown in Figure 6.6, estimator is stable, parameters converge to their nominal values and three DOF linear roll model is s.l.i.

101

```
                                                   Directional
  Iteration  Func-count    Residual    Step-size   derivative
      0            8      0.00624665
      1           19      0.00618656            1   -5.29e-013
      2           30      0.00618656        0.998   -6.84e-017
      3           41      0.00618656    -6.46e-011  -1.35e-019
No improvement in search direction: Terminating.

Cf =

   4.0000e+004


Cr =

   3.5000e+004


Izz =

   1.7000e+003


Ixx =

   399.9746


Cphi =

   2.9998e+003


Kphi =

   3.9998e+004


Tao =

     0.0250

>>
```

Figure 6.6: Output of the three DOF linear roll model identifiability study with parameters C_f, C_r, I_{zz}, I_{xx}, C_φ, K_φ, and τ

6.5. IDENTIFIABILITY OF THE THREE DEGREE OF FREEDOM NONLINEAR ROLL MODEL

Finally identifiability of the three DOF nonlinear roll model with the parameters K_φ, C_φ, I_{xx}, I_{zz}, τ, a_1, a_2, a_3, a_4, a_6, a_7, $\delta_{\varphi f}$, and $\delta_{\varphi r}$ with lateral, yaw, and roll velocities is examined. Result of the identifiability analysis is given in Figure 6.7. As can be understood from Figure 6.7 estimator is stable and estimated parameters converge to their nominal values and thus three DOF nonlinear roll model is s.l.i.

The same information on the identifiability of the model can be obtained with the other approach [38] that involves the simulation of the model with nominal parameters and then estimation of parameter values by using different initial parameter values than nominal parameters. If the estimation process is performed with a few iterations, model may be identifiable.

Identifiability study is important and it should be done before the experiment and according to result of it experiment configuration can be changed or it may be redesigned. Numerical Local Approach is easier to apply when it compared with the analytical identifiability method.

```
                                              Directional
  Iteration  Func-count   Residual    Step-size    derivative
       0          14    9.13833e-023
Optimization terminated: directional derivative along
 search direction less than TolFun and infinity-norm of
 gradient less than 10*(TolFun+TolX).

a1 =

   -50


a2 =

   900


a3 =

      40000


a4 =

     3


a6 =

   -0.7000


a7 =

   -0.3000


Izz =

      1700


Ixx =

   400


Cphi =

      3000


Kphi =

      40000


Tao =

    0.0250

rollsteerf =

    0.1000

rollsteerr =

    0.1000

>>
```

Figure 6.7: Output of the three DOF nonlinear roll model identifiability study
with parameters K_φ, C_φ, I_{xx}, I_{zz}, τ, a_1, a_2, a_3, a_4, a_6, a_7, $\delta_{\varphi f}$, and $\delta_{\varphi r}$

104

6.6. PARAMETER ESTIMATION

After examining the sensitivity and the identifiability of the handling models, parameter values are to be estimated. Data used for identification are obtained from the simulations of the ADAMS model and the parameters are estimated using Simulink Parameter Estimation Toolbox.

As can be seen from the sensitivity analysis, sensitivities of the lateral velocity, yaw velocity, and roll velocity to parameters are high at a range of frequencies. To cover these frequencies, sine chirp input with 0-2 Hz frequency range is used

Data used for identification is taken from the simulation of the ADAMS vehicle model with a transient PAC 2002 [8] tire model. This tire model is an advanced form of the Magic Formula tire model and it calculates the combined lateral and longitudinal tire forces by considering the transient properties of the tire. Basic handling response data namely lateral, yaw and roll velocity, lateral acceleration and the steering wheel input are acquired as the measured response set. Linear bicycle model, one DOF roll model, three DOF linear and nonlinear roll models are identified from this measured response sets.

For linear models low amplitude steering input is used for acquiring data from ADAMS to satisfy the low lateral acceleration and low slip angle assumption.

For acquiring data following sensors and instruments are assumed to be used:

- Lateral and longitudinal velocity sensor
- Gyro for yaw and roll velocity
- Accelerometer for lateral acceleration
- Steering wheel angle measurement system
- Steering wheel robot

Steering wheel input with the responses lateral, longitudinal, yaw, and roll velocities and lateral acceleration are given in Figure 6.9 to Figure 6.14 and calculated front and rear axle slip angles are given in Figure 6.15 and Figure 6.16. Amplitude of the steering wheel input is 20 degree and frequency range of steering input is 0-2 Hz which covers high sensitivity regions of the outputs to parameters and natural frequencies of the outputs. Longitudinal velocity used in the simulation is 20 m/s. Identified models are validated by using the data taken from the double lane change simulation of the ADAMS model at 20 m/s longitudinal velocity. Steering wheel input and responses acquired from the double lane change analysis are given in Figure 6.17 to Figure 6.22 and calculated front and rear axle slip angles are given in Figure 6.23 and Figure 6.24. Schematic of double lane change analysis is shown in Figure 6.8.
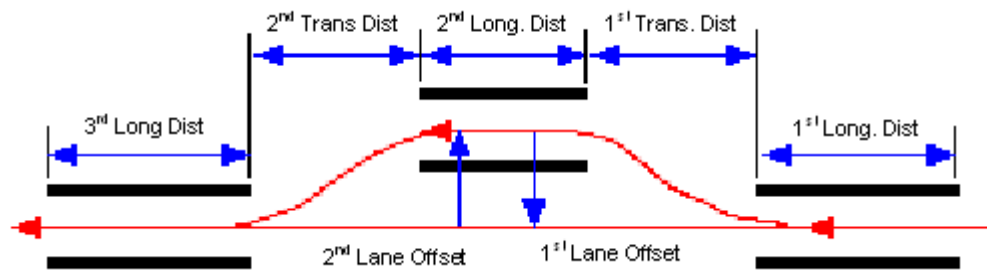
Figure 6.8: Double lane change maneuver [7]

106
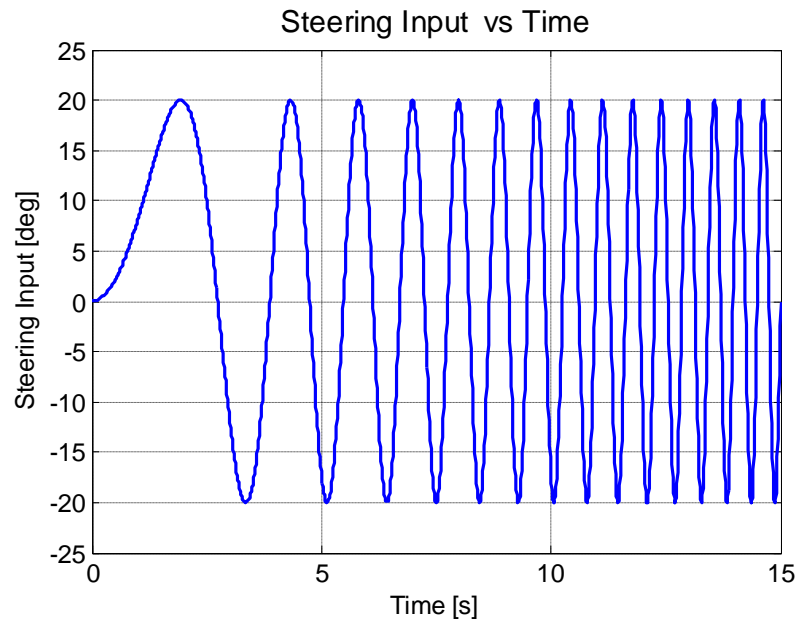
Figure 6.9: Steering wheel input for the estimation process
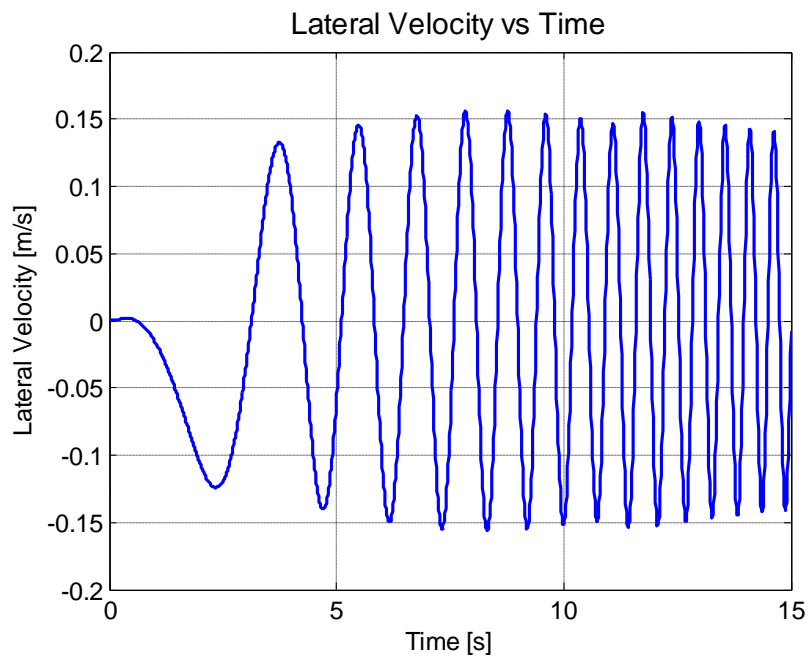
Figure 6.10: Lateral velocity response for the estimation process
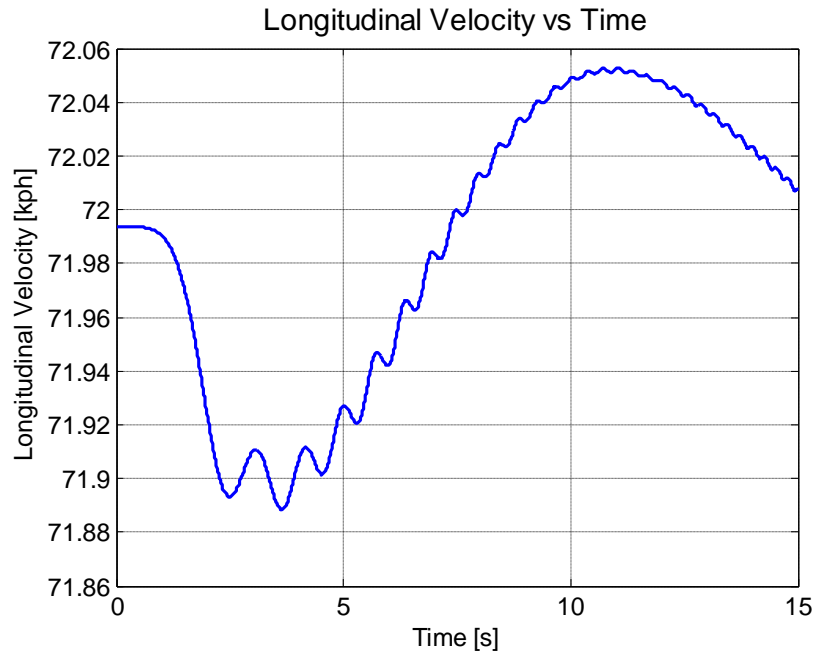
Figure 6.11: Longitudinal velocity response for the estimation process
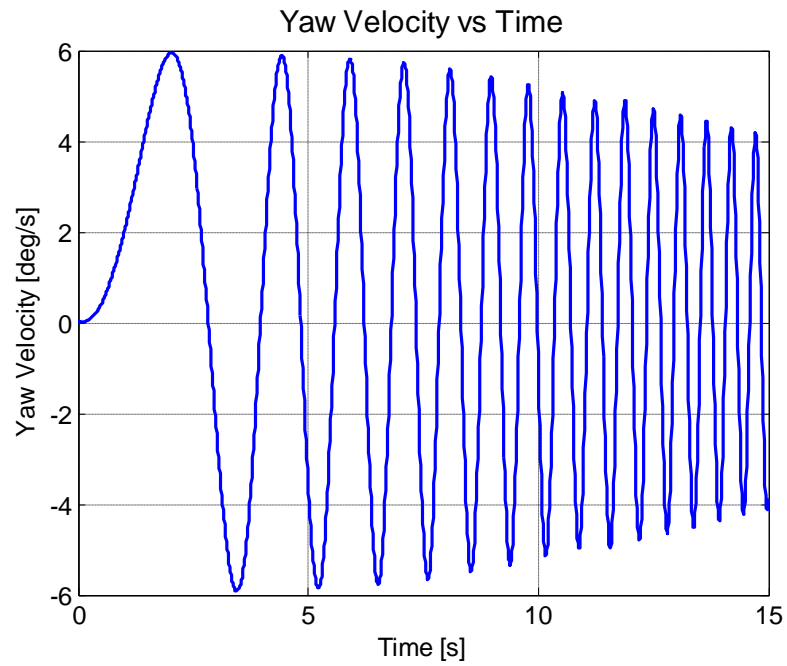
Figure 6.12: Yaw velocity response for the estimation process
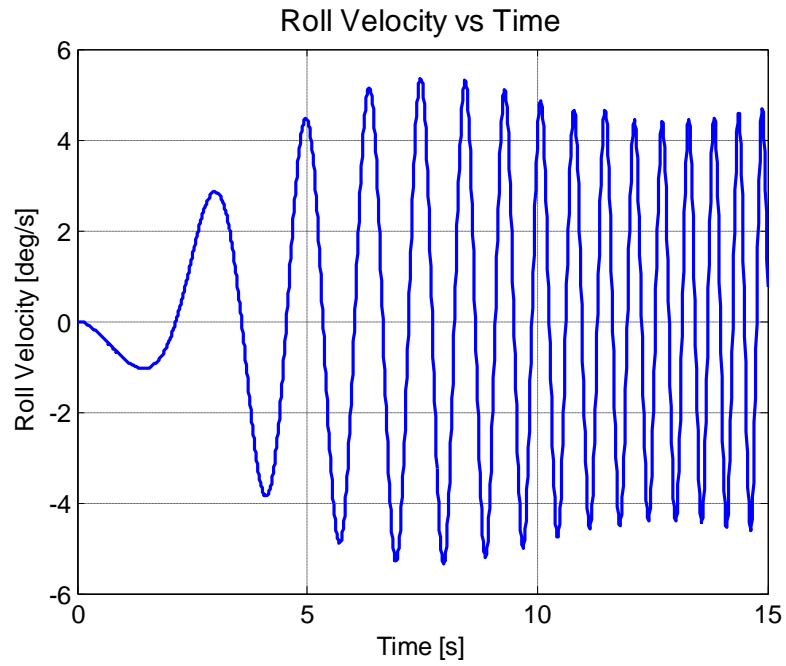
Figure 6.13: Roll velocity response for the estimation process
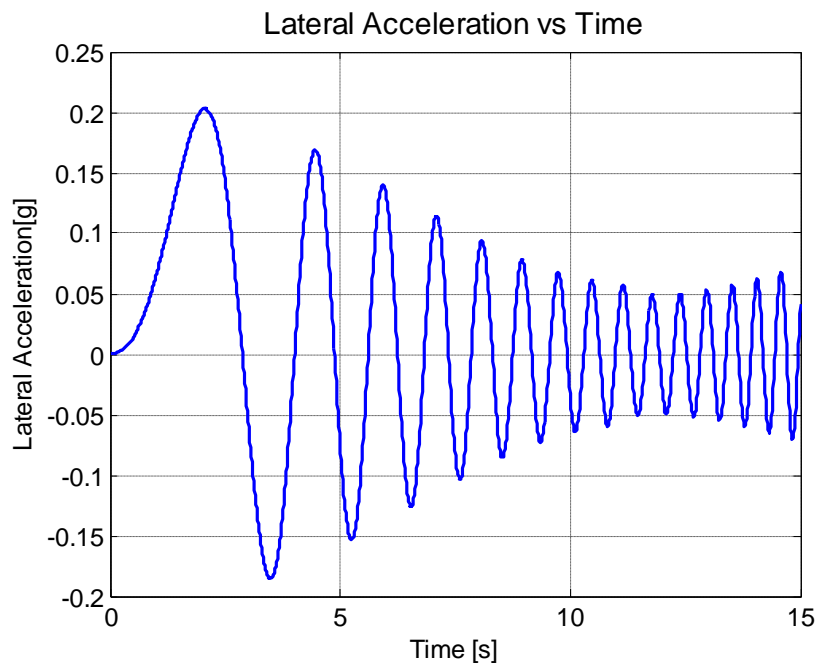
Figure 6.14: Lateral acceleration response for the estimation process
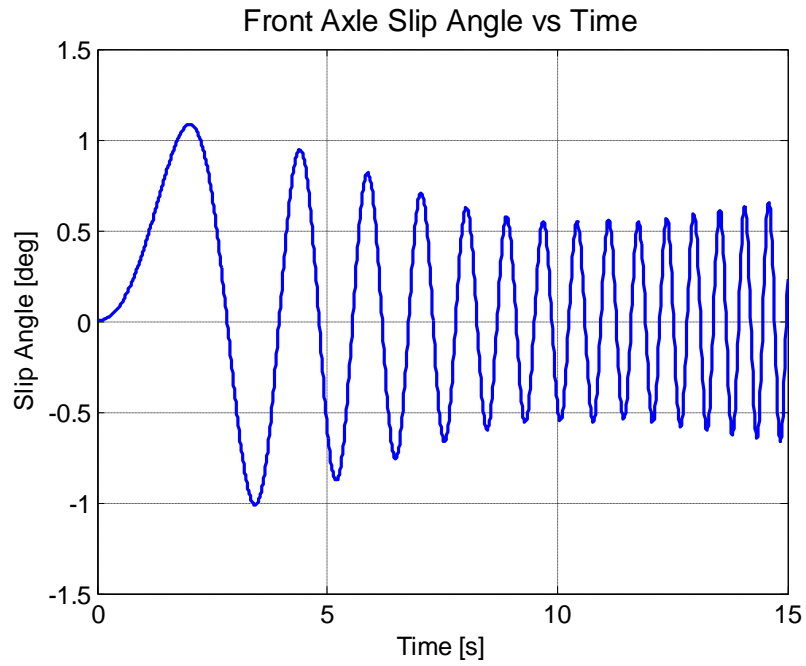
Figure 6.15: Front axle slip angle for estimation process
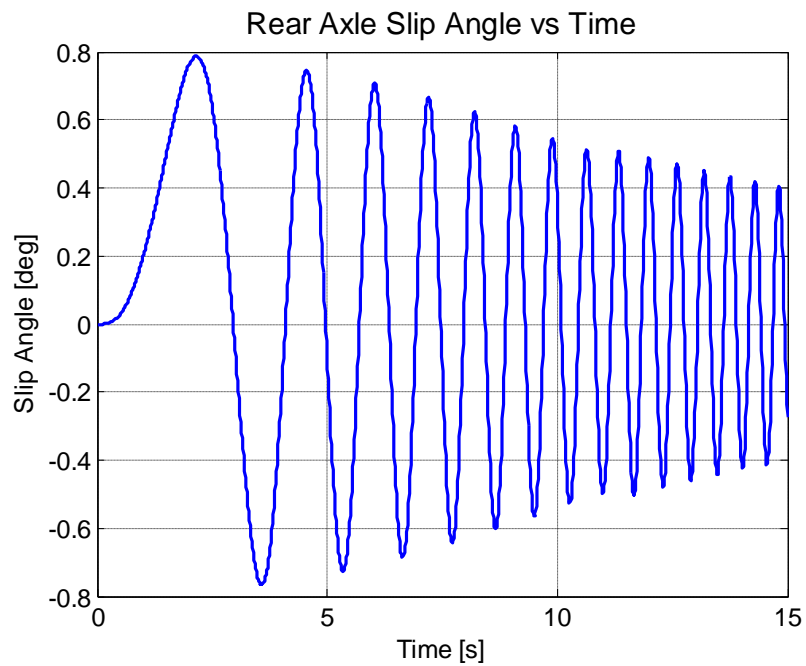
Figure 6.16: Rear axle slip angle for estimation process

110
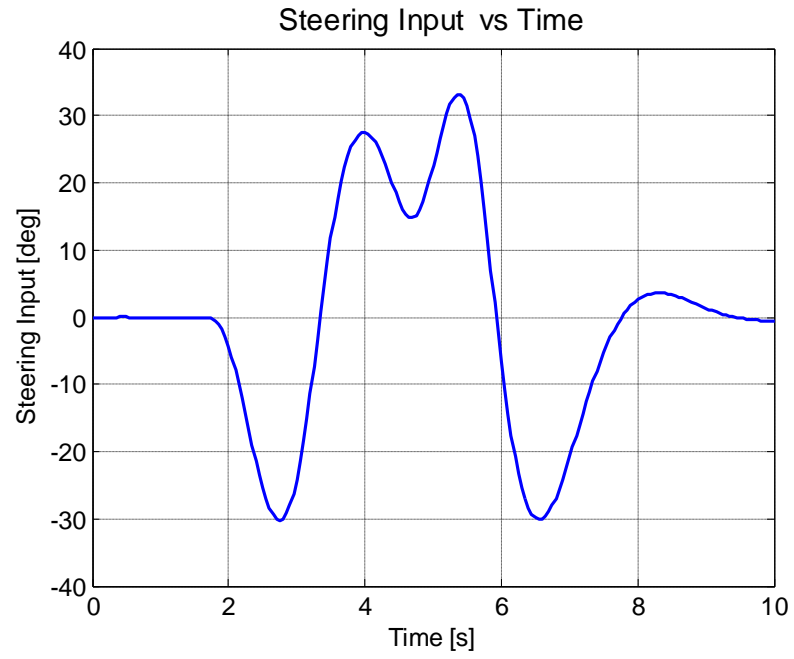
Figure 6.17: Steering wheel input for validation process
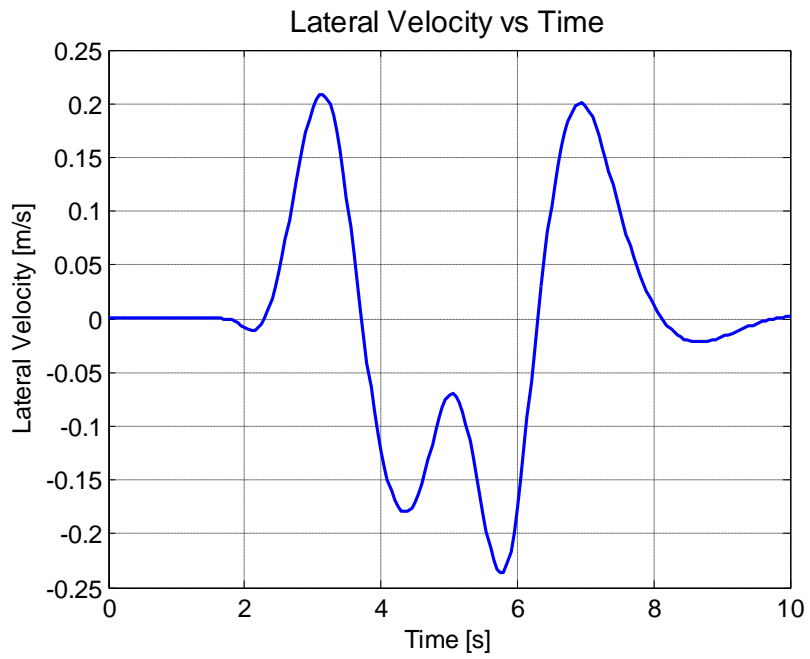
Figure 6.18: Lateral velocity response for validation process
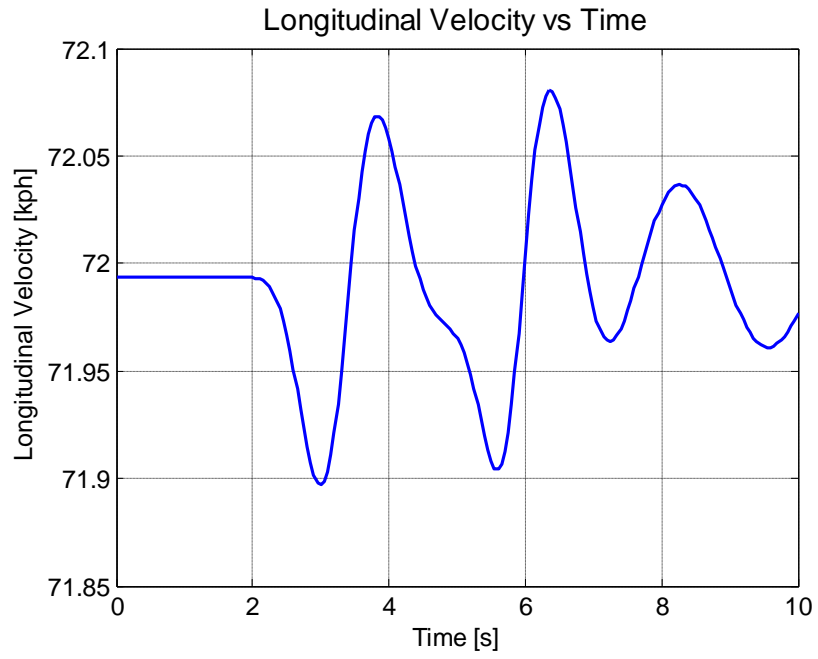
Figure 6.19: Longitudinal velocity response for validation process
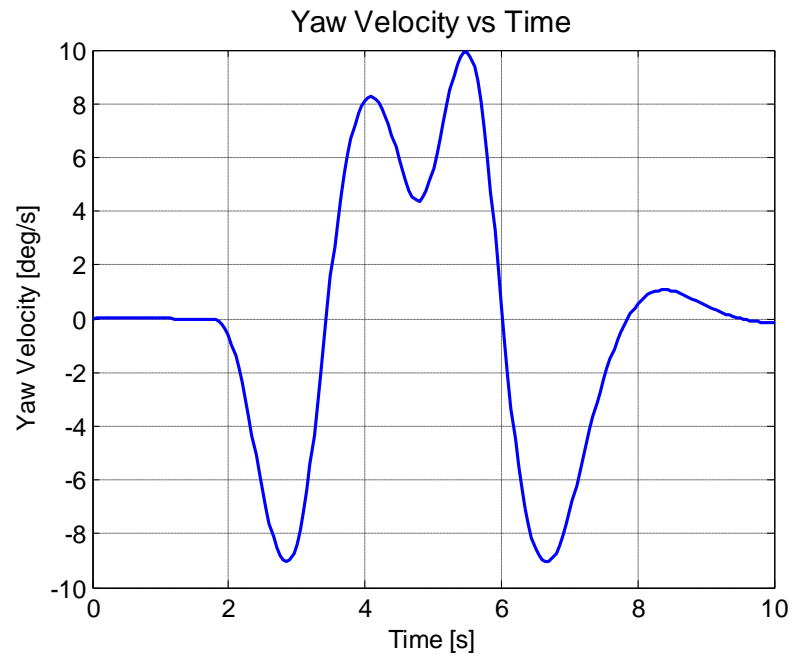
Figure 6.20: Yaw velocity response for validation process

112
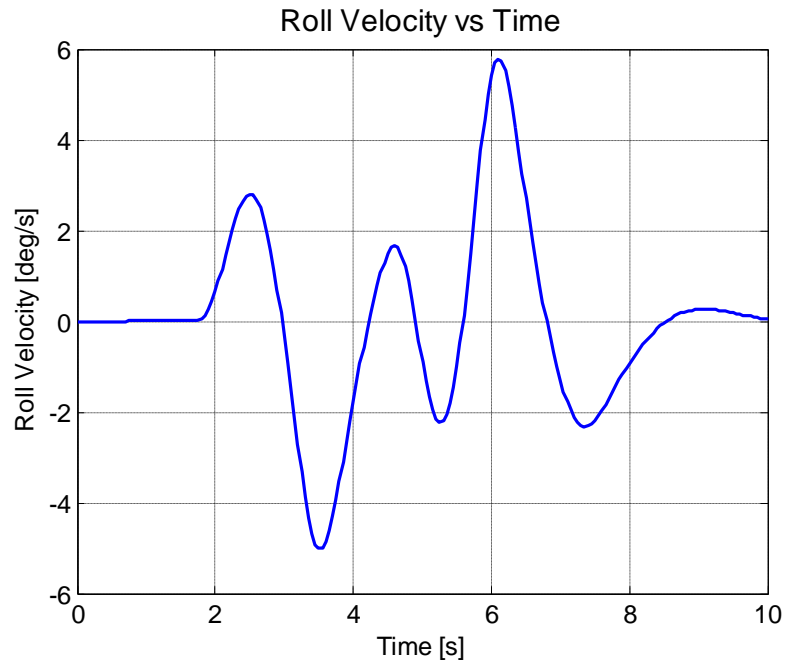
Figure 6.21: Roll velocity response for validation process
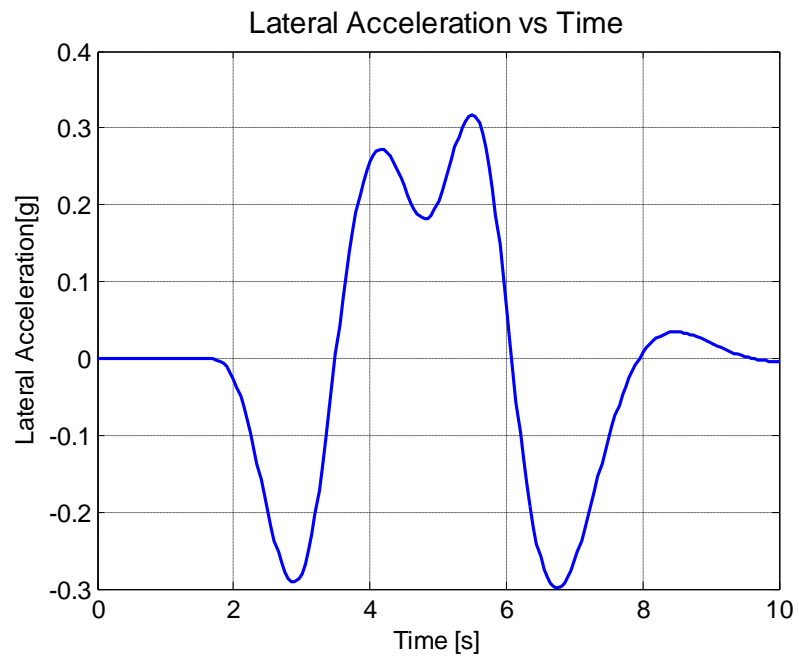
Figure 6.22: Lateral acceleration response for validation process
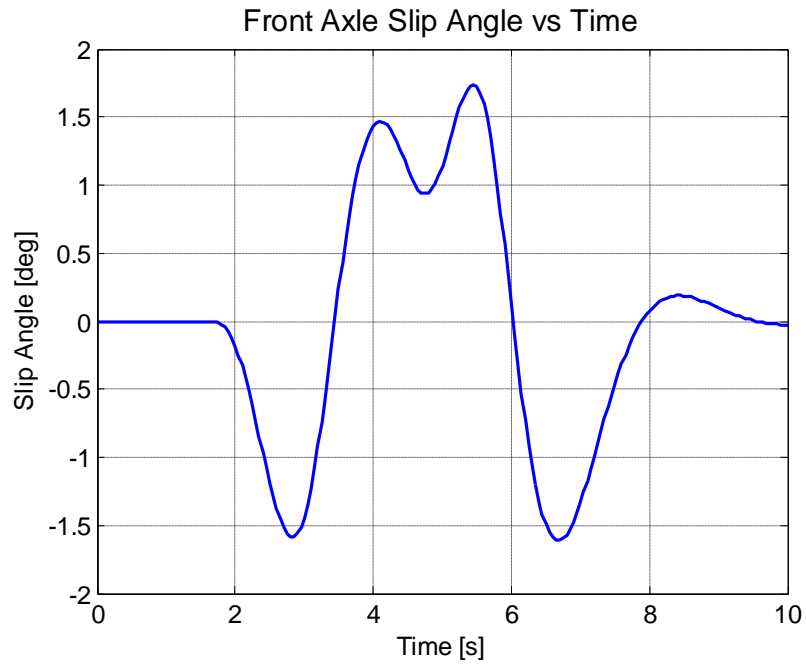
Figure 6.23: Front axle slip angle for validation process
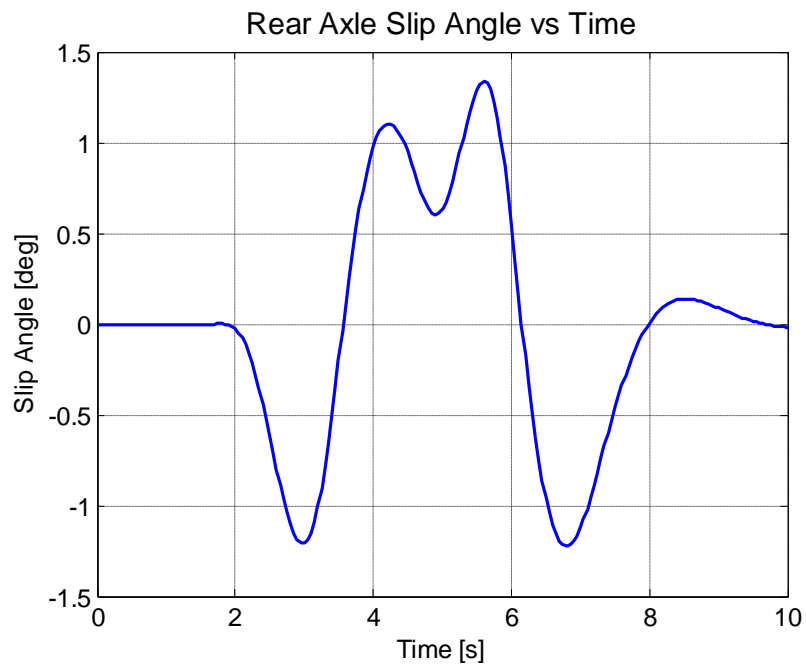
Figure 6.24: Rear axle slip angle for validation process

To be able to compare the estimated cornering stiffness values, the cornering stiffness values of ADAMS/Chassis vehicle model can be estimated from PAC2002 [8] tire model file as [7, 8, 39];

Nominal tire load, F_{z0}=3800N

a_3=-12.536

a_4=1.3856

Front tire vertical load: F_{zf}=3022N

Rear tire vertical load: F_{zr}=2092N

$$C_f = a_3 \cdot F_{z0} \cdot \sin\left[2 \cdot \tan^{-1}\frac{F_{zf}}{a_4 \cdot F_{z0}}\right] = 41130 \text{ N/rad} \qquad (6.6)$$

$$C_r = a_3 \cdot F_{z0} \cdot \sin\left[2 \cdot \tan^{-1}\frac{F_{zr}}{a_4 \cdot F_{z0}}\right] = 32690 \text{ N/rad} \qquad (6.7)$$

6.6.1. THE BICYCLE MODEL WITH STEADY STATE TIRE MODEL PARAMETER ESTIMATION

The linear bicycle model has two limitations which are small slip angle and low lateral acceleration. The bicycle model has seven parameters and three of these are treated as unknowns which are front and rear cornering stiffness values and the yaw moment of inertia. Parameters of the bicycle model are estimated using only lateral velocity, only yaw velocity, and both lateral velocity and yaw velocity.

Unknown parameters: $\{C_f, C_r, J\}$

Simulink model of the two DOF linear bicycle model used in identification is given in Figure 6.25.
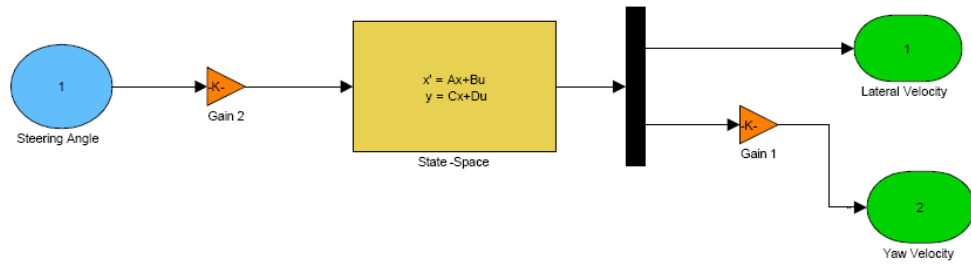
Figure 6.25: Simulink model of the two DOF linear bicycle model.

As can be seen from Figure 6.14, the lateral acceleration is lower than 0.3g and front and rear slip angles are lower than 4 degrees as shown in Figure 6.15 and Figure 6.16, so linear bicycle model assumption is valid.

6.6.1.1. ESTIMATION WITH LATERAL VELOCITY DATA

In this part, estimation process is performed using only lateral velocity response. Table 6.3 summarizes the estimation result:

Table 6.3: Estimated and measured parameter values for the bicycle model with steady state tire model using only lateral velocity response

Estimated	C_f=141240 N/rad	C_r=75724 N/rad	J=1613 kgm^2
Actual	C_f=82260 N/rad	C_r=65380 N/rad	J=1724 kgm^2
Error [%]	71.7	15.8	-6.4

Measured and estimated responses are given in Figure 6.26 and Figure 6.27.
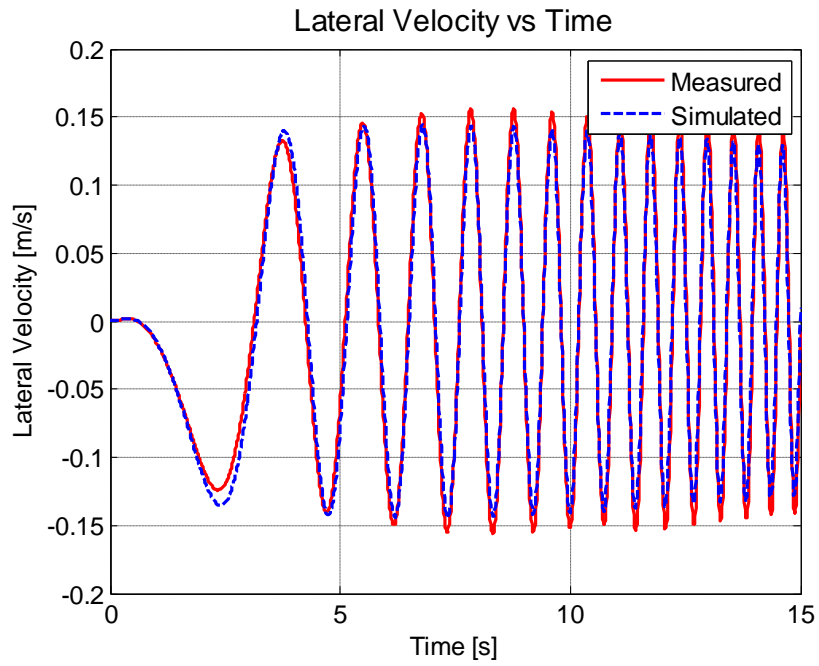
Figure 6.26: Lateral velocity responses - estimated using lateral velocity data.
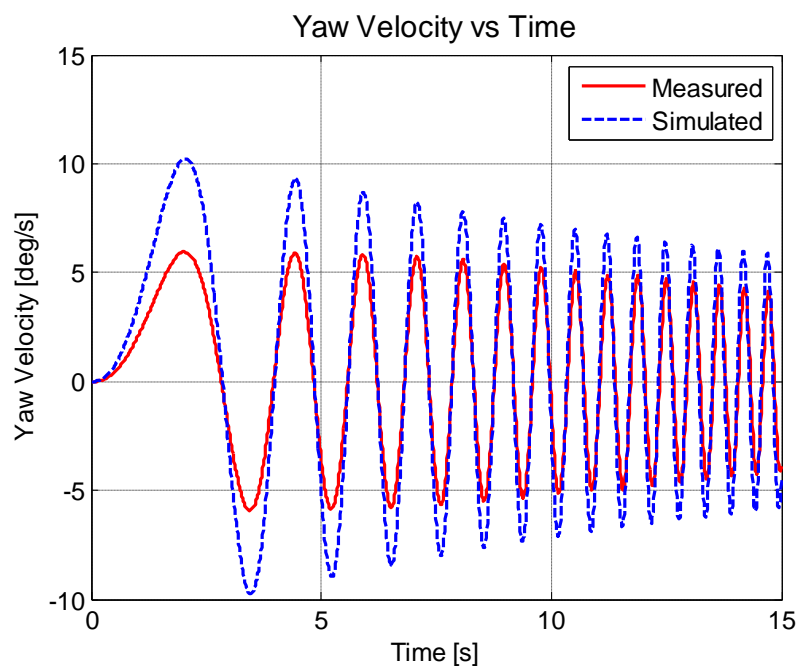
Figure 6.27: Yaw velocity responses - estimated from lateral velocity data

117

Measured and estimated responses for model validation are given in Figure 6.28 to Figure 6.29.
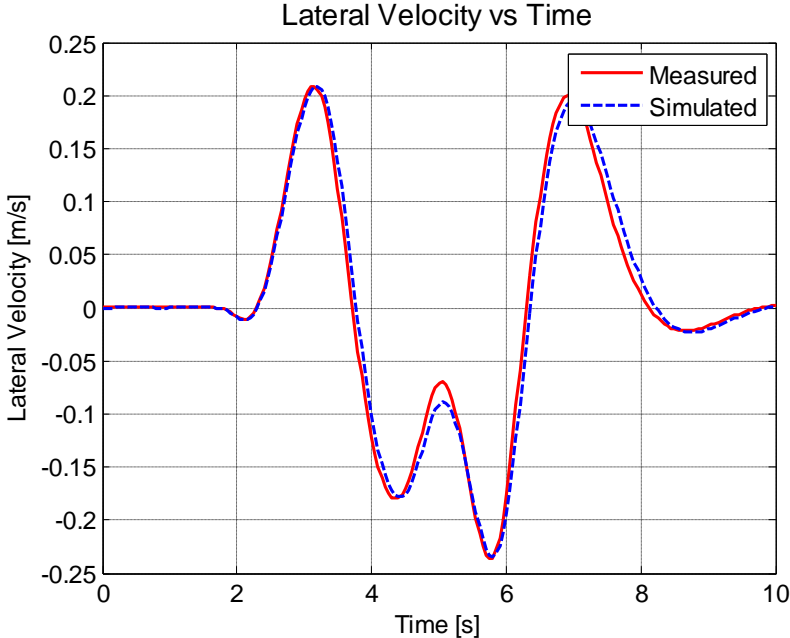
Figure 6.28: Lateral velocity responses - estimated from lateral velocity for model validation
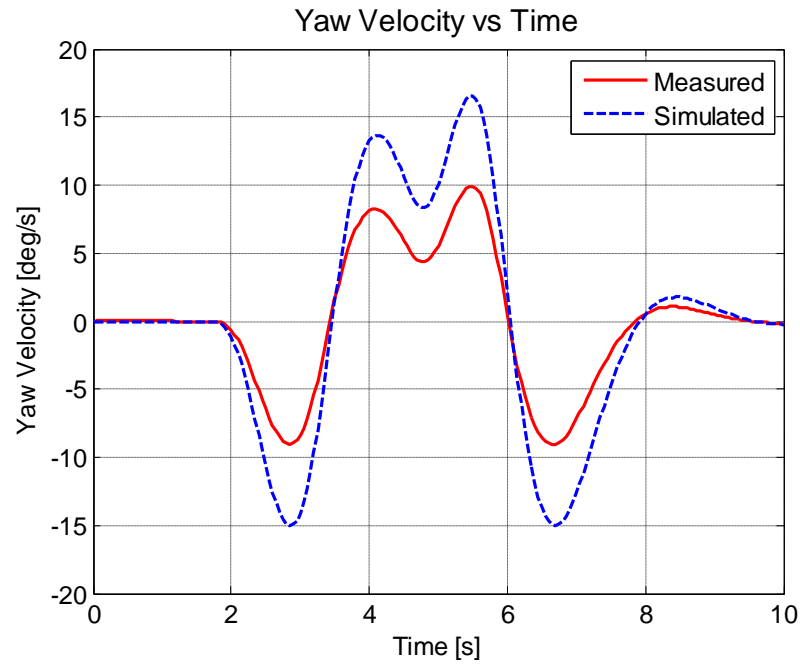
Figure 6.29: Yaw velocity responses - estimated from lateral velocity for model validation.

As shown in Figure 6.26 to Figure 6.28, only the lateral velocity is estimated accurately so using only lateral velocity response for estimation may not produce accurate results.

6.6.1.2. ESTIMATION WITH YAW VELOCITY DATA

In this part, linear bicycle model is estimated using only yaw velocity data. Table 6.4 summarizes the estimation result:

Table 6.4: Estimated and measured parameter values for the bicycle model with steady state tire model using only yaw velocity data

Estimated	C_f=53794 N/rad	C_r=48628 N/rad	J=1274 kgm^2
Actual	C_f=82260 N/rad	C_r=65380 N/rad	J=1724 kgm^2
Error [%]	-34.6	-25.6	-26

Measured and estimated responses are given in Figure 6.30 and Figure 6.31.
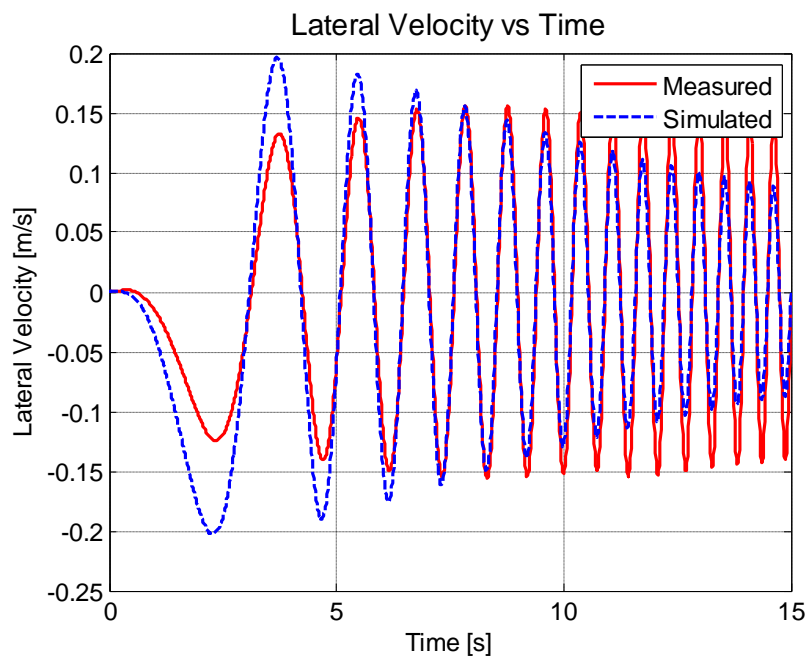
Figure 6.30: Lateral velocity responses - estimated using yaw velocity data.
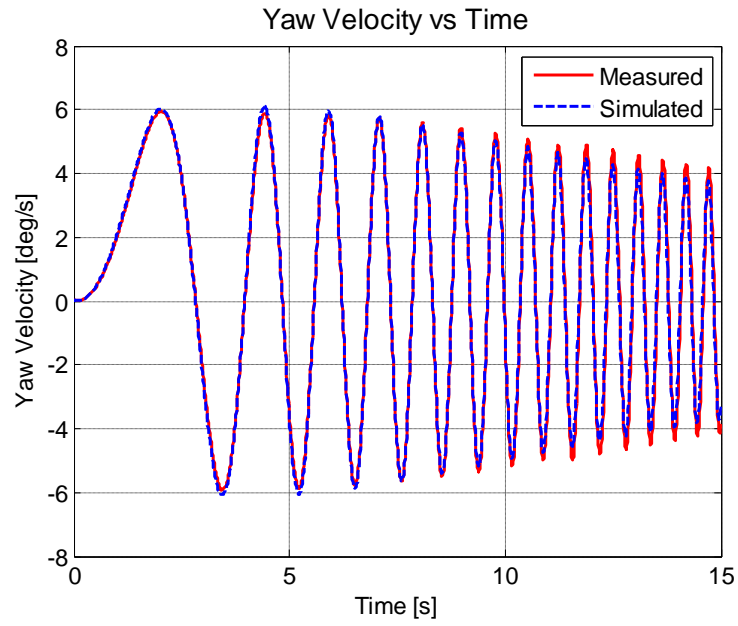
Figure 6.31: Yaw velocity responses - estimated using lateral velocity data.

Estimated and measured responses are given in Figure 6.32 and Figure 6.33.
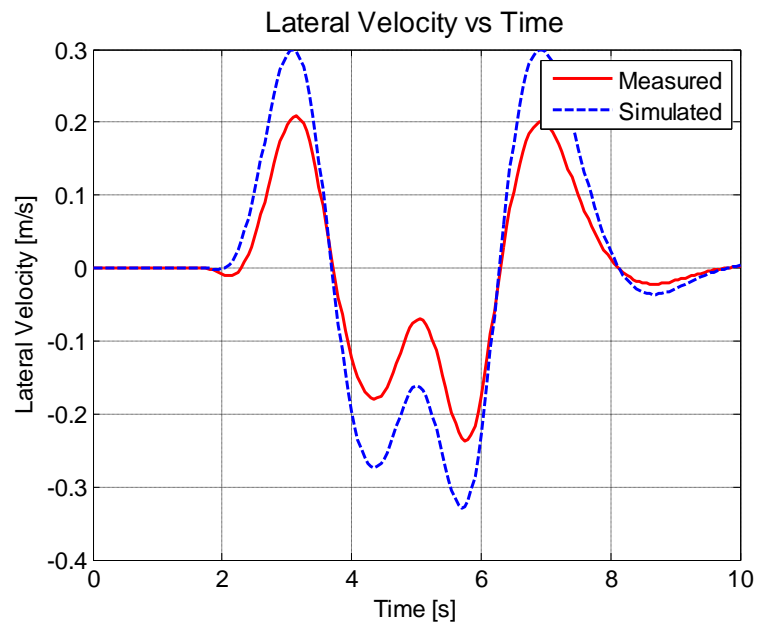
Figure 6.32: Lateral velocity responses - estimated from yaw velocity data for model validation
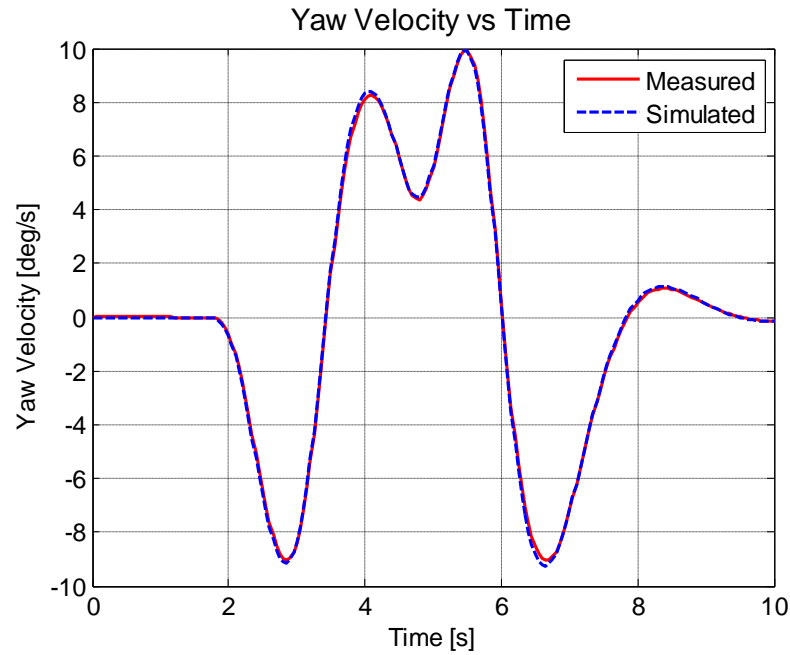
Figure 6.33: Yaw velocity responses - estimated from yaw velocity data for model validation

From the estimation results, it can be seen that even though identified model predicts the yaw velocity response quite well, it does not represent the lateral velocity response adequately and thus using only yaw velocity for estimation may not produce accurate results.

6.6.1.3. ESTIMATION WITH LATERAL VELOCITY AND YAW VELOCITY DATA

Since estimation with only lateral and only yaw velocity data may not produce accurate results, the parameters are now estimated from both lateral and yaw velocity data. Estimation result is given in Table 6.5

Table 6.5: Estimated and measured parameter values for bicycle model with steady state tire model using lateral velocity and yaw velocity data

Estimated	C_f=79636 N/rad	C_r=64852 N/rad	J=1634 kgm^2
Actual:	C_f=82260 N/rad	C_r=65380 N/rad	J=1724 kgm^2
Error [%]	-3.2	-0.8	-5.2

Measured and simulated responses are given in Figure 6.34 and Figure 6.35.
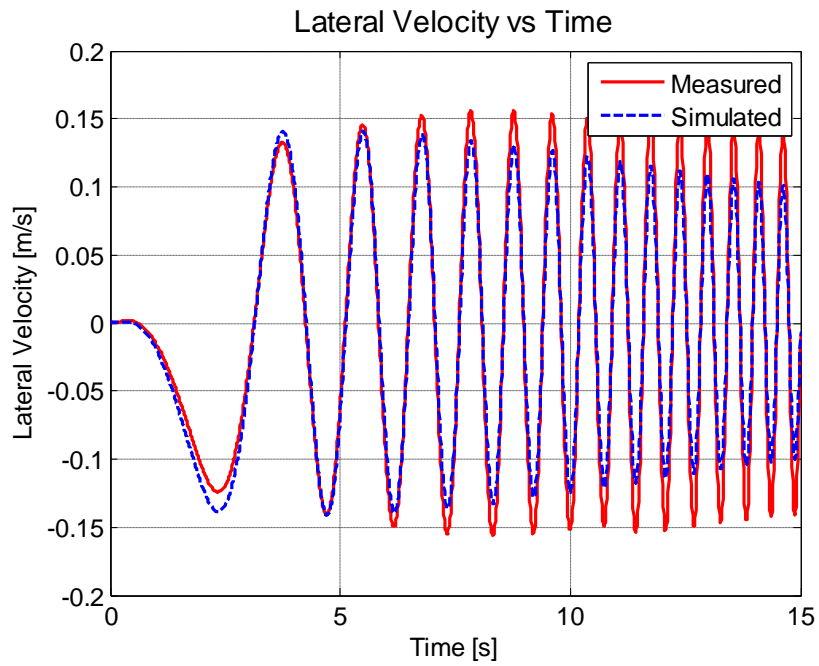
Figure 6.34: Lateral velocity responses - estimated using both lateral and yaw velocity data.
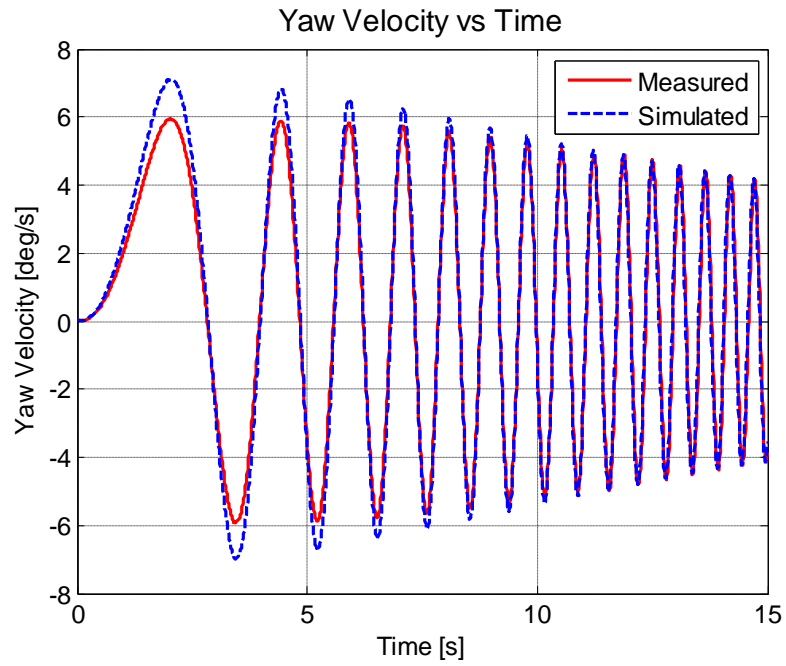
Figure 6.35: Yaw velocity responses - estimated using both lateral and yaw velocity data.

Estimated and measured responses for model validation are given in Figure 6.36 and Figure 6.37.
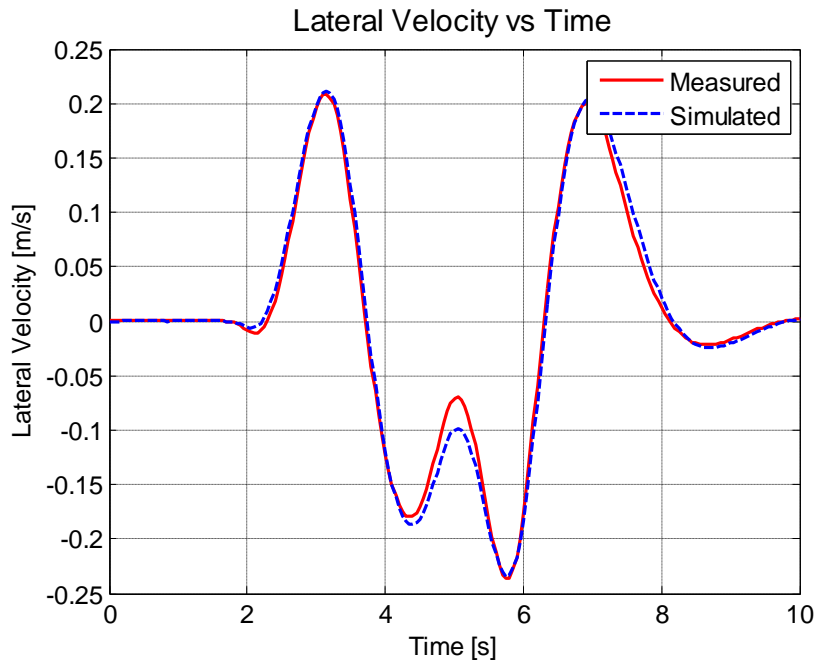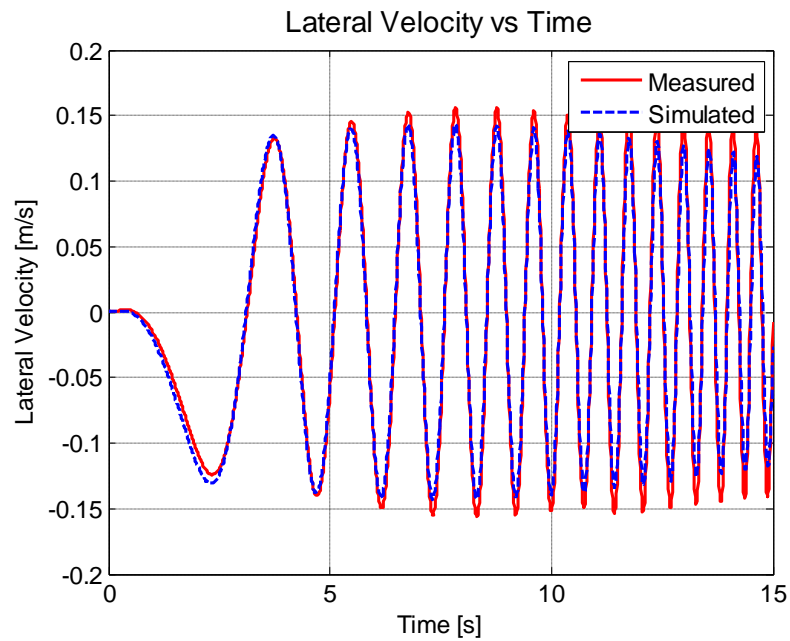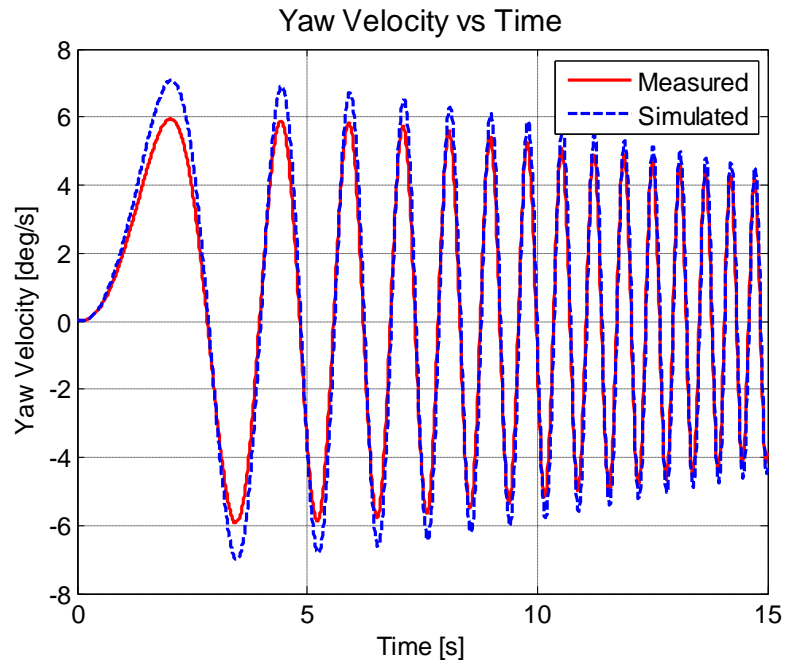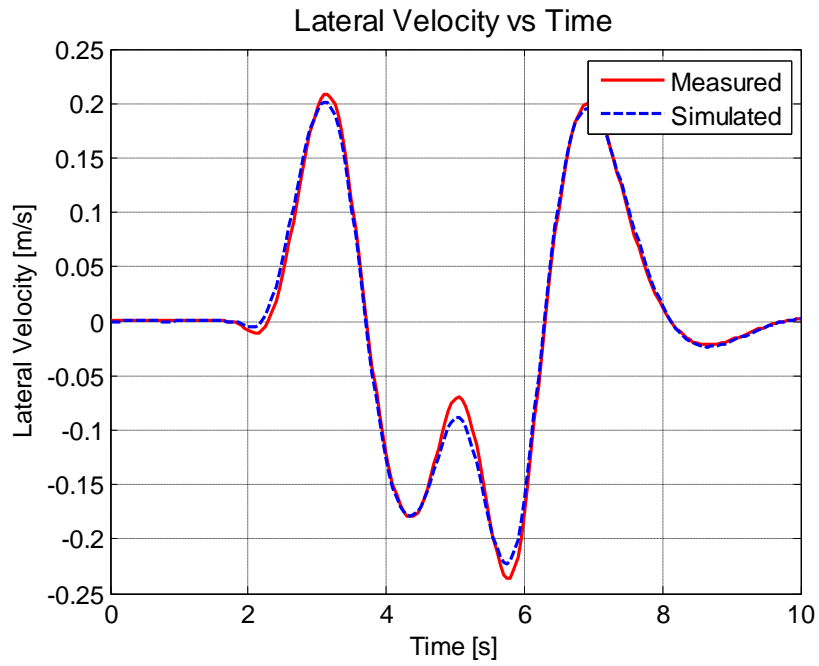
Figure 6.36: Lateral velocity responses - estimated using both lateral and yaw velocity
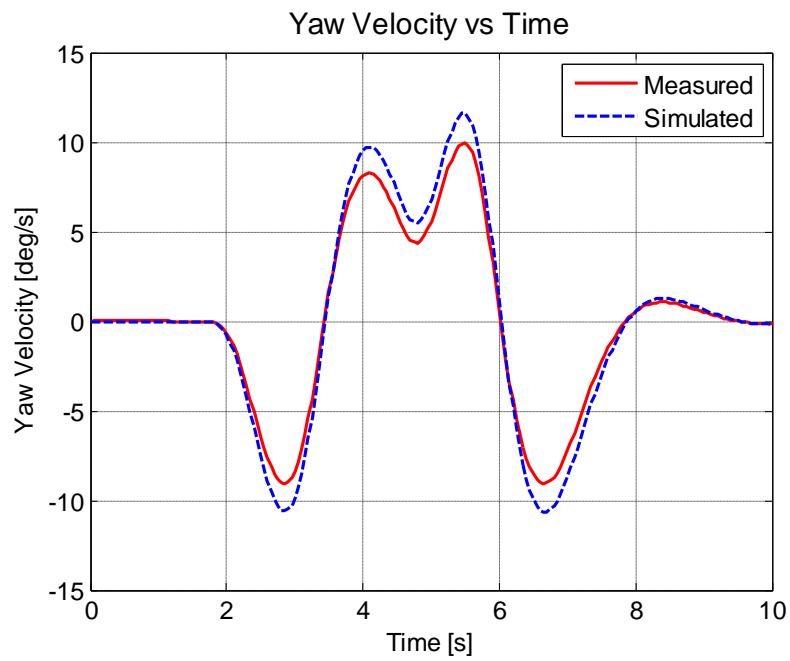
Figure 6.37: Yaw velocity responses - estimated using both lateral and yaw velocity

When the lateral velocity and yaw velocity are used for identification, identified model produced both lateral and yaw velocity successfully as can be seen from the responses. When using both data for identification, appropriate weighting factors are given to lateral velocity and yaw velocity data to add each response in estimation equally or according to aim of the study.

Parameters of the bicycle model can be estimated from the lateral velocity, yaw velocity, and both lateral and yaw velocity. When these parameters are estimated from both lateral and yaw velocity, these responses can be tracked successfully and estimated parameters are close to their real values obtained from the ADAMS model. However, there are still some small differences between the estimated and the simulated data. When these differences are examined, their periodic characteristics which show the model deficiency can be observed. When the parameters are estimated from yaw velocity, estimation result is not so accurate for the lateral velocity, and only yaw velocity can be reconstructed well. Similarly when the parameters are estimated from lateral velocity, only lateral velocity can be reconstructed well. When both lateral and yaw velocity are used together with appropriate weighting factor for test data, both lateral velocity and yaw velocity can be estimated successfully. Also, since cornering force changes with slip angle nonlinearly for high slip angles, steering input used should be low to obtain tire linearity.

Bicycle model with linear tire model can be improved by modeling transient properties of the tire. Since a highly transient input, chirp input, is used in identification transient characteristic of the tires affect the system responses. This effect can be observed by comparing the simulation of the ADAMS/Chassis model with transient and steady state tire models. Characteristic of the ADAMS tire model such as steady state and transient, combined-uncombined cornering and braking, parking and comfort etc. can be changed easily, that is, in the ADAMS tire file different tire models can be obtained by changing these characteristic.

Lateral Velocity vs Time
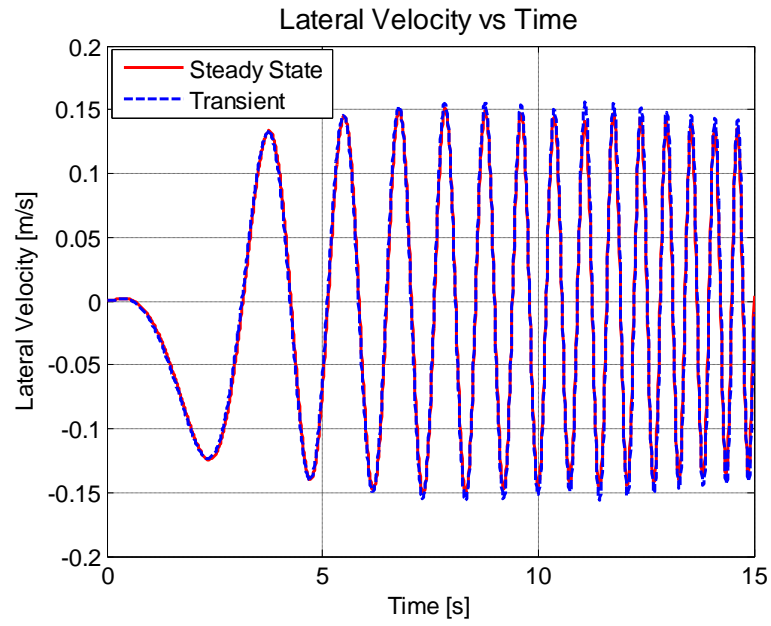
Figure 6.38: Lateral velocity responses of ADAMS model with transient and steady state tire models

Yaw Velocity vs Time
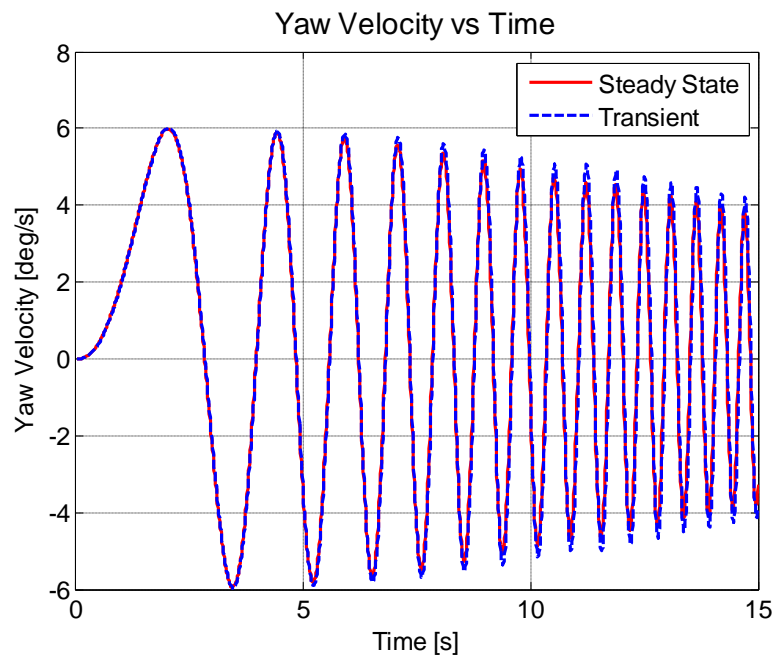
Figure 6.39: Yaw velocity responses of ADAMS model with transient and steady state tire models
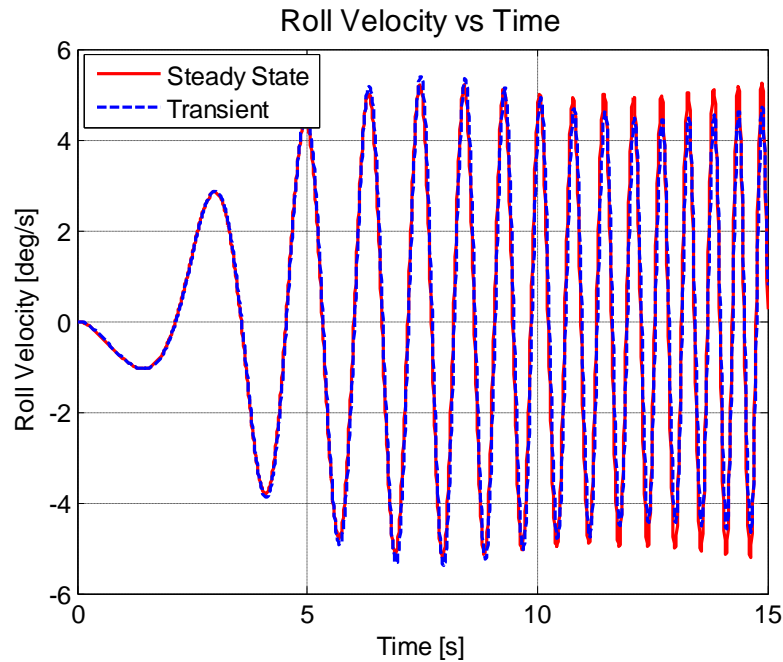
Figure 6.40: Roll velocity responses of ADAMS model with transient and steady state tire models

Figure 6.38 to Figure 6.40 show the differences between lateral, yaw, and roll velocities of steady state and transient tire models. Since these responses are taken from the ADAMS simulation with low amplitude steering input, differences are small; yet when the steering input amplitude is increased these differences increase. Even if they are small, they may still affect the estimated parameters. Thus, unmodeled system response can be compensated by the change in estimated parameters.

Using three DOF nonlinear roll model with Magic Formula tire model, effects of tire dynamics on vehicle responses can be shown in Figure 6.41 to Figure 6.43.
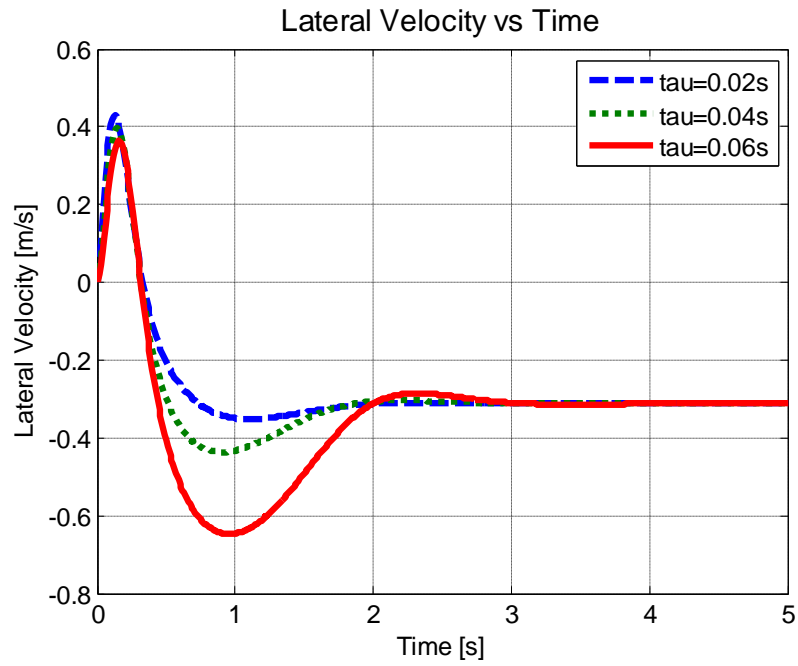
Figure 6.41: Effect of tire dynamics on lateral velocity for different relaxation time constant
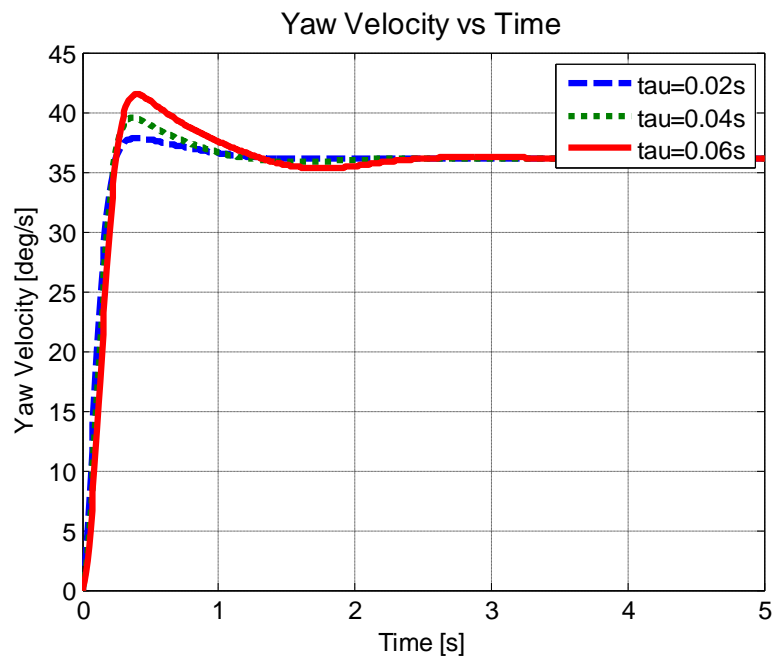
Figure 6.42: Effect of tire dynamics on yaw velocity for different relaxation time constant

129
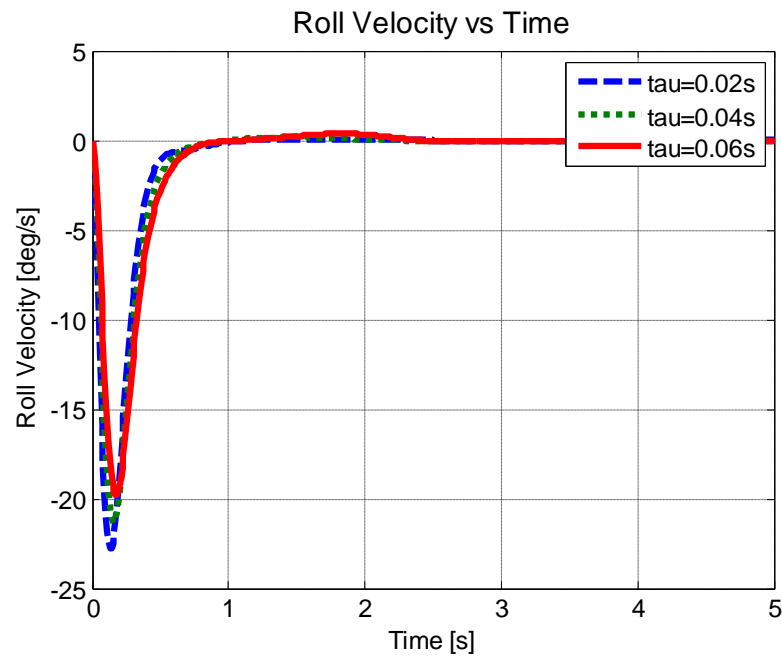
Figure 6.43: Effect of tire dynamics on roll velocity for different relaxation time constant.

As can be seen from Figure 6.41, Figure 6.42, and Figure 6.43, tire dynamics are effective on the transient responses of the vehicle as expected, and thus for nonlinear roll model identification which requires high input amplitude it must be included in the model.

6.6.2. BICYCLE MODEL WITH TRANSIENT TIRE MODEL PARAMETER ESTIMATION

Linear bicycle model with transient tire dynamics can be constructed in Simulink environment simply by adding the transient tire model to bicycle model as shown in Figure 6.44.
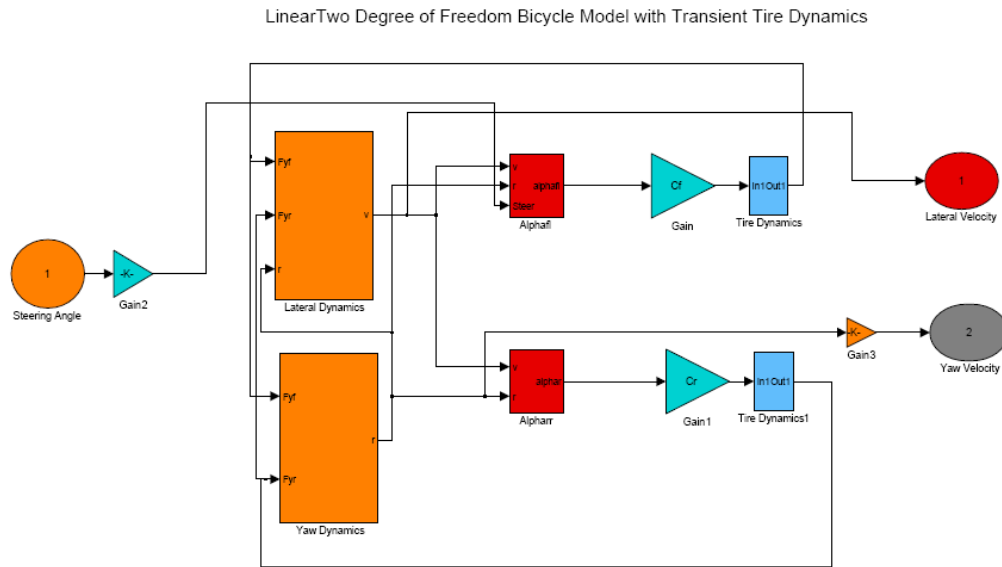
Figure 6.44: Simulink model of the two DOF bicycle model with transient tire.

Similar to the bicycle model with the steady state tire model, the bicycle model with the transient tire model are estimated from only lateral velocity, only yaw velocity, and from both lateral and yaw velocity data. In addition to front and rear cornering stiffness values and yaw moment of inertia, another tire parameter, relaxation time constant is also estimated. Since front and rear cornering stiffness values are close to each other and all tires are the same, the same tire relaxation time constant may be used for all tires.

Unknown parameters: $\{C_f, C_r, I_{zz}, \tau\}$

The bicycle model parameters are estimated from both lateral and yaw velocity data, and the estimation results are given in Table 6.6. When the identification is from one set of data only, results are similar to the bicycle model with steady state tire model, that is only yaw or lateral velocity response is identified successfully and those results are given in Appendix B.

131

Table 6.6: Estimated and measured parameter values for bicycle model with transient tire model using both lateral velocity and yaw velocity data

Estimated	C_f=80437 N/rad	C_r=66310 N/rad	J=1750 kgm^2	τ=0.026s
Actual	C_f=82260 N/rad	C_r=65380 N/rad	J=1724 kgm^2	-
Error [%]	-2.2	1.4	1.5	-

Estimated and measured responses are given in Figure 6.45 and Figure 6.46.

Figure 6.45: Lateral velocity responses - estimated from both lateral and yaw velocity data.

Figure 6.46: Yaw velocity responses - estimated from both lateral and yaw velocity data.

Estimated and measured responses for model validation are given in Figure 6.47 and Figure 6.48.

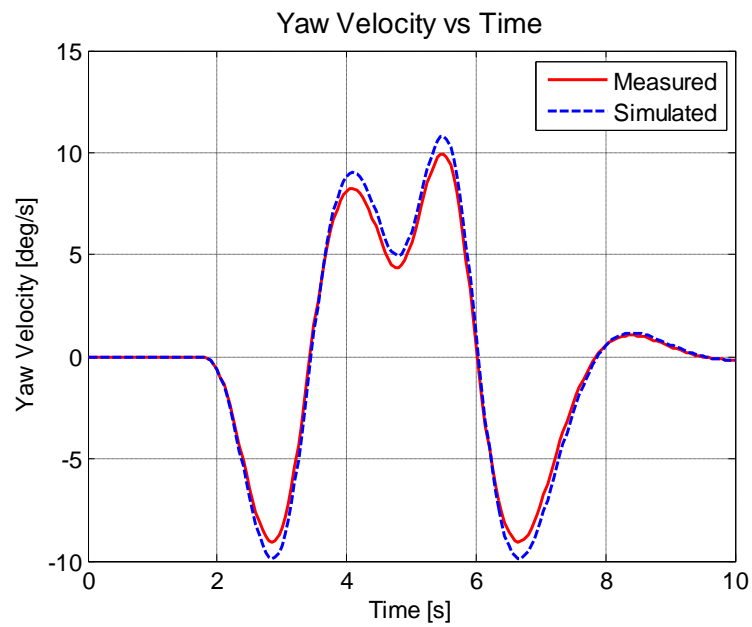**Figure 6.47: Lateral velocity responses - estimated from both lateral and yaw velocity data for validation process**
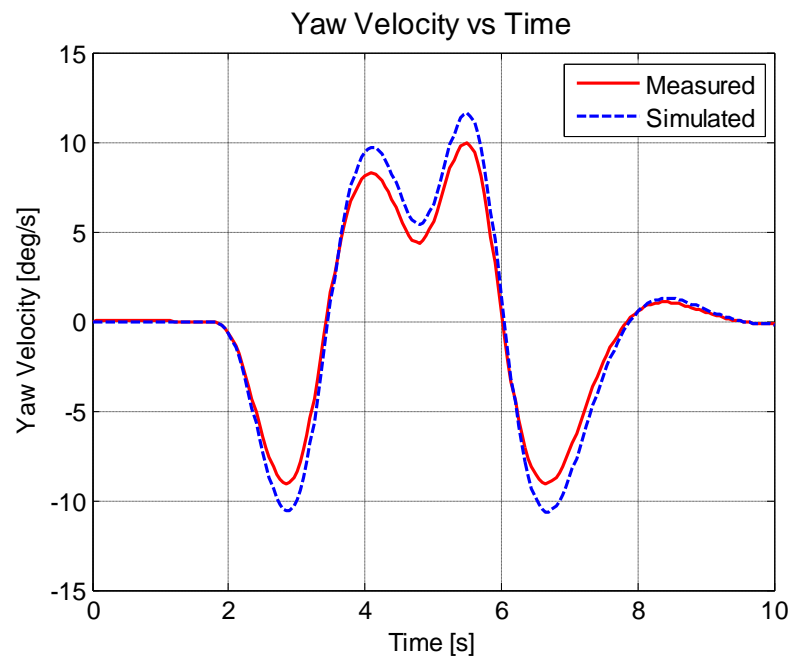
Figure 6.48: Yaw velocity responses - estimated from both lateral and yaw velocity data for validation process for validation process.

As in the case of the bicycle model with the steady state tire model, when the parameters are estimated from both lateral and yaw velocity data estimation results are successful and both responses can be tracked quite well by the identified model.

6.6.3. ONE DEGREE OF FREEDOM ROLL MODEL PARAMETER ESTIMATION

In the previous parts parameters of the bicycle model were estimated. However, as explained before to be able to explain the dynamics of the vehicle handling completely, roll motion should also be considered. Adding the roll degree of freedom to planar dynamics increases the accuracy of the model, yet it has its own disadvantage; adding the roll degree of freedom also increases the complexity of model and in turn the complexity of estimation process.

The most simple roll model is the one DOF vehicle roll model which has three parameters to be identified; namely the roll stiffness, roll damping and the roll moment of inertia. Calculations or measurements of these parameters are difficult so they are better estimated.

In the one DOF roll model, lateral acceleration can be assumed as the model input and the roll velocity can be assumed as the model output. State space model constructed in Simulink is shown in Figure 6.49.

Unknown parameters: $\{C_{\phi}, K_{\phi}, I_{xx}\}$

One Degree of Freedom Vehicle Roll Model
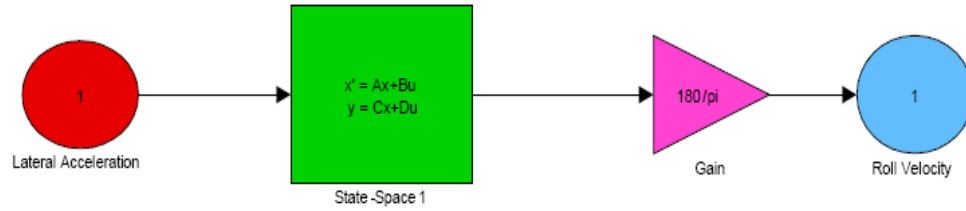
Figure 6.49: One DOF vehicle roll model.

Estimated parameters are given in Table 6.7.

Table 6.7: Estimated parameters for one degree of freedom roll model

Estimated	C_φ=2535 Nms	K_φ=37759 Nm	I_{xx}=384 kgm^2

Estimated and measured responses are given in Figure 6.50.
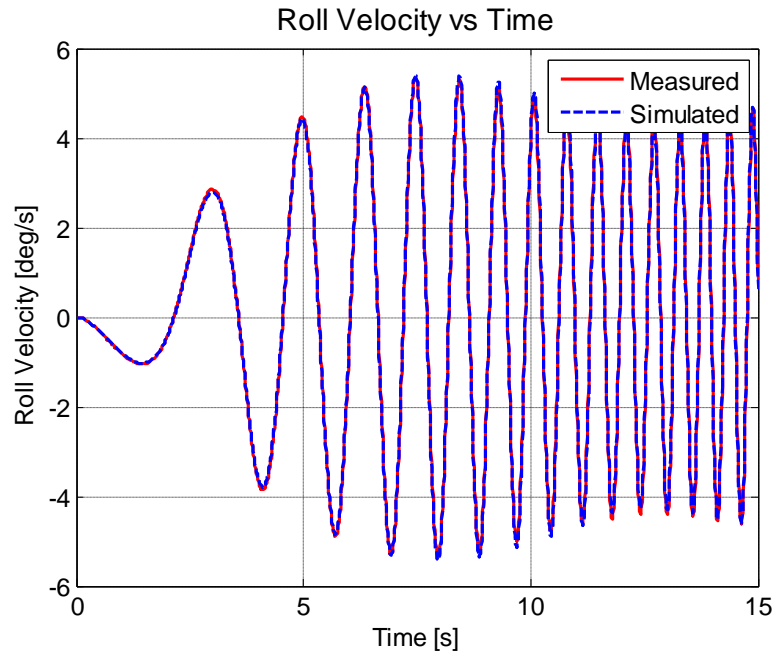
Figure 6.50: Roll velocity responses for estimation process

Estimated and measured responses for model validation are given in Figure 6.51.
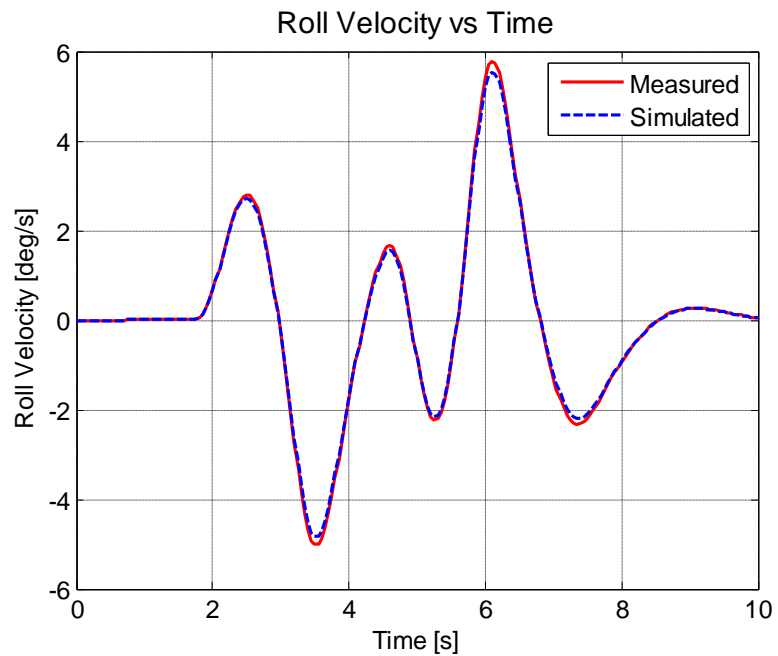
Figure 6.51: Roll velocity responses for validation process

Roll velocity is highly sensitive to distance between roll axis and center of gravity and thus accurate knowledge of this value is vital for correct parameter estimation. However, position of the roll center changes as suspension moves during maneuver and so the distance between roll axis and center of gravity will change and this will affect the estimated parameters.

6.6.4. THREE DEGREE OF FREEDOM LINEAR ROLL MODEL PARAMETER ESTIMATION

The bicycle model represents only plane dynamics of vehicles and it does not comprise the roll degree of freedom. However, roll motion and lateral motion of the vehicles are coupled and thus roll motion has effects on the lateral motion. When the measured and estimated responses of the bicycle model are compared it can be observed that there is error which shows periodic characteristic which means that the identified model has model deficiency. This deficiency can be decreased by increasing the model order and more accurate results can be obtained. However, an increase in model order brings its own disadvantages. Number of parameters to be estimated increases and thus numerical calculations becomes more difficult.

Three DOF roll model considers the coupled planar and roll degrees of freedom and now the parameters of the more accurate vehicle model are estimated.

Simulink model of the three DOF linear roll model is given in Figure 6.52.

THREE DEGREE OF FREEDOM LINEAR ROLL MODEL
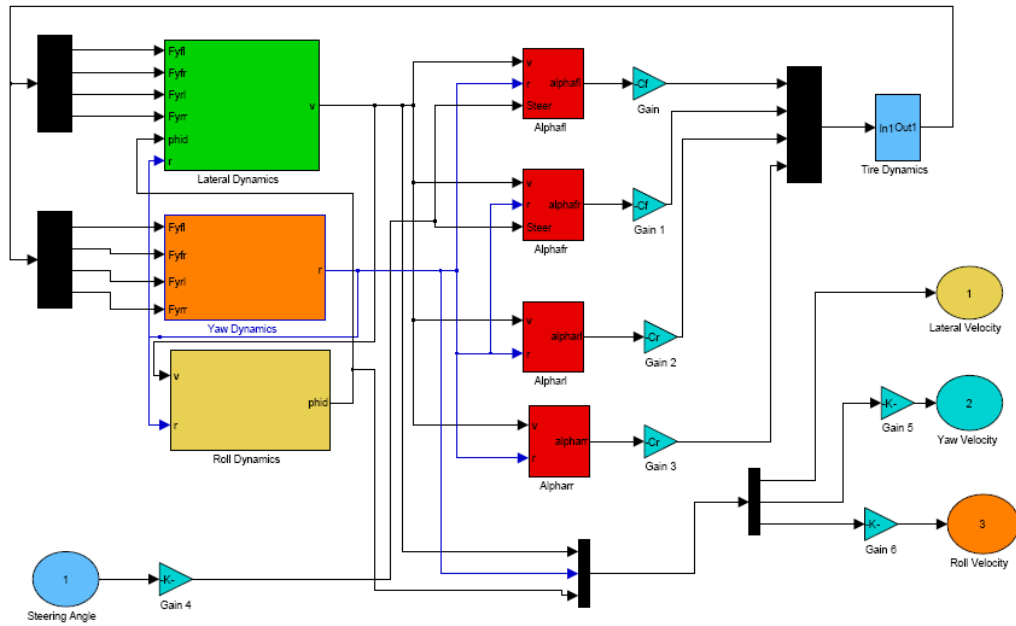
Figure 6.52: Linear three DOF roll model

Unknown parameters: $\{C_f, C_r, K_\phi, C_\phi, I_{xx}, I_{zz}, \tau\}$

The data are taken from the simulation of the ADAMS model and it is the same as the one used for the bicycle model identification.

Result of the estimation process is given in Table 6.8.

Table 6.8: Estimated and measured parameter values for three degree of freedom linear roll model

Parameter	Estimated	Actual	Error [%]
C_f [N/rad]	74618	82260	-9.3
C_r [N/rad]	66542	65380	1.8
I_{zz} [kgm^2]	1766	1724	2.4
I_{xx} [kgm^2]	363	-	-
K_φ [Nm]	41330	-	-
C_φ [Nms]	2409	-	-
τ [s]	0.017	-	-

Measured and estimated responses are given in Figure 6.53 to Figure 6.55.
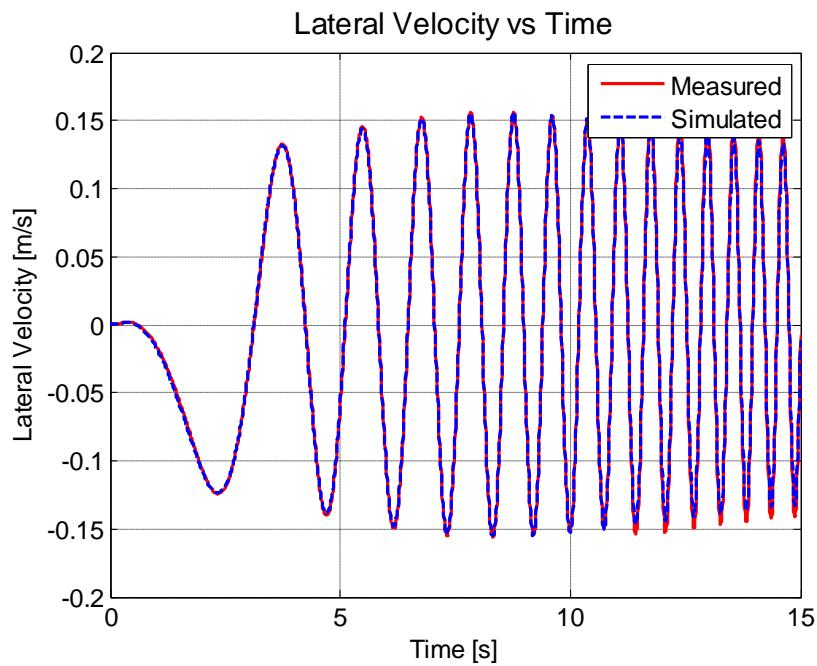
Figure 6.53: Lateral velocity responses for identification process.
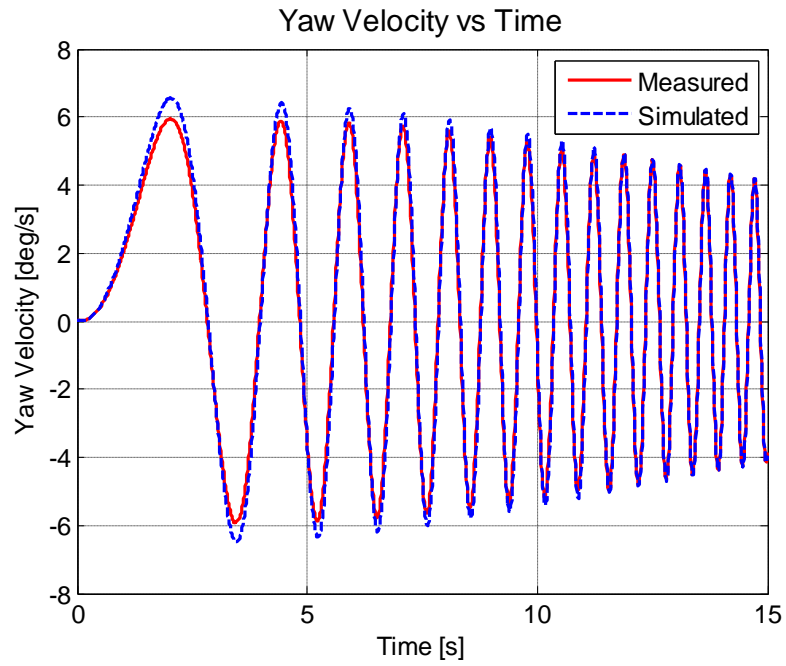
Figure 6.54: Yaw velocity responses for identification process
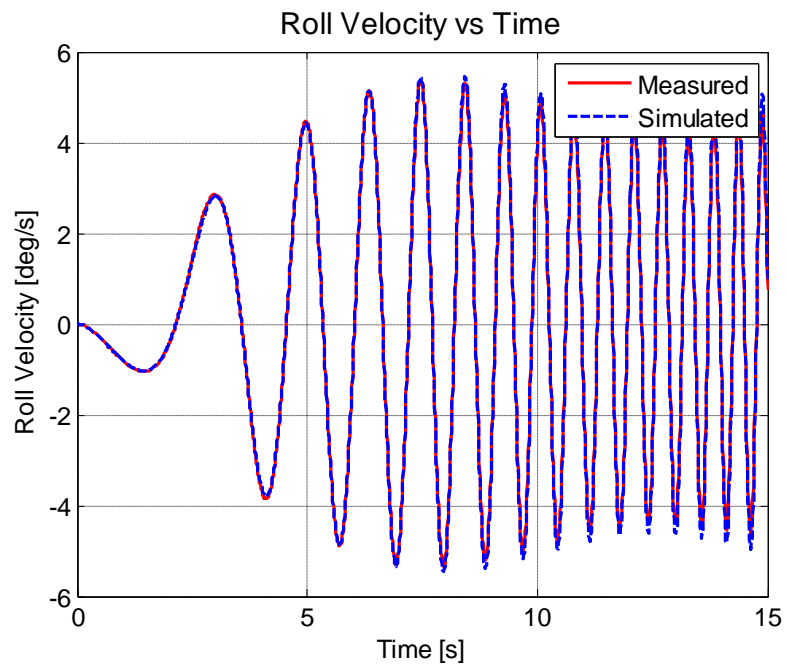
Figure 6.55: Roll velocity responses for identification process

Estimated and measured responses for model validation are given in Figure 6.56 to Figure 6.58.
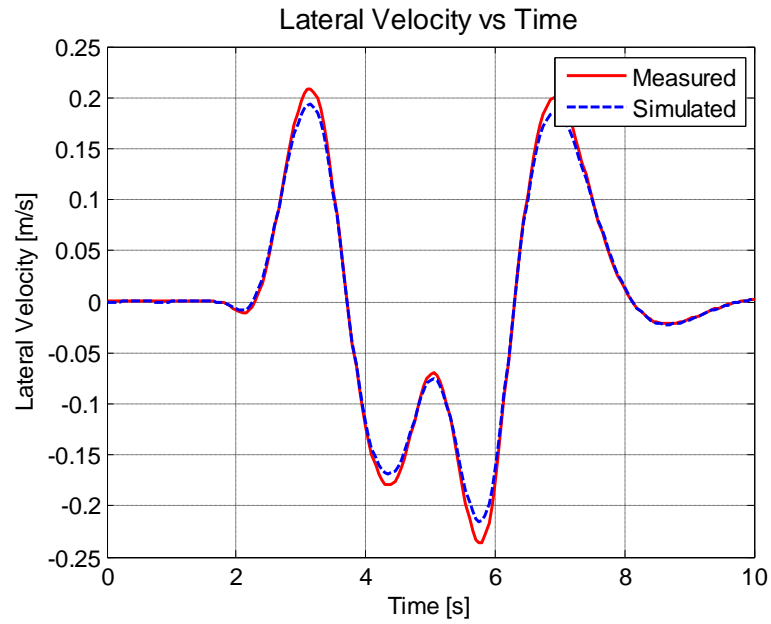
Figure 6.56: Lateral velocity responses for validation process

Figure 6.57: Yaw velocity responses for validation process
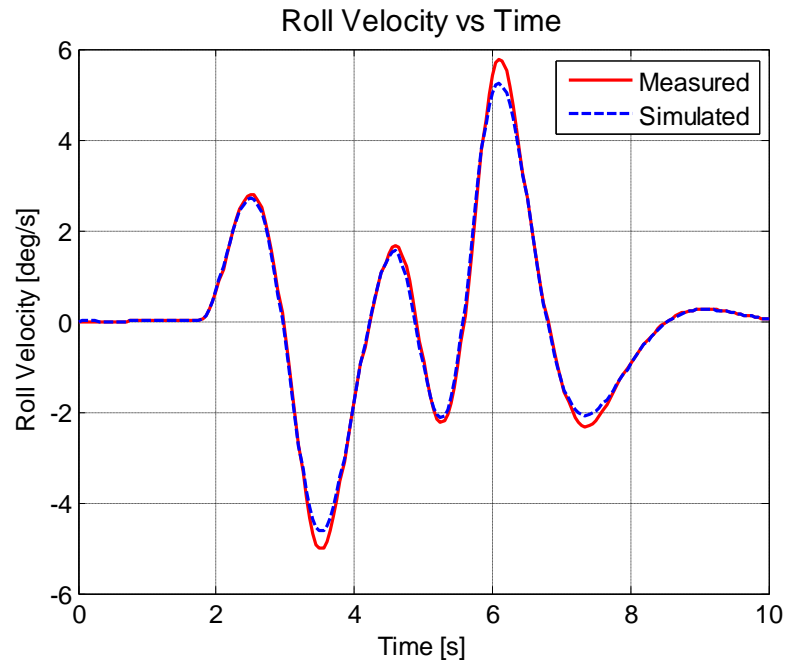
Figure 6.58: Roll velocity responses for validation process.

Using lateral velocity, yaw velocity, and roll velocity three DOF linear roll model can be identified. As can be seen from measured and estimated responses estimated responses track the measured responses successfully. When the results of the linear bicycle model and the linear roll model are compared, it can be seen that considering the effect of the roll motion on the lateral motion, more accurate estimate is obtained. As can be seen in Figure 6.59 and Figure 6.60 the error between measured and estimated responses of the roll model is smaller than the error between measured and estimated responses of the bicycle model.
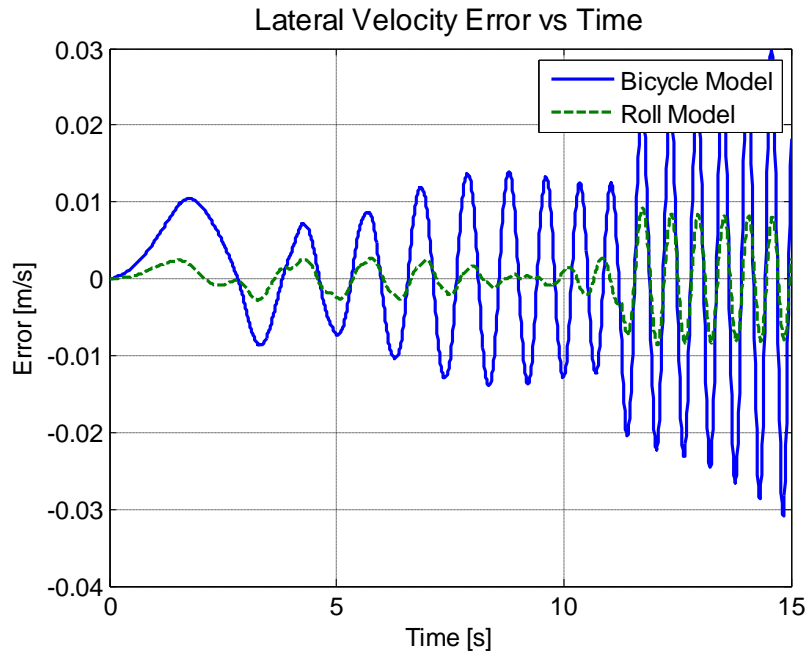
Figure 6.59: Error between measured and estimated lateral velocities of bicycle and roll model.
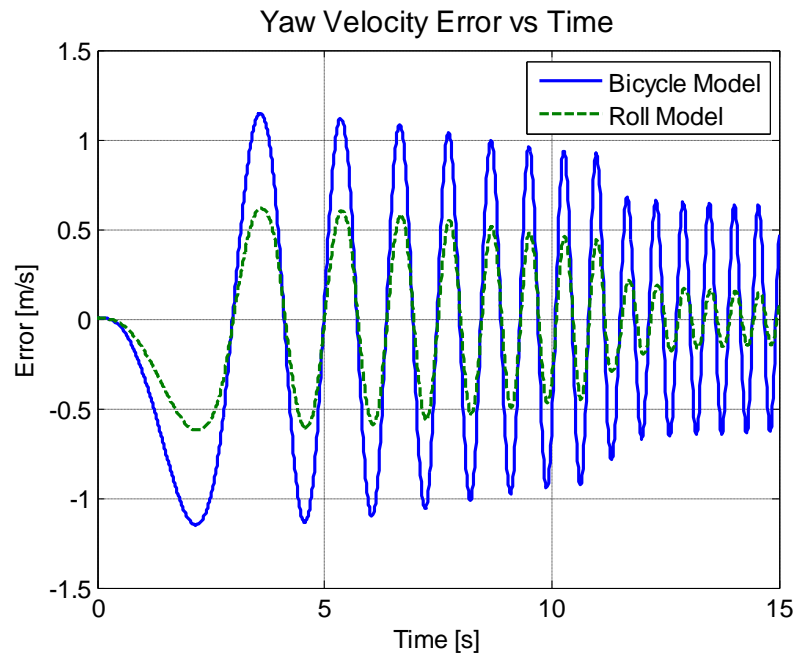
Figure 6.60: Error between measured and estimated yaw velocities of bicycle and roll model.

Till now, linear handling models have been identified and their identifications have been relatively straight forward. When the bicycle model is identified by using two vehicle output data; namely lateral velocity and yaw velocity, two states of the bicycle model, identification results are successful. On the other hand, even if one set of response data is sufficient for the identification of the bicycle model (for a specified parameter set) from the structural identifiability point of view, only one output set used in the identification is identified successfully. To illustrate, when the bicycle model is identified by using only lateral velocity data, only lateral velocity is identified successfully. This may be due to the fact that unmodeled part of the vehicle may affect the estimated parameters for the specified output. Since the input used in the identification is sine chirp input which covers a certain frequency range, transient properties of the tire should also be modeled. Three DOF linear roll model tracks the measured responses successfully in the linear operating region of the vehicle, and it may be used for the control applications effectively.

Handling models can also be identified by firstly identifying state space or transfer function parameters and then by identifying physical parameters from these parameters. However, to be able to identify physical parameters from state space or transfer function parameters, a nonlinear set of equations must be solved; and this is not easy. Since in vehicle handling identification, aim is to estimate physical parameters rather than model parameters, estimation of physical parameters directly is easier. When the physical parameters are estimated from model parameters by equation solving or by optimization methods, constraints cannot be imposed directly on physical parameters so estimation process may become difficult.

However, for more severe maneuvers, that is, when the slip angles and lateral acceleration are high, linear models cannot be used since tire behavior changes nonlinearly with tire inputs like slip angle and vertical tire load. Therefore, tire should be modeled such that those nonlinearities can also be included in the analysis. Consequently, more advanced and more complex vehicle handling models

145

are required. Thus, the identification of a nonlinear handling model with Magic Formula tire model is attempted.

6.6.5. THREE DEGREE OF FREEDOM NONLINEAR ROLL MODEL PARAMETER ESTIMATION

In this section three DOF nonlinear roll model is used with the Magic Formula tire model. Data used in the identification is taken from the simulation of the ADAMS vehicle. PAC2002 [8] tire model which calculates combined cornering and braking/traction tire forces by considering dynamic tire characteristics is used with ADAMS model. First order transient tire model is used in the model to be identified.

When the slip angle of the tire is higher than approximately 4 degree, linear tire model which relates the cornering force to slip angle linearly cannot be used; and more advanced and complex nonlinear tire models should be used. These nonlinear models calculate the tire cornering force as a function of various inputs like slip angle and vertical tire load, and they can be used for wider operating conditions. When the combined cornering and braking tire characteristic is also considered more accurate tire models with a better representation of the real tire behavior is obtained, yet determining the values of the high number of unknown parameters pose a difficulty. There are various nonlinear tire models, each one of which has its own specific advantages and disadvantages. Some of these are Fiala tire model, look-up table model, Allen tire model, and Magic Formula tire model.

Detailed comparison of Fiala tire model and Magic Formula tire model have been given in [40]. In Magic Formula tire model, cornering stiffness changes with vertical tire load and camber angle, yet in Fiala tire model cornering stiffness does not change with vertical load on it and camber angle. On the other hand, Fiala tire model Formula calculates tire forces with a lower number of parameters as compared with the Magic Formula tire model, which is the advantage of the Fiala tire model [40].

146

In this study various nonlinear tire models including, Fiala tire model, lookup table tire model, polynomial tire model, and Magic Formula tire model have been examined and among these the best estimation results have been obtained with Magic Formula tire model. In vehicle tests with a high amplitude transient steering input stimulating tires highly, lateral load on tires change so cornering stiffness of the tires changes. Since Fiala tire model assumes constant cornering stiffness, this model may be used up to some slip angle. When the lookup table tire model is used, increased number of parameters may pose a problem and also shape of the estimated tire forces may not be correspond to measured tire forces. In polynomial tire model estimation results are good, that is, estimated responses track the measured responses well, yet these models can only be used for the slip angle which is obtained in test; at higher slip angle nonphysical tire behavior may result due to certain characteristics of the polynomials as also indicated in [39]. Therefore, the Magic Formula tire model is used in the nonlinear roll model due to its proved accuracy and applicability in vehicle handling dynamics.

Magic Formula tire model has various parameters and estimations of all of them are a difficult task with simple vehicle tests. More advanced test routines are needed to estimate the parameters. As explained in chapter 2, tires are tested with some specialized test setup to measure forces acting between the tire and the road. Then Magic Formula tire parameters are estimated from those test data. With this test, combined and pure braking and cornering tire force measurement can be performed and Magic Formula tire model parameters can be estimated. However, these parameters may also be estimated from vehicle handling tests. Estimation is performed for the coefficients of the Magic Formula tire models which are; a_0, a_1, a_2, a_3, a_4, a_6, a_7. These parameters are the basic parameters of the Magic Formula tire model and they are not dependent on the vertical loads or other variables. Since in the estimation model vertical load in each tire is modeled, estimation of these parameters produces more reliable results.

147

In ADAMS vehicle model used in this study, four wheels of the vehicle are the same and since tire model coefficients (a_0, a_1..) to be estimated are independent of the other variables like the vertical load on the tires, only one tire model parameter set is treated as the unknown tire parameter set.

To be able to estimate the parameters of the Magic Formula tire parameters, wide operating points should be covered and thus ADAMS vehicle model is disturbed with steering wheel input at high amplitude.

To be able to determine the effects of the tire parameters to cornering force, sensitivity study is first performed. With this study, change of sensitivities of the cornering force to tire parameters with tire slip angle at different vertical tire load is studied and the required tire slip angle is found. According to the results, as can be seen from Figure 6.61 to Figure 6.63, sensitivities of cornering force to tire parameters related with cornering stiffness are high at low slip angle. On the other hand, sensitivities of the cornering force to tire parameters related with maximum force are high at high slip angles. Sensitivities of the cornering force to tire parameters related with curvature factor are not so high. Therefore to be able to estimate tire model parameters high slip angles are required.
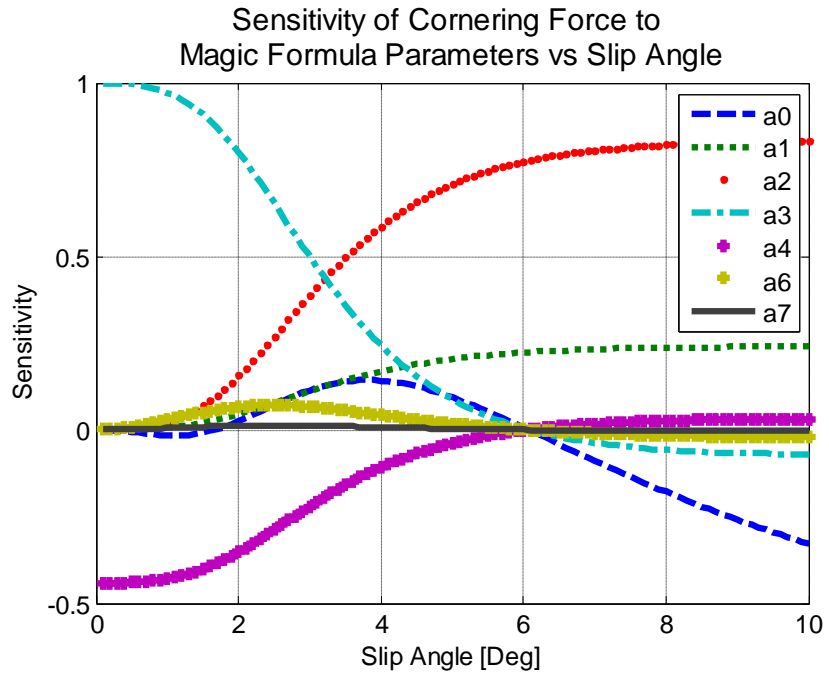
Figure 6.61: Sensitivity of cornering force to Magic Formula tire parameters at 2 kN vertical tire load
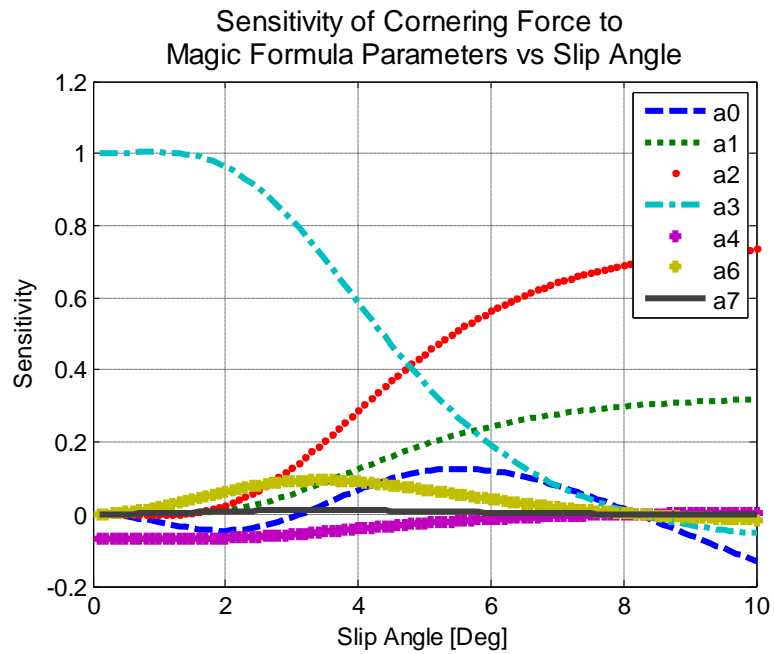
Figure 6.62: Sensitivity of cornering force to Magic Formula tire parameters at 3 kN vertical tire load

149
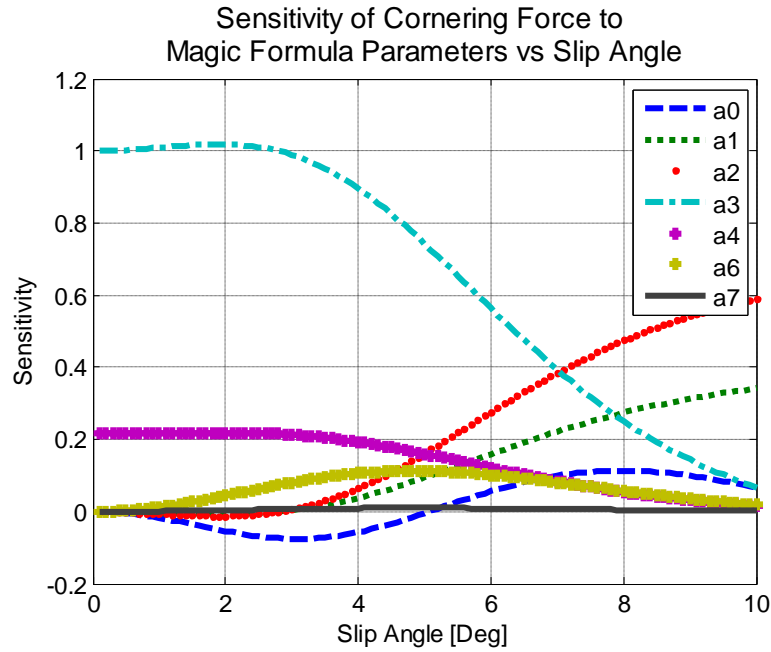
Figure 6.63: Sensitivity of cornering force to Magic Formula tire parameters at 4 kN vertical tire load

Shape factor of the Magic Formula tire model a_0 is usually fixed to value of 1.3 and so in the identification it is assumed to be 1.3. Further total roll stiffness is the sum of front and rear roll stiffness and roll damping is the sum of the front and rear roll damping. However, to decrease the number of parameters it is assumed that front and rear roll stiffness values as well as front and rear roll damping are equal to each other.

Unknown parameter set becomes: $\{I_{zz}, I_{xx}, C_{\varphi}, K_{\varphi}, \tau, a_0, a_1, a_2, a_3, a_4, a_6, a_7, \delta_{\varphi f}, \delta_{\varphi r}\}$

Simulink model of the three DOF nonlinear roll model is shown in Figure 6.64.
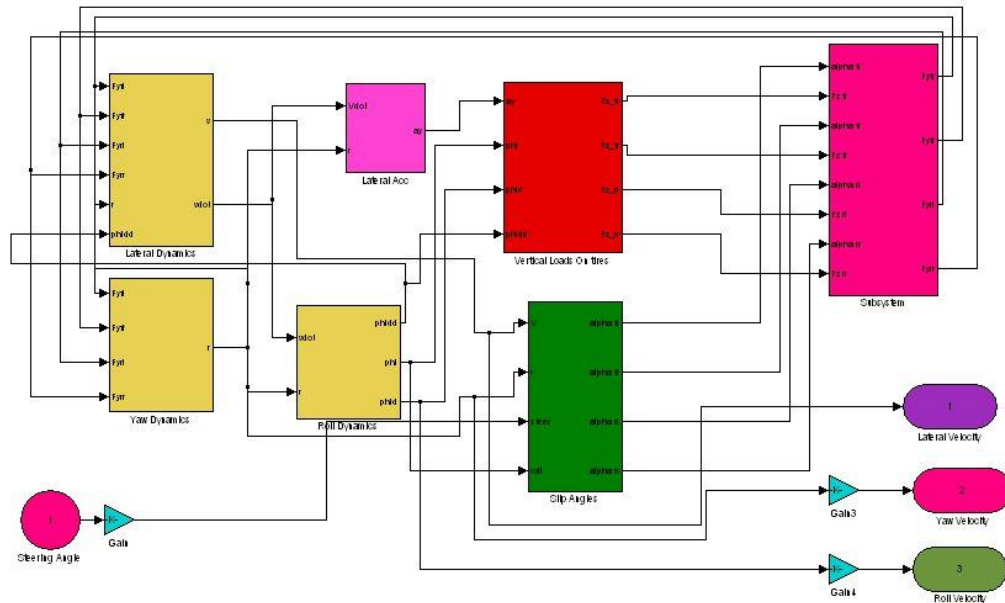
Figure 6.64: Simulink model of three DOF nonlinear roll model

To be able to excite the system over a wide operating point, data set is taken from simulation of ADAMS/Chassis model with high amplitude steering input. Vehicle longitudinal velocity used in the ADAMS simulation is fixed to 15 m/s. At 20m/s vehicle longitudinal velocity very high slip angles are observed at the first 2-3 second of the maneuver and then slip angles drops to low values rapidly. At 15m/s longitudinal velocity, smoother slip angle responses are obtained and therefore more accurate estimation is obtained. Data set used in the identification is given in Figure 6.65 to Figure 6.70 and estimated slip angles with vertical tire loads are given in Figure 6.71 to Figure 6.78.
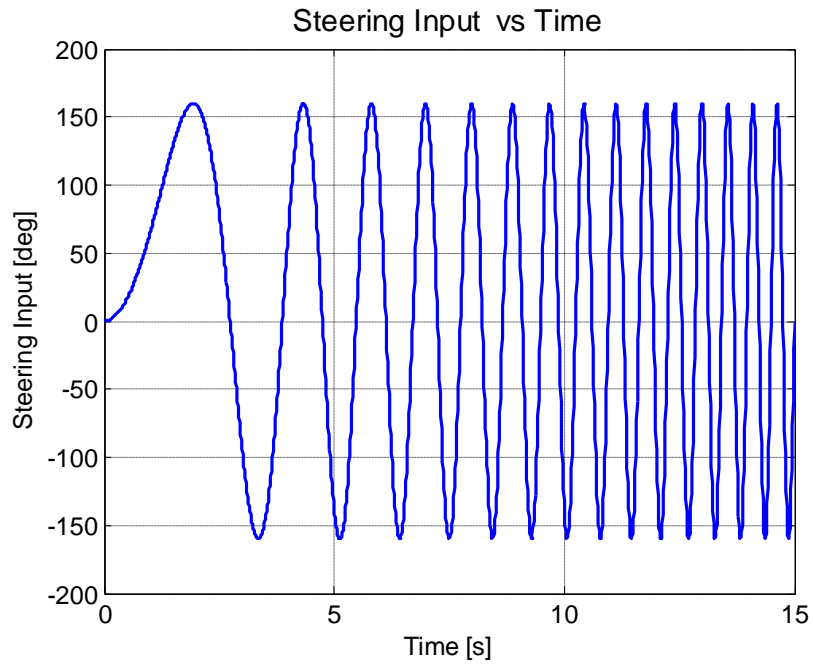
Figure 6.65: Steering wheel input for estimation process
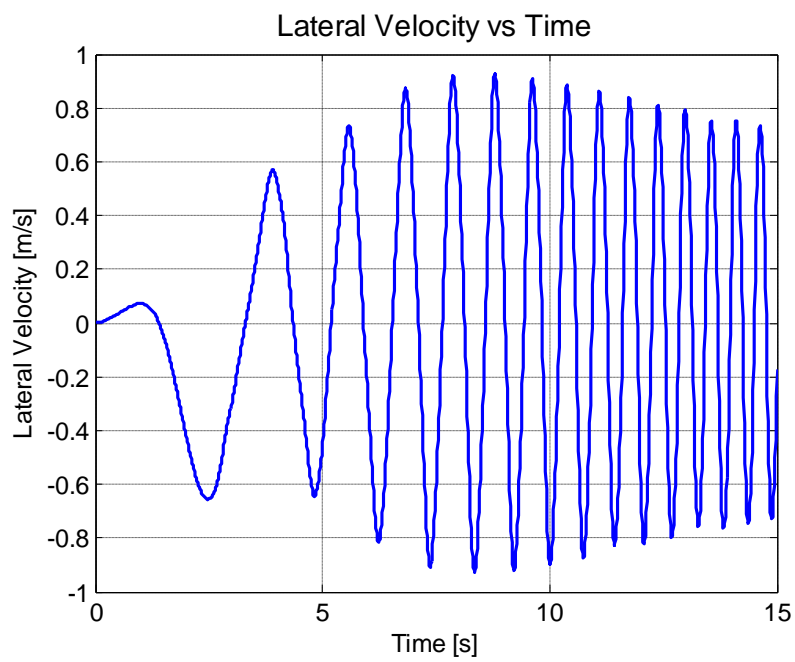
Figure 6.66: Lateral velocity response for estimation process

152
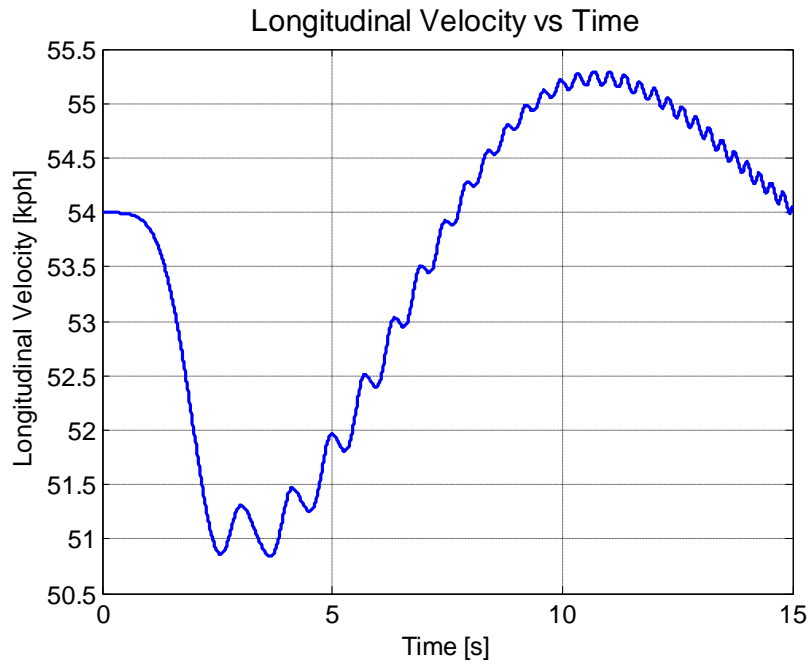
Figure 6.67: Longitudinal velocity response for estimation process
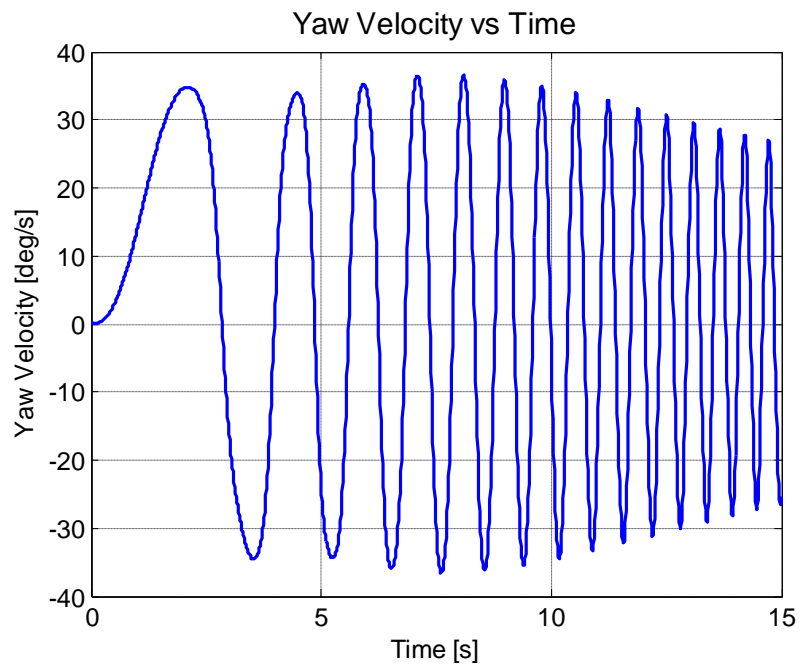
Figure 6.68: Yaw velocity response for estimation process

153
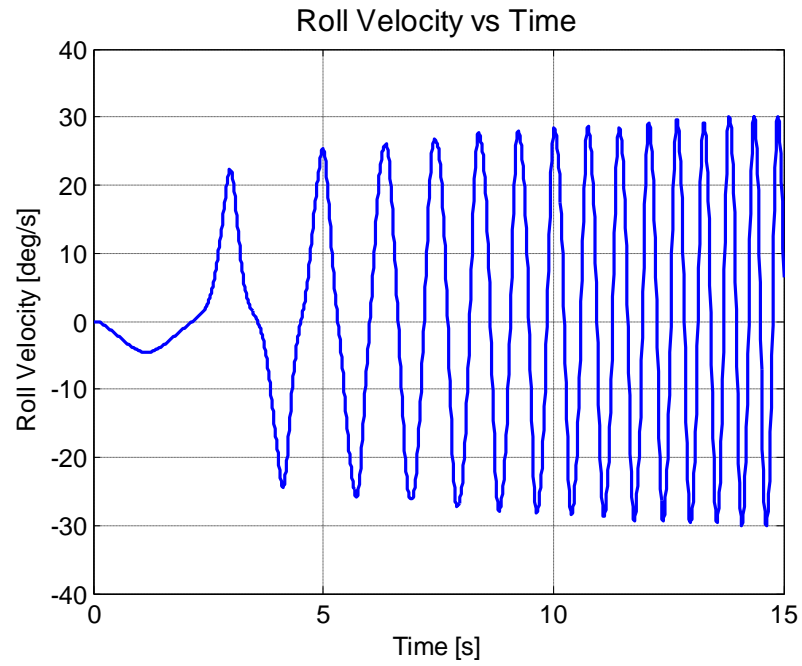
Figure 6.69: Roll velocity response for estimation process
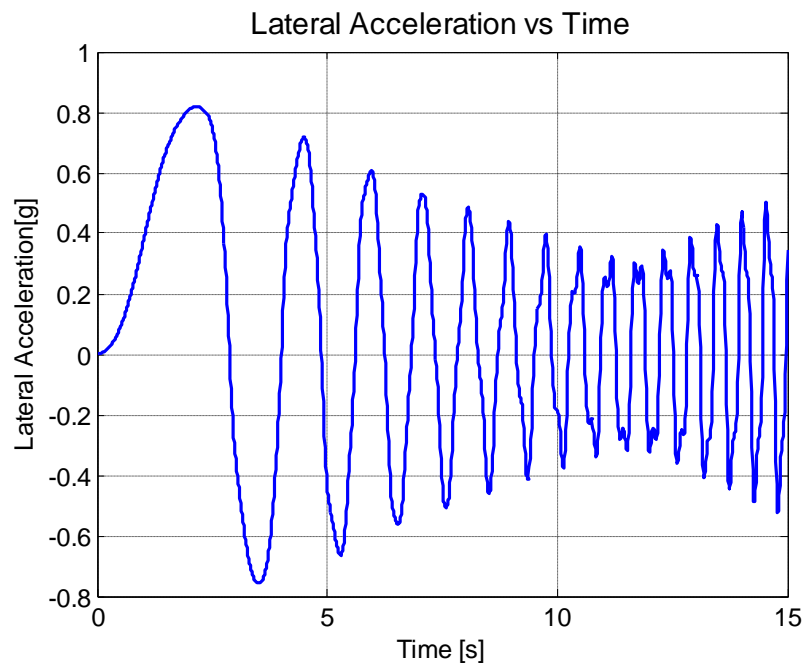
Figure 6.70: Lateral acceleration response for estimation process
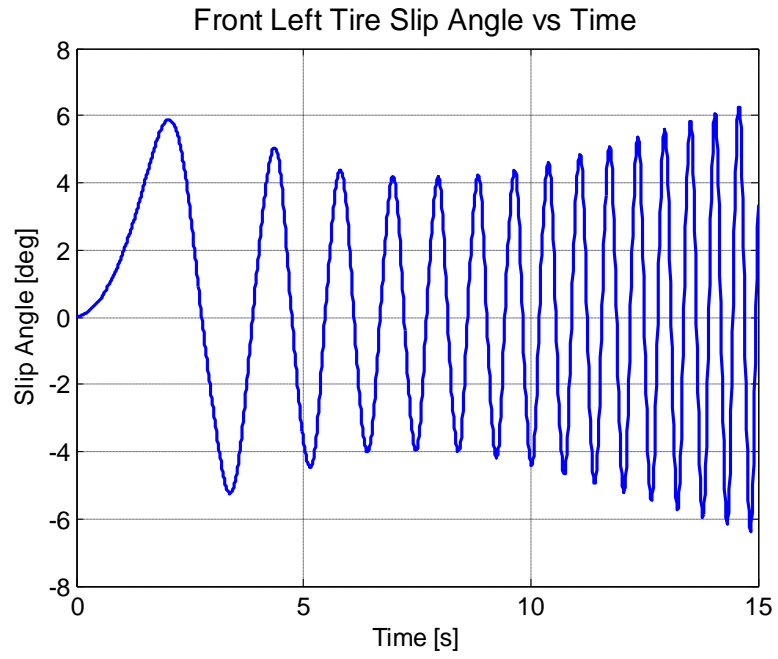
Figure 6.71: Front left tire slip angle
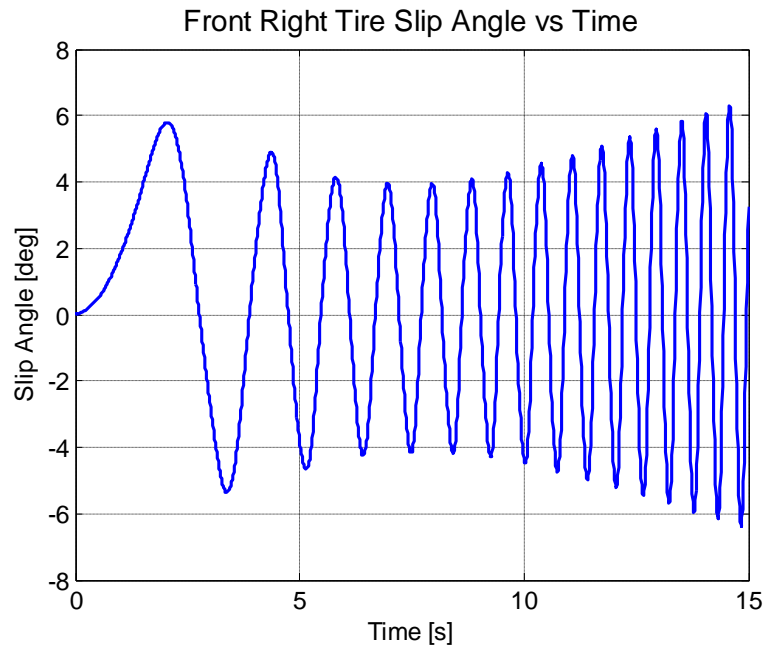
Figure 6.72: Front right tire slip angle

155
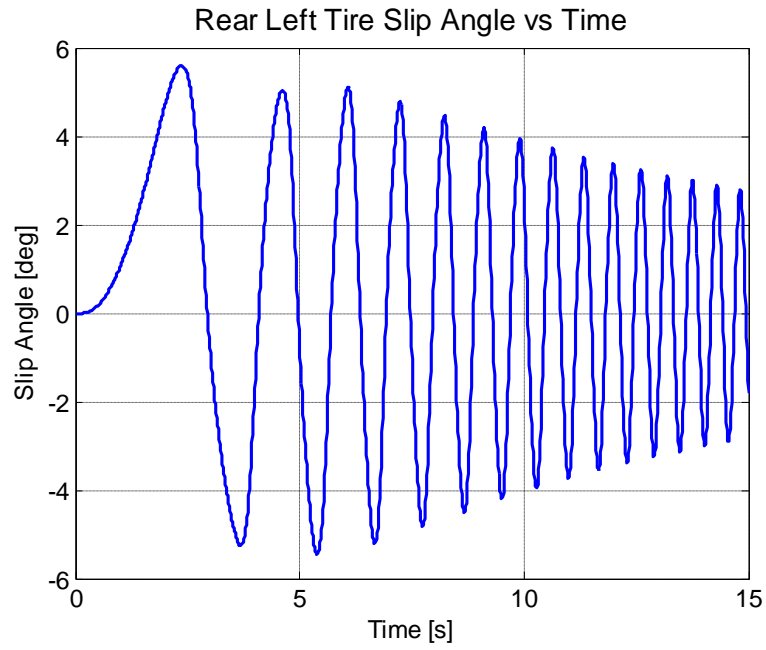
Figure 6.73: Rear left tire slip angle
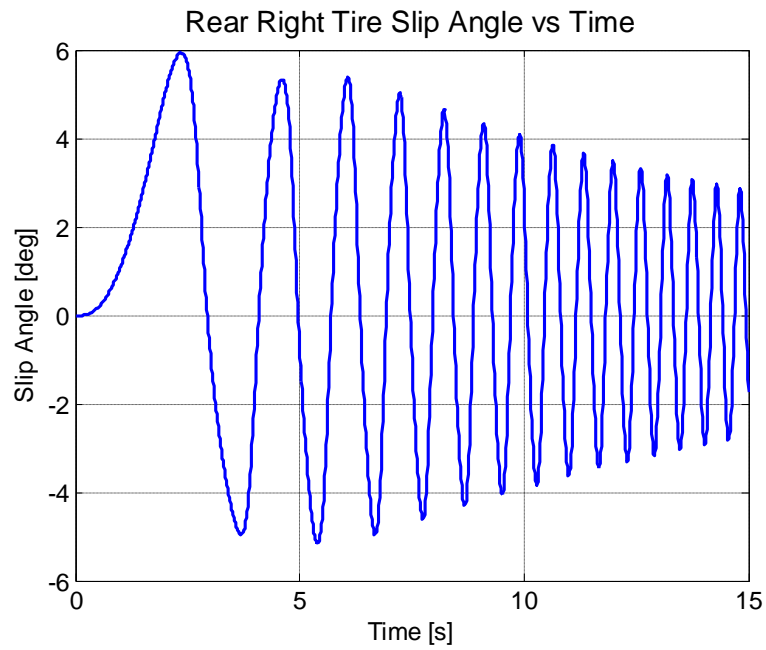
Figure 6.74: Rear right tire slip angle
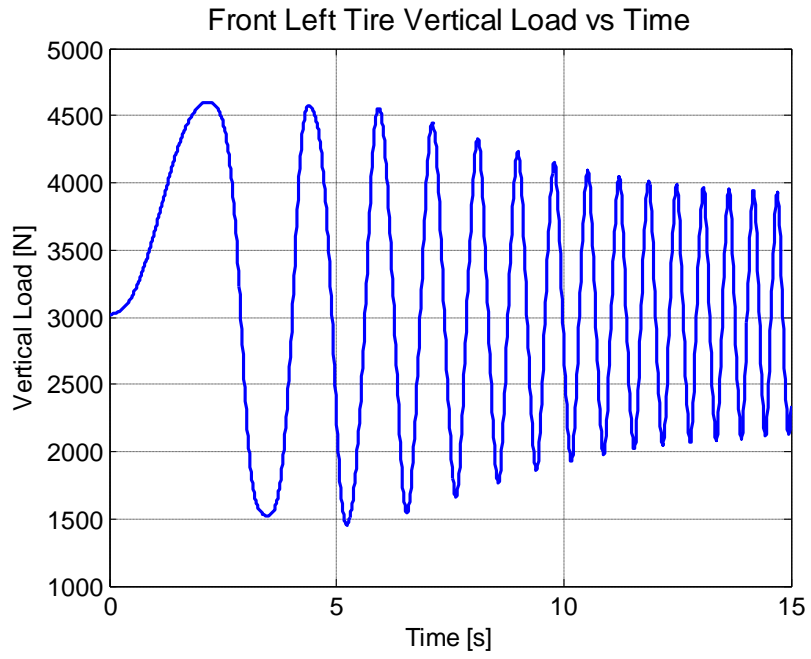
Figure 6.75: Front left tire vertical load
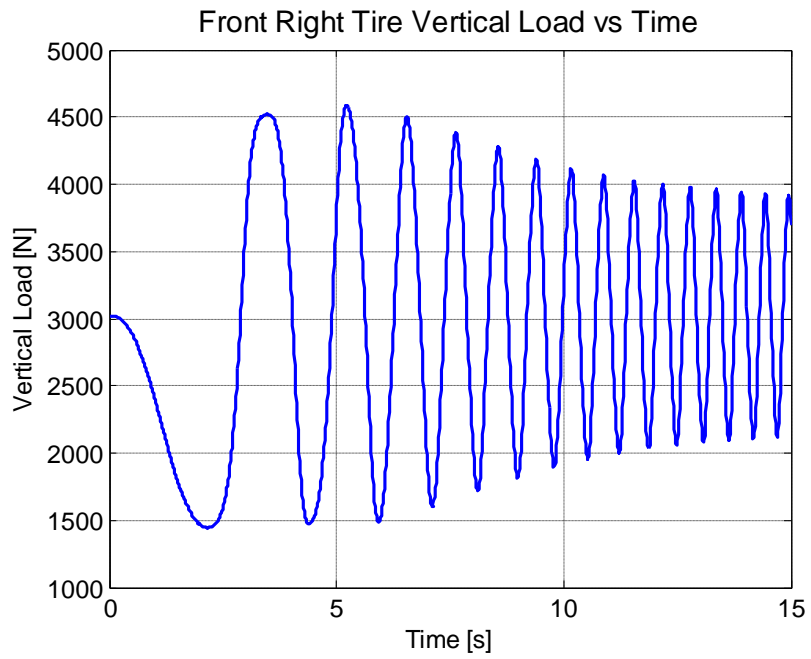
Figure 6.76: Front right tire vertical load
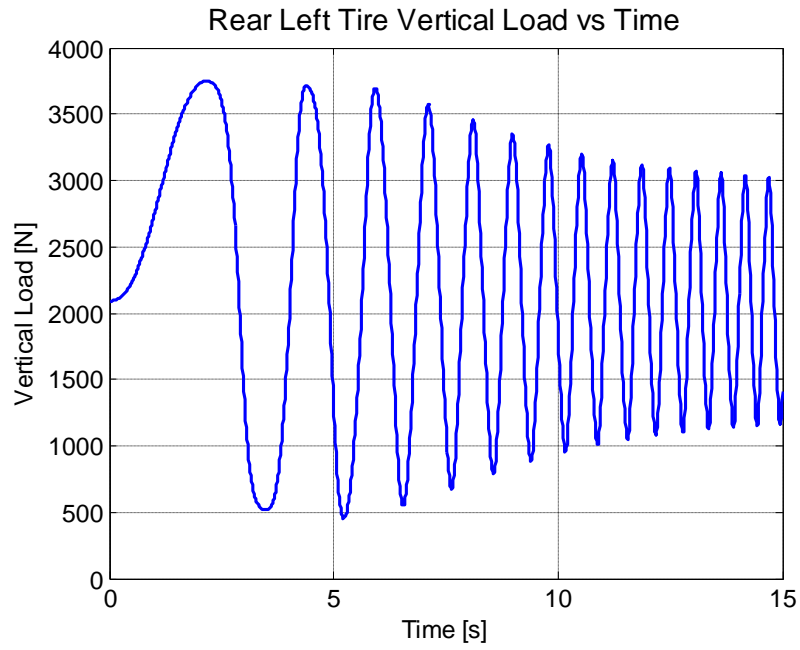
Figure 6.77: Rear left tire vertical load
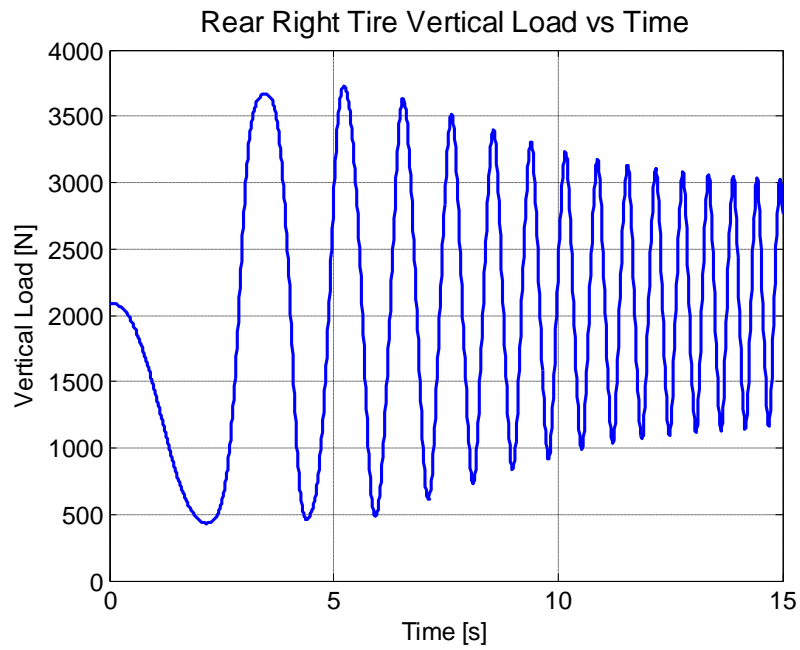
Figure 6.78: Rear right tire vertical load

158

As can be seen from slip angle versus time graphs, and vertical load versus time graphs, slip angle and load transfer are high enough to estimate tire model parameters; that is the vehicle maneuver stimulates the system such that Magic Formula tire can be identified.

To validate the identified system another data set is taken and is given in Figure 6.79 to Figure 6.84. To excite the vehicle in a wider operating range, a steering input with a wide range of frequencies together with high amplitude, shown in Figure 6.79, is used.
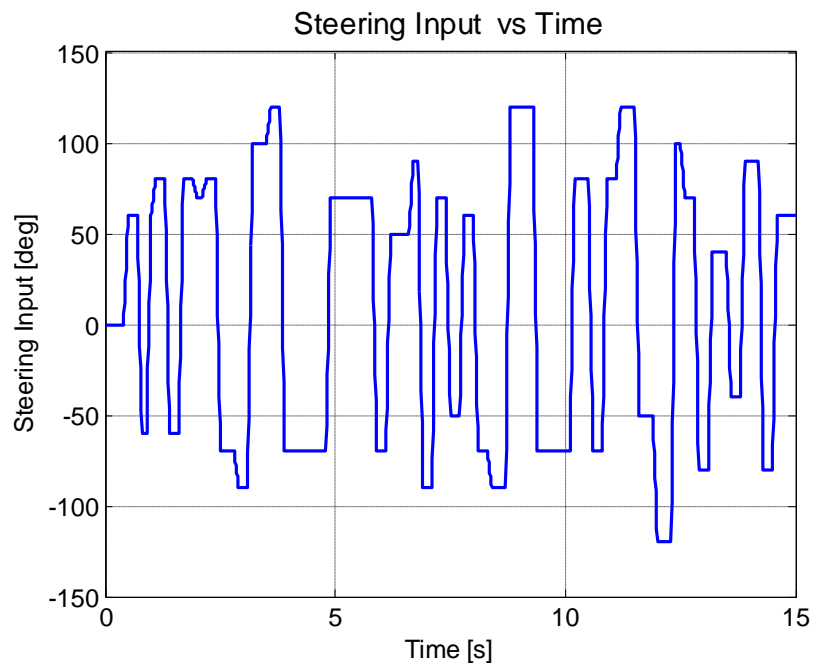
Figure 6.79. Steering wheel input for validation process
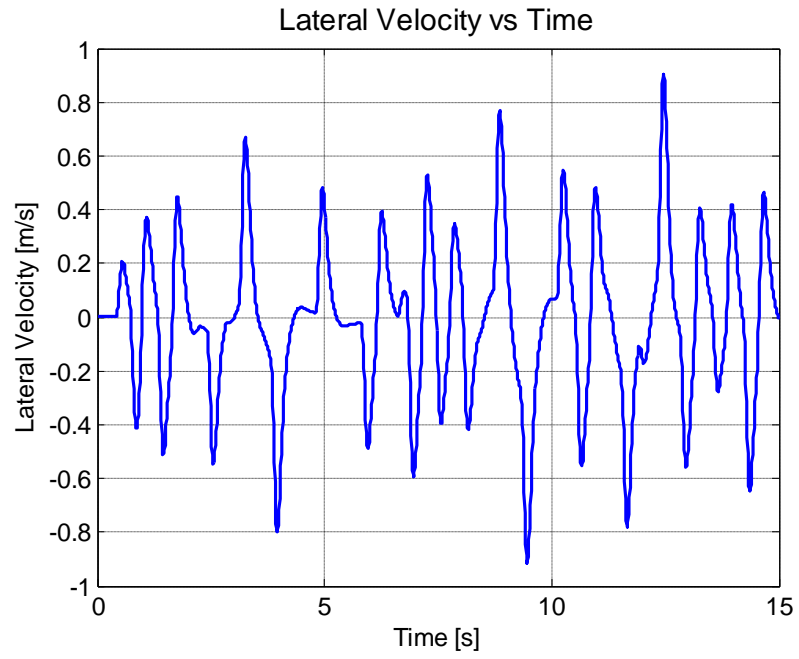
Figure 6.80: Lateral velocity response for validation process
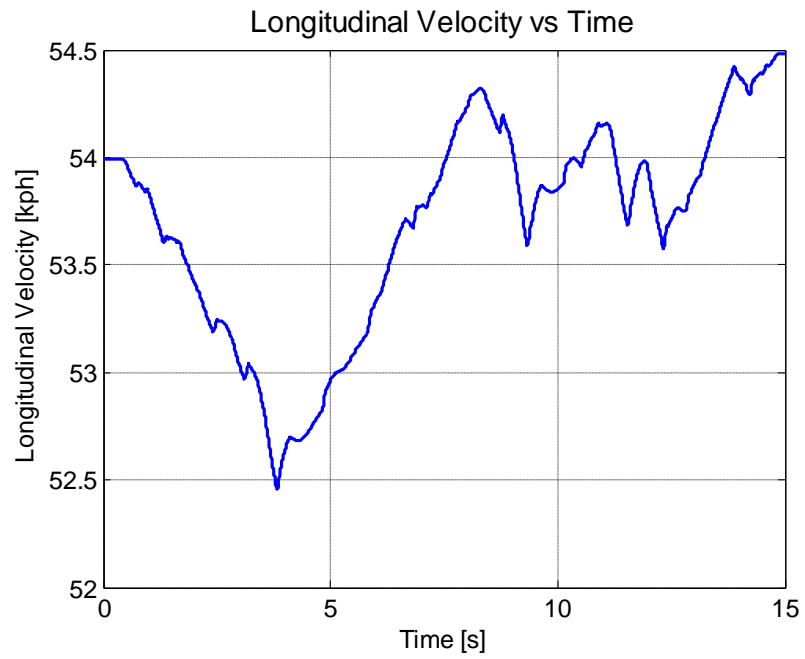
Figure 6.81: Longitudinal velocity response for validation process
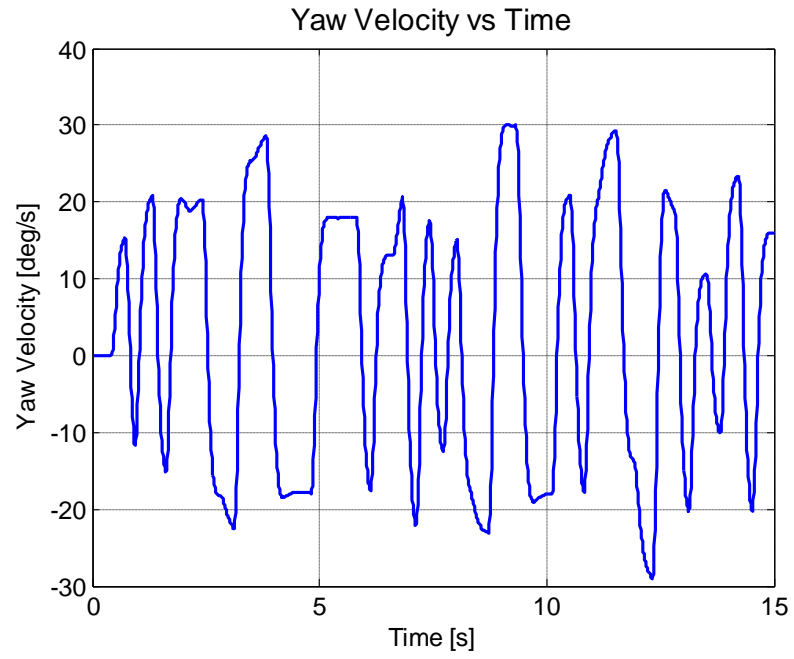
Figure 6.82: Yaw velocity response for validation process
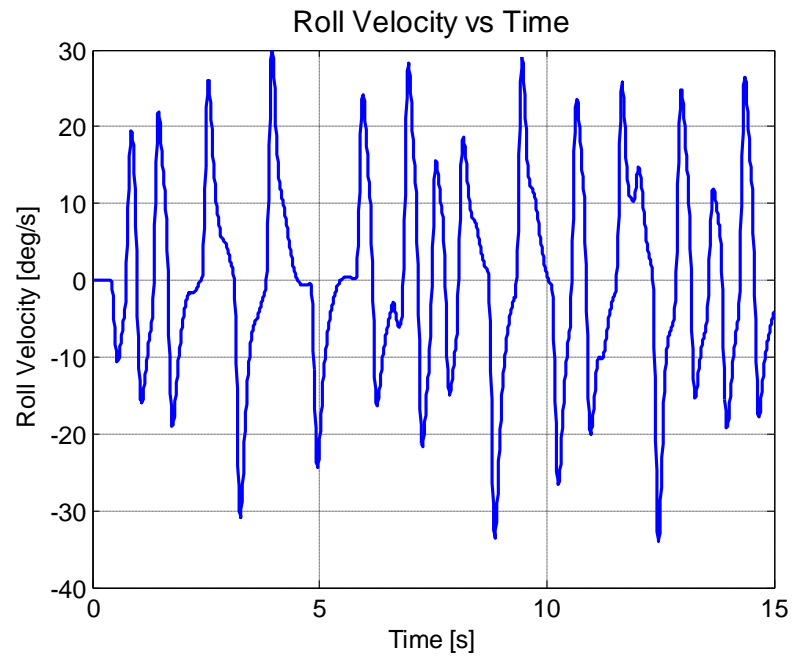
Figure 6.83: Roll velocity response for validation process
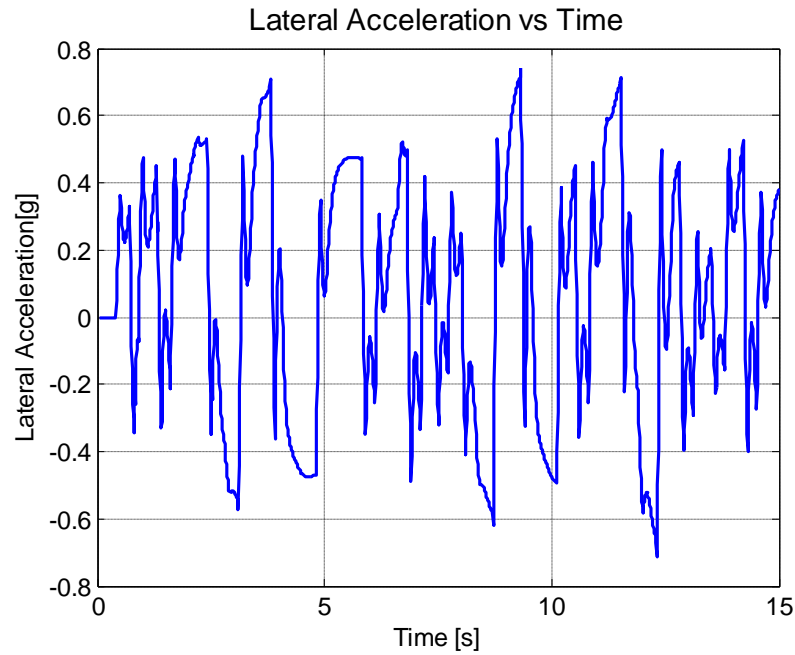
Figure 6.84: Lateral acceleration response for validation process

When the estimated and measured responses are compared from the estimation and validation processes, it can be seen that identified model track the actual responses satisfactorily. Tire forces taken from the ADAMS/Chassis model and the identified model are also compared in Figure 6.89 to Figure 6.92. From these figures it is seen that characteristic of the measured and identified tire forces are similar.

To simplify the estimation process upper and lower parameters constrained are inserted so that the parameter space to be searched is constrained. Also appropriate weighting factors are given to different responses according to result of the estimation. Estimated parameters are given in Table 6.9. Typical weighting factors used in the estimation for lateral, yaw, and roll velocities are 70, 1.2, and 1.6 respectively and these are determined according to aim of identification, order of magnitude of the responses, practical problems in experimentation etc.

Table 6.9: Estimated parameter values for the three DOF nonlinear roll model

I_{zz}=2051 kgm^2	I_{xx}=398 kgm^2	C_φ=2520 Nms	K_φ=37905 Nm	τ=0.026 s
a_0=1.3	a_1=-47	a_2=1291	a_3=67327	a_4=7.81
a_6=0.59	a_7=-1.97	$\delta_{f\varphi}$=0.29	$\delta_{r\varphi}$=0.01	

When the estimated parameters are examined, it can be seen that front roll steer coefficient, $\delta_{f\varphi}$, is large. This may due to the effect of the unmodeled part of the vehicle on the estimated parameter. It can be avoided by lowering the upper constraint on the roll steer coefficient, but in this case quality of the estimate decrease slightly. However, when the estimated and measured tire cornering forces are compared, it can be seen that estimation process is successful. Moreover, when the severity of the maneuver is increased, from the sensitivity analysis, it is expected to obtain more accurate result, yet due to nonlinearities of the vehicle, estimation process becomes more difficult. Other studies using different lower and upper constraints on parameters have been performed and sometimes slightly different Magic Formula tire model parameters have been estimated. This can be due to lack in the modeling or estimation of tire inputs such as vertical load and slip angle with low accuracy, or due to optimization algorithms, etc.

Cornering force characteristics of the identified tire model is given Figure 6.85.
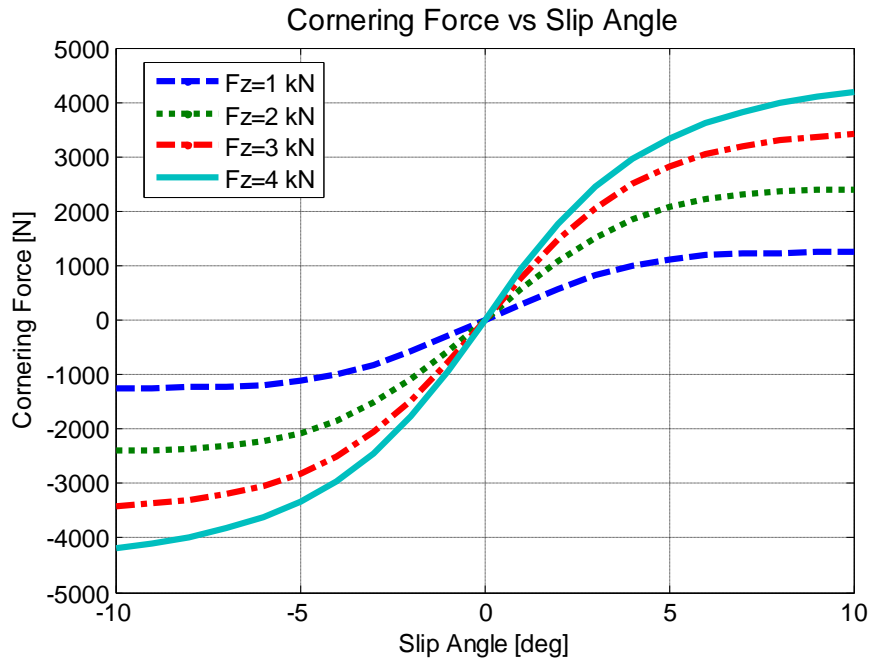
Figure 6.85: Cornering force characteristic of identified tire model

Estimated and measured responses are given in Figure 6.86 to Figure 6.88.
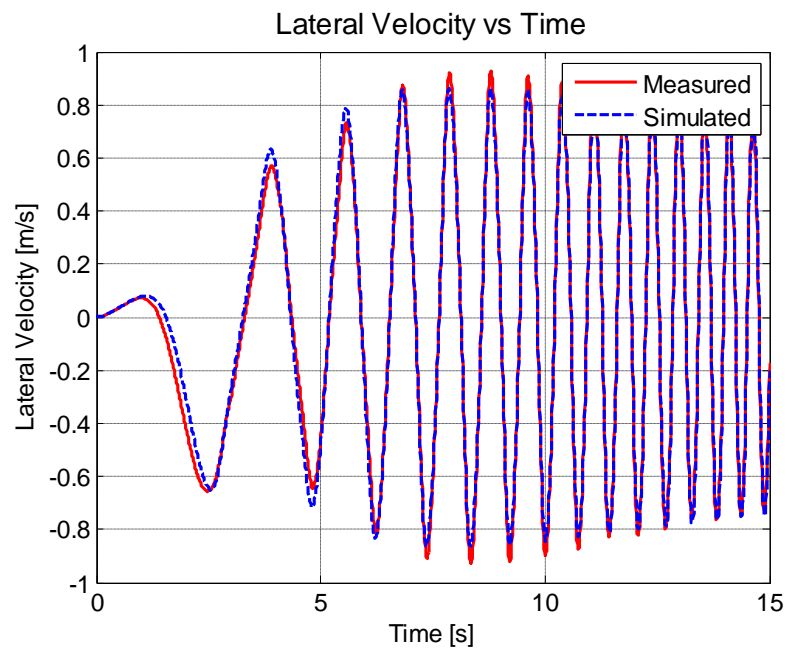
Figure 6.86: Estimated and measured lateral velocity responses

Yaw Velocity vs Time
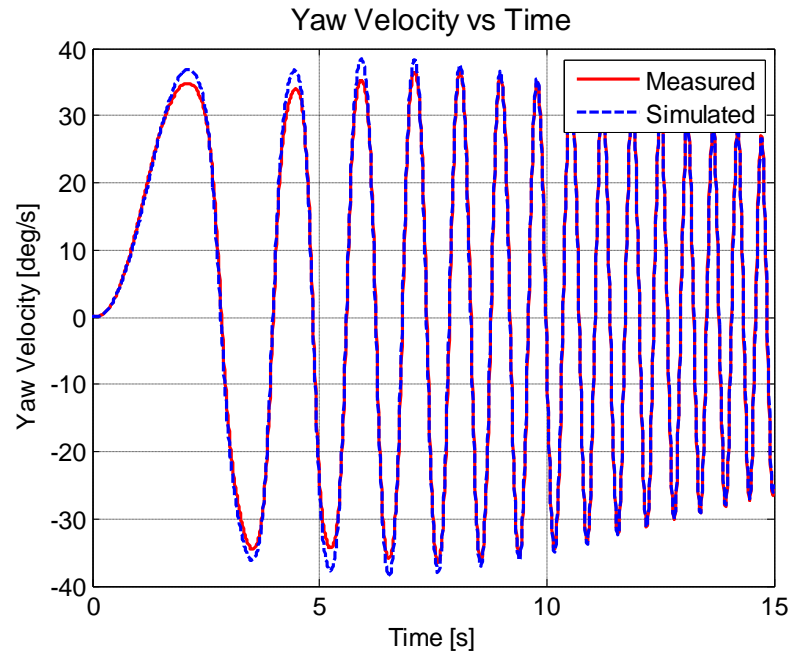
Figure 6.87: Estimated and measured yaw velocity responses

Roll Velocity vs Time
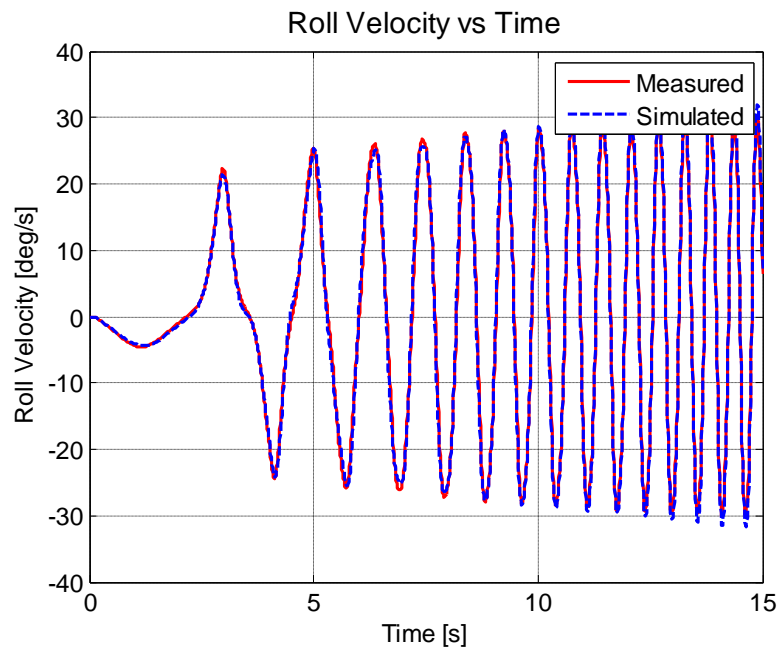
Figure 6.88: Estimated and measured roll velocity responses

Measured and estimated tire lateral forces are given in Figure 6.89 to Figure 6.92.
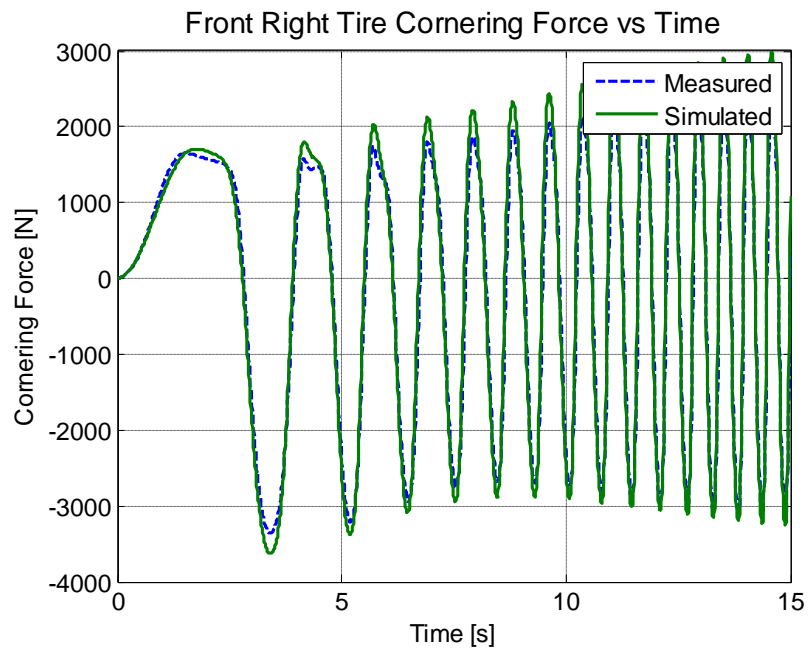
Figure 6.89: Estimated and veasured front right tire cornering force
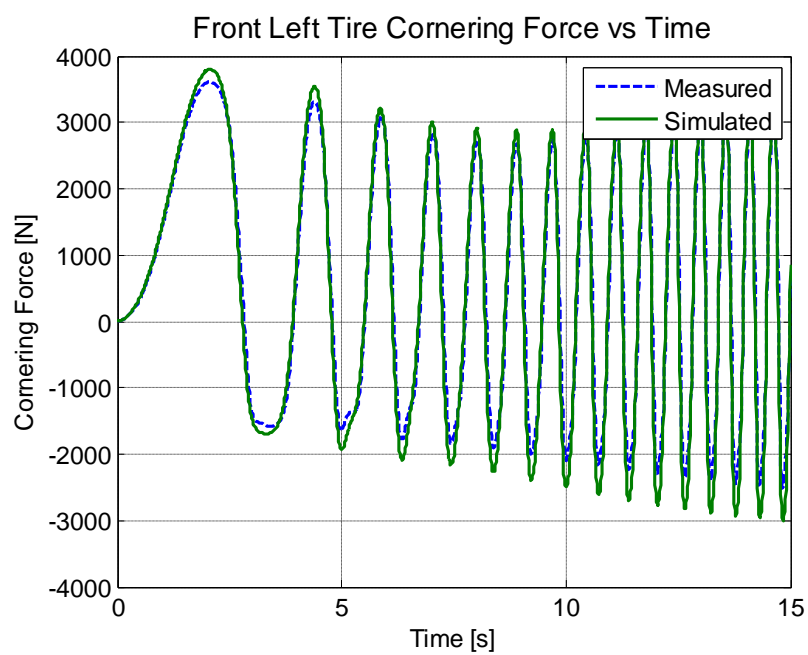
Figure 6.90: Estimated and measured front left tire cornering force
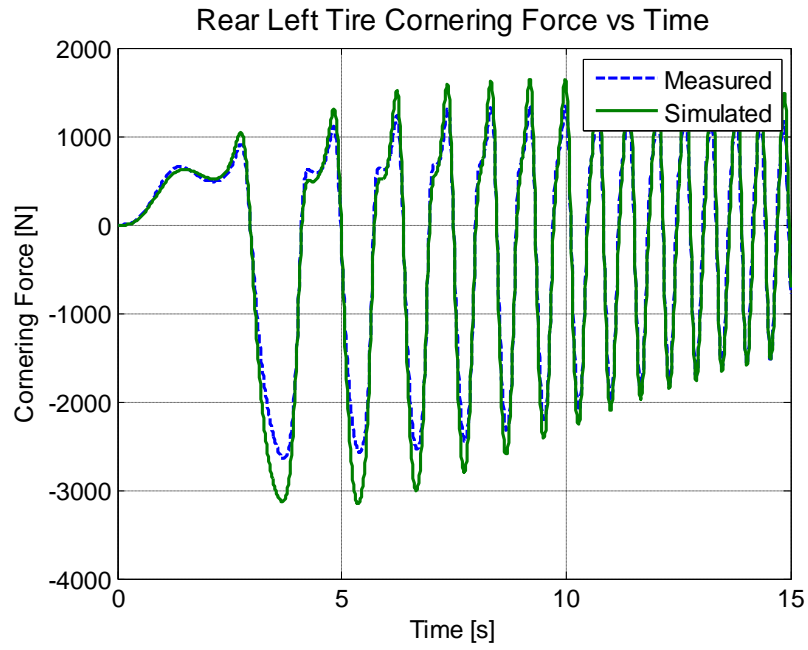
Figure 6.91: Estimated and measured rear left tire cornering force
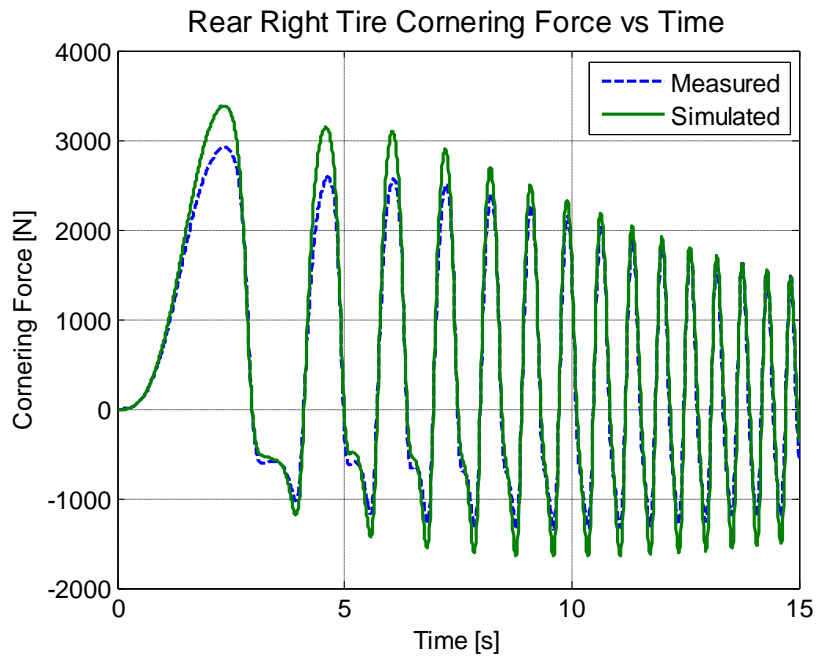
Figure 6.92: Estimated and measured rear right tire cornering force

Estimated and validated responses for model validation are given in Figure 6.93 to Figure 6.95.
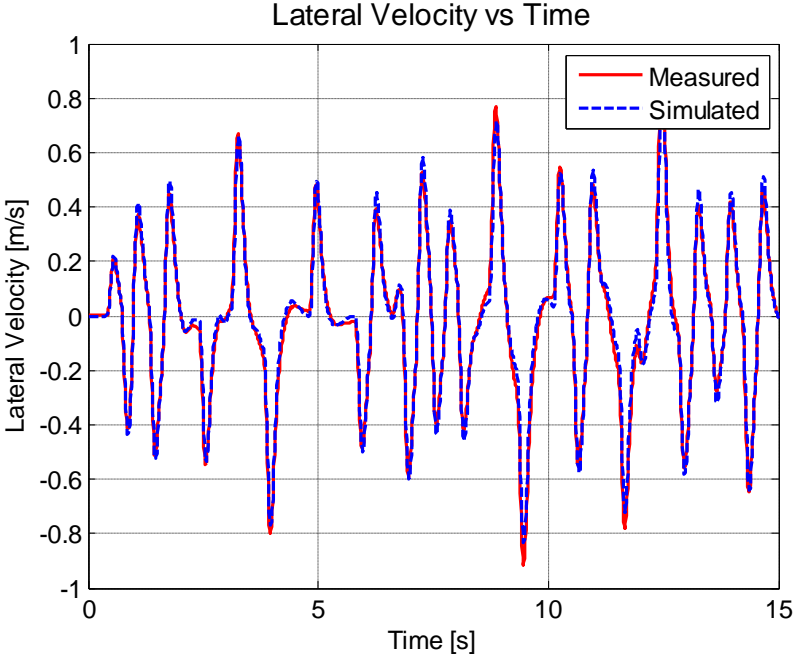
Figure 6.93: Estimated and measured lateral velocity responses for validation process
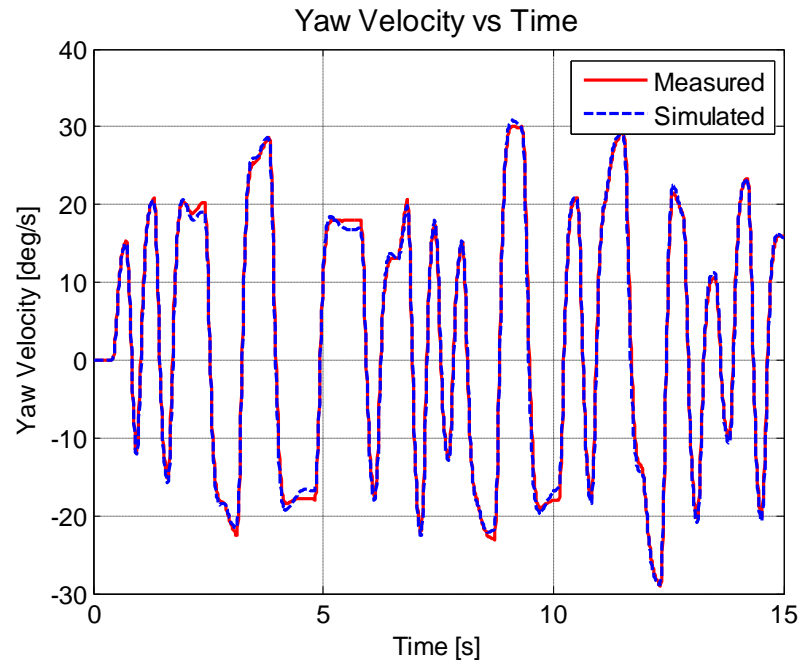
Figure 6.94: Estimated and measured yaw velocity responses for validation process
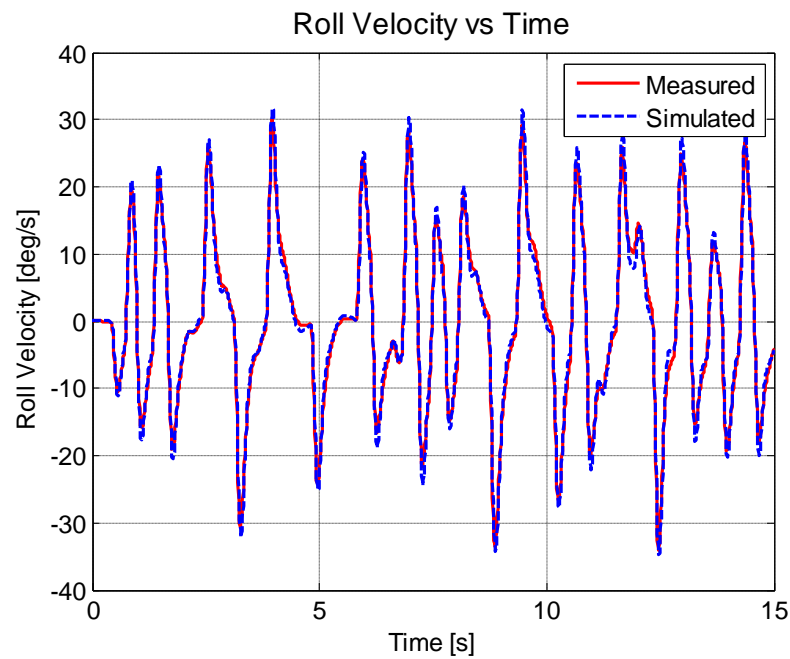
Figure 6.95: Estimated and measured roll velocity responses for validation process

169

Though the ADAMS vehicle model with PAC2002 [8] tire model are quite complex (it has more than 100 parameters), their handling response characteristics can be predicted successfully even for highly severe maneuvers. Tire system is highly nonlinear and complex, and there are uncertainties in it; thus modeling of the tire is a difficult process especially for wide operating ranges. As shown in this study, Magic Formula tire parameters together with vehicle parameters can be estimated such that the estimated vehicle responses track actual responses successfully. However, estimated parameters may not correspond to their actual values, since these parameters may compensate the unmodeled part of the system in the simple handling model. To ease the estimation and to guarantee estimate, physical parameters upper and lower parameter constrained are imposed on the parameters for estimation process.

CHAPTER 7

DISCUSSION AND CONCLUSION

The objective of this study was the identification of handling models from multibody dynamics vehicle model. In particular, identification of Magic Formula tire model parameters was studied in some detail.

In this study, a methodology was given for identification of low order vehicle handling model from Multibody dynamics vehicle models. Simple handling models which are two DOF linear bicycle model and one DOF roll model, and more complex vehicle handling models which are three DOF linear and nonlinear roll model were identified form the test data acquired from the simulation of ADAMS/Chassis vehicle model. Three DOF nonlinear roll model was constructed with the well known and commonly used Magic Formula tire model with transient characteristics. ADAMS/Chassis vehicle model has subsystems which are front and rear suspension subsystems, steering subsystem, chassis subsystem and front and rear tire subsystems and it has nearly 100 degrees of freedom. Tire model used in the ADAMS/Chassis vehicle model is a version of the Magic Formula tire model which calculates combined braking/traction and cornering force considering transient characteristic of tire. Therefore, ADAMS/Chassis vehicle model is assumed to represent real vehicle dynamics completely.

In this study four vehicle models; namely the bicycle model with steady state and transient tire models, one DOF roll model, three DOF linear roll model, and three DOF nonlinear roll model with Magic Formula tire model were used. At small slip angles tire cornering force is linearly proportional to slip angles and thus at linear

operating range of the vehicle linear tire model can be used. However at high slip angle tire cornering force changes nonlinearly with slip angle and thus Magic Formula tire model was used. To use Magic Formula vertical load on each tire is required so in the three DOF nonlinear roll model lateral load transfer were also modeled. Transient property of the tire alters cornering forces thus it was also included. These models were constructed in Simulink environment and the cost function was formed directly by the Simulink Parameter Estimation Toolbox.

To determine the effects of parameters on the model responses and to determine frequency range of test input, a detailed sensitivity analysis was performed in frequency domain for bicycle model and three DOF roll model for different longitudinal velocities. Sensitivities of the lateral, yaw, and roll velocities to model parameters were calculated. According to these results, frequency ranges at which sensitivity values are high and natural frequencies of the model are included were selected as the steering input parameters. Sine chirp input with the determined frequency range was used as the steering input.

To determine whether the model to be identified is unique or not, structural identifiability analysis for each model with different outputs and output set were performed. For structural identifiability analysis there are various methods. Algebraic methods are sometimes very difficult to apply especially for the nonlinear models with large number of parameters. In this thesis, Numerical Local Approach is used for identifiability analysis. According to this method data is acquired from the simulation of the model with nominal parameter values. Then using these nominal parameters values as the initial values at estimation, quadratic cost function is optimized with a second order optimization method like Gauss-Newton. If the estimator is stable, then model is s.l.i and estimated parameters converge to their nominal values. According to result of this method, the bicycle model with steady state and transient tire models with the selected unknown parameters are identifiable for only lateral velocity, for only yaw velocity, and for both lateral and yaw velocities. That is by using only one output bicycle model can be identified.

However, structural identifiability analysis does not guarantee accurate identification. As shown in the parameter estimation chapter, identification using lateral and yaw velocity responses produce more accurate results. After the bicycle model, identifiability of the one DOF roll model with specified parameters was shown. Finally, it was shown that linear and nonlinear roll model with lateral velocity, yaw velocity, and roll velocity outputs with specified parameters are structurally locally identifiable.

After identifiability and sensitivity analysis, handling models were identified. Optimization process was performed by nonlinear least square, simplex search and genetic algorithms and sometimes with combination of these. The bicycle model with steady state and transient tire model was identified by using only lateral velocity, only yaw velocity, and both lateral and yaw velocity. According to identification results using both responses improves identification results. One DOF roll model requires lateral acceleration and roll velocity. Three DOF linear roll model was identified by using lateral velocity, yaw velocity, and roll velocity. For vehicle maneuvers performed in linear operating ranges, identification process is relatively easy, and estimated responses track the measured responses accurately.

Identified linear models were validated by data taken from the double lane change simulation. Result of the validation process showed the validity of the identified model. Three DOF nonlinear roll model was constructed with Magic Formula tire model and it included lateral load transfer to calculate vertical load on tire. According to sensitivity analysis, high slip angles are required to identify tire model. Therefore, identification data is taken from the simulation with a high amplitude steering input to cover a high slip angle region. With this dataset, parameters of the tire and vehicle were identified from the lateral velocity, yaw velocity, and roll velocity data. It was shown that estimated responses track the measured responses successfully. Tire cornering forces taken from the ADAMS and from the identified model were also compared and it was observed that they correspond to each other well. To validate the identified model another data set was

taken and the identified model was successfully validated. More accurate results of the Magic Formula tire model identification are obtained from advanced tire test setups. The tire to be identified is tested under different loading and operating conditions like different camber angles, vertical loads, slip angles and combined braking and cornering, and thus tire characteristics are identified experimentally. However, by making vehicle tests and using standard sensor sets, cornering force characteristic of the Magic Formula tire model was identified in this study, together with suspension parameters and inertial vehicle parameters. Large number of unknown vehicle parameters brings about its own disadvantage such that different parameters even unphysical parameters can be estimated. Constraining the parameter values may solve this problem, yet to do this a priori knowledge about vehicle is required. Nonetheless, constraining parameters may decrease the accuracy of the estimation. Therefore there is a trade off and according to the aim of the study desired precautions may be taken. In literature on vehicle handling identification there are a limited number of studies about nonlinear vehicle handling identification especially related with Magic Formula tire model. Work towards the identification of the Magic Formula parameters given in this study is believed to be a contribution to the limited amount of investigation available in the literature.

As a future study more complicated vehicle handling models comprising longitudinal motion may be identified. Also while identifying nonlinear roll model, front and rear tire may be modeled separately and thus a more general model can be obtained. In addition, in this study practical difficulties like noise in data, signal to noise ratio, or placement of sensor, steering robot, etc. are not considered; yet in future studies these issues can also be taken into account for a more realistic study.

REFERENCES

[1]   Jazar, Reza, N., "Vehicle Dynamics: Theory and Application" Springer, 2008.

[2]   Ljung, L., "System Identification: Theory for the User". Prentice Hall PTR, 2nd Edition, 1999.

[3]   Arikan, K., B., "Identification of Handling Models for Road Vehicles", PhD. Thesis, The Graduate School of Natural and Applied Sciences, Middle East Technical University, 2008.

[4]   Tekin, G., "Design and Simulation of an Integrated Active Yaw Control System for Road Vehicles", M.Sc. Thesis, The Graduate School of Natural and Applied Sciences, Middle East Technical University, 2008.

[5]   Şahin, M., "Design and Simulation of an ABS for an Integrated Active Safety System for Road Vehicles", M.Sc. Thesis, The Graduate School of Natural and Applied Sciences, Middle East Technical University, 2007.

[6]   MSC Software Corporation, "ADAMS/Chassis Help Documentations".

[7]   MSC Software Corporation, "ADAMS/Chassis Software".

[8]   MSC Software Corporation, "ADAMS/Tire Help Documentations".

[9]   Bolhasani, M.R., Azadi, S., "Parameter Estimation of Vehicle Handling Dynamics Using Genetic Algorithm", Scientia Iranica, Vol. 11, Nos. 1&2, pp 121-127.

[10]   Alloum, A.,Charara, A, Machkour, H., "Parameters Nonlinear Identification for Vehicle's Model", Proceedings of the 1997 IEEE International Conference on Control Applications Hartford, CT October 5-7, 1997.

[11] Abdellatif, H., Heimann, B., Hoffmann, J., "Nonlinear Identification of Vehicle's Coupled Lateral and Roll Dynamics", Proceedings. of the 11th IEEE Mediterranean Conference on Control and Automation, MED03, Rhodes, Greece, 2003.

[12] Arndt, M., Ding, E., L., Massel, T., "Identification of Cornering Stiffness During Lane Change Maneuvers", Proceedings of the 2004 IEEE International Conference on Control Applications Taipei, Taiwan, September 2-4, 2004.

[13] Sierra, C., Tseng, E., Jain, A. and Peng, H., (2006), "Cornering stiffness estimation based on vehicle lateral dynamics", Vehicle System Dynamics, 44:1, 24 – 38.

[14] Wesemeier, D., & Isermann, R., "Identification of vehicle parameters using stationary driving maneuvers.", Control Engineering Practice, (2008), doi:10.1016/j.conengprac.2008.10.008.

[15] Abdellatif, H., Heimann, B., "Accurate Modeling and Identification of Vehicle's Nonlinear Lateral Dynamics", Preprints of the 16th IFAC World Congress, Praha2005, Prag, Czech Republic, 2005.

[16] Ryu, J., "State and Parameter Estimation for Vehicle Dynamics Control Using GPS", PhD. Thesis, Department of Mechanical Engineering and The Committee on Graduate Studies, Stanford University, 2004.

[17] Bolzern, P., Cheli, F., Falciola, G. and Resta, F. (1999), "Estimation of the Non-Linear Suspension Tire Cornering Forces from Experimental Road Test Data", Vehicle System Dynamics, 31:1, 23 – 34.

[18] Yu, N., "Yaw-Control Enhancement for Buses by Active Front-Wheel Steering", PhD. Thesis, The Graduate School Department of Mechanical and Nuclear Engineering, The Pennsylvania State University, 2007.

[19] Cabrera, J. A., Ortiz, A., Carabias, E. and Simon, A. (2004), "An Alternative Method to Determine the Magic Tire Model Parameters Using Genetic Algorithms", Vehicle System Dynamics, 41:2,109 – 127.

[20] Oosten, van J.,J.,M., and Bakker, E., "Determination of Magic Tyre Model Parameters", Proceedings of 1st International Colloquium on Tyre models for Vehicle Dynamics Analysis, held in Delft, The Netherlands, October 21-22, 1991.

[21] Cadiou, J. C., Hadri, A. El., **"Transversal Tyre Road Characteristic Estimation"**, Proc. Instn Mech. Engrs, Vol. 218, Part D: J. Automobile Engineering.

[22] Klein, V., Morelli, E., A., "Aircraft System Identification: Theory and Practice". American Institute of Aeronautics and Astronautics, 2006.

[23] CORRSYS-DATRON, CORRSYS-DATRON,
http://www.corrsys-datron.com
http://www.corrsys-datron.com/data_acq_sw.htm, 2 February 2010.

[24] CORRSYS-DATRON, CORRSYS-DATRON,
http://www.corrsys-datron.com
http://www.corrsys-datron.com/optical_sensors.htm, 1 October 2009.

[25] Industrial Measurement Solutions Pty Ltd, Industrial Measurement Solutions,
http://www.measure.com.au/
http://www.measure.com.au/vehicle_dynamics_and_mapping/in_vehicle_robots/index.php, 1 October 2009.

[26] Industrial Measurement Solutions Pty Ltd, Industrial Measurement Solutions,
http://www.measure.com.au/
http://www.measure.com.au/vehicle_dynamics_and_mapping/mechanical_sensors/index.php, 1 October 2009.

[27] Pintelon, R., Schoukens, J., "System Identification A Frequency Domain Approach", IEEE press, 2001.

[28] Nelles, O., **"Nonlinear System Identification: From Classical Approaches to Neural Networks and Fuzzy Models",** Springer, 2001.

[29] Rao, S., S., "Engineering Optimization Theory and Practice". Wiley, 3rd Edition, New York, 1996.

[30] Chong, Edwin K. P., Zak, Stanislaw H., "An Introduction to Optimization". 3rd Edition, Wiley-Intersience, 2008.

[31] The Mathworks Inc., "MATLAB Simulink Parameter Estimation User's Guide", 2008.

[32] Pacejka, H., B., Bakker, E., "The Magic Formula Tyre Model", Proceedings of 1st International Colloquium on Tire models for Vehicle Dynamics Analysis, held in Delft, The Netherlands, October 21-22,1991.

[33] Loeb, J.S., Guenther, D.A., Chen, H.F., Ellis J.R., "Lateral Stiffness, Cornering Stiffness and Relaxation Length of the Pneumatic Tire", SAE Technical Paper Series, Document Number 900129, SAE International Congress and Exposition, 1990.

[34] Heydinger, G.J., Garrott, W.R., Chrstos, J.P., "The Importance of Tire Lag on Simulated Transient Vehicle Response", SAE Technical Paper Series, Document Number. 910235, 1991.

[35] Rajamani, R., "Vehicle Dynamics and Control", Springer, 2006.

[36] Nalecz, Andrzej G., "Application of Sensitivity Methods to Analysis and Synthesis of Vehicle Dynamics Systems", Vehicle System Dynamics, 18(1989), pp.1-44.

[37] Walter, E., Pronzato, L, "Identification of Parametric Models from Experimental Data", Springer, 1997.

[38] Bonate, P. L., Howard, D. R., "Pharmacokinetics in Drug Development: Clinical Study Design and Analysis, Volume 1", AAPS Press, 2004.

[39] Pacejka H. B., "Tyre and Vehicle Dynamics", Elsevier, 2nd Edition, 2006.

[40] Blundell, M. V., "The Modelling and Simulation of Vehicle Handling Part 3: Tyre Modelling", Proc Instn Mech Engrs, Vol 214, Part K.

APPENDIX A

SENSITIVITY ANALYSIS

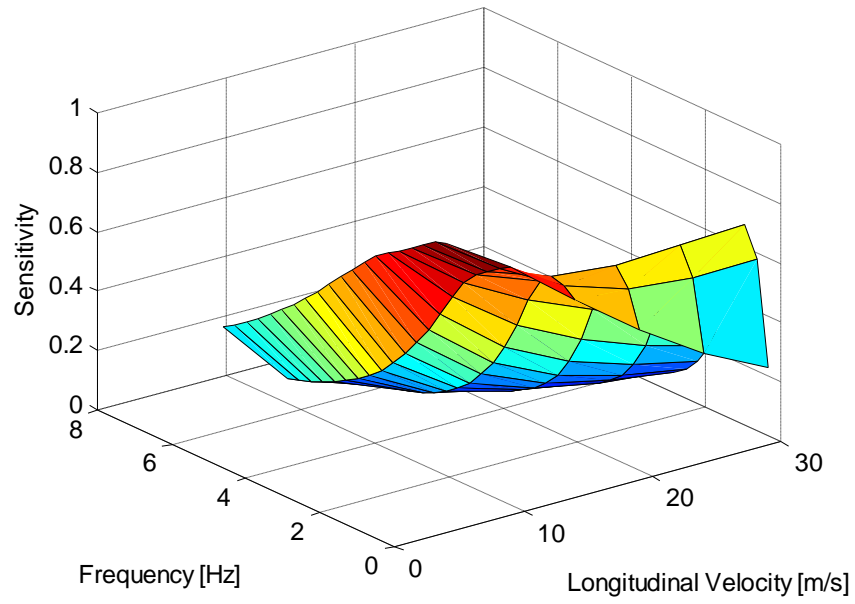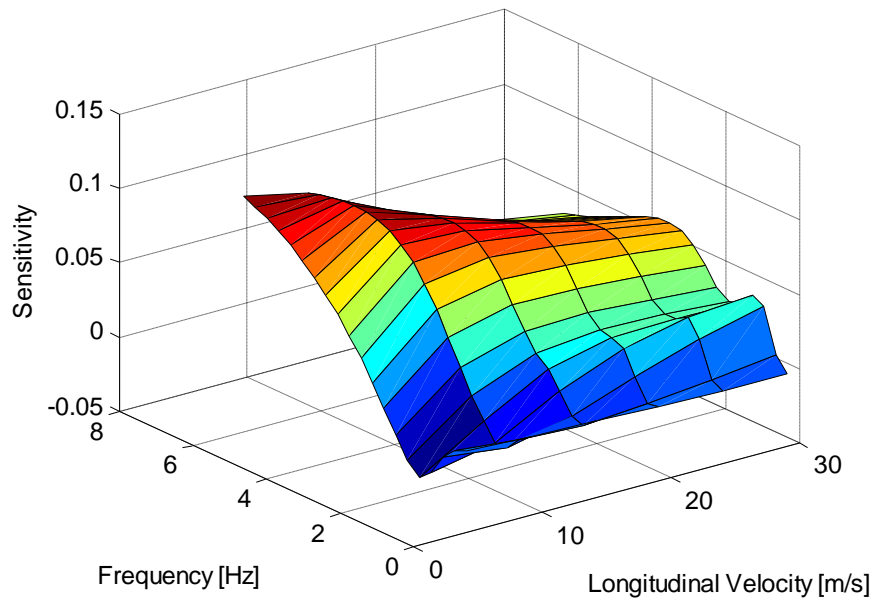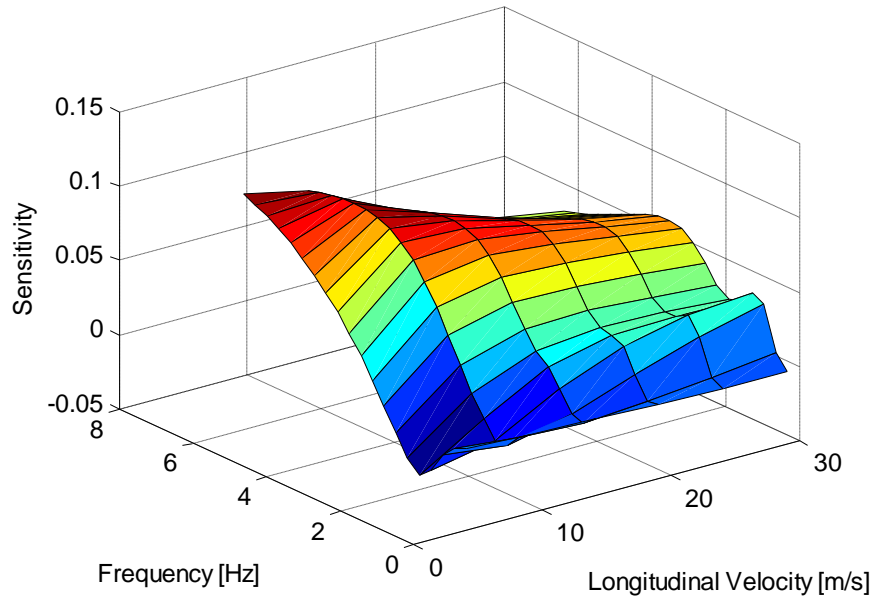## A.1. BICYCLE MODEL SENSITIVITY ANALYSIS
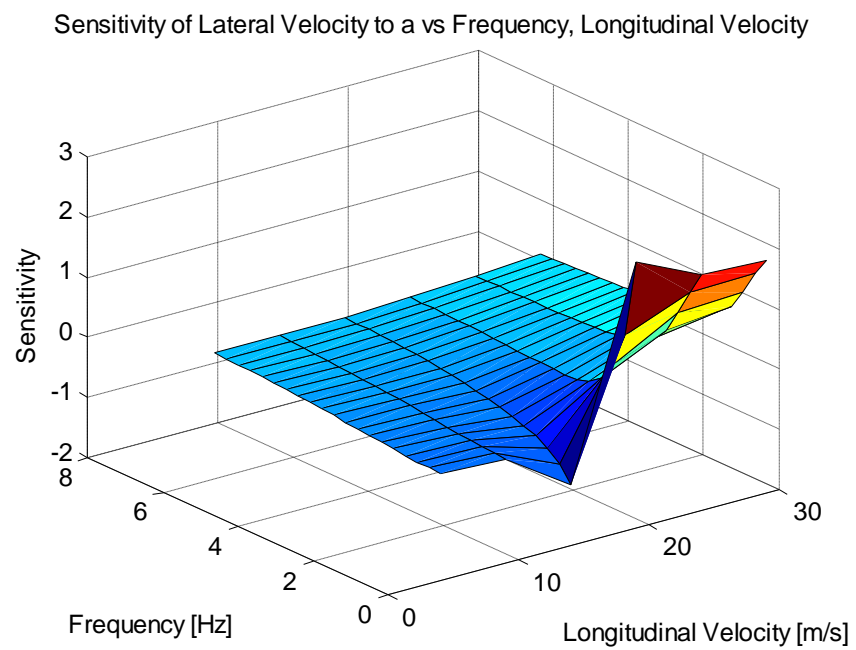
Figure A.1: Sensitivity of lateral velocity to a

Sensitivity of Lateral Velocity to b vs Frequency, Longitudinal Velocity
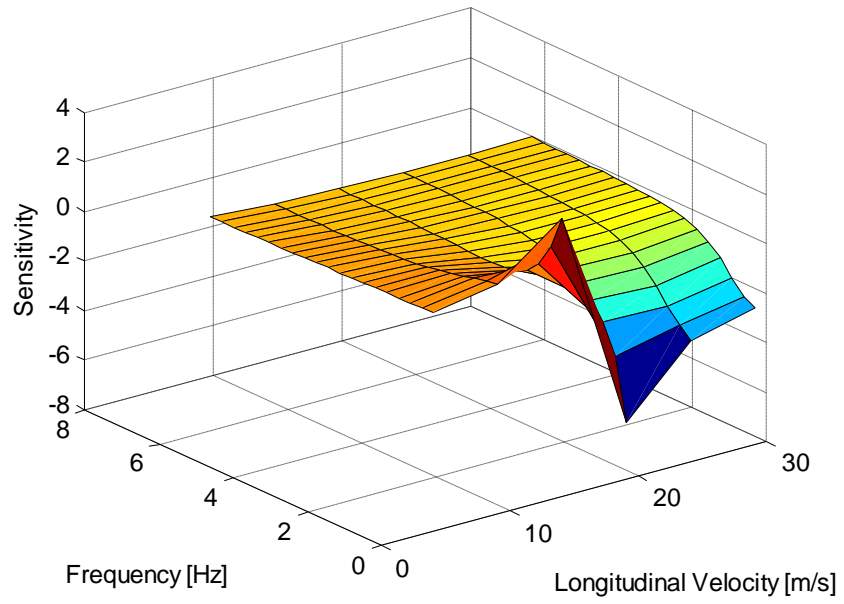
Figure A.2: Sensitivity of lateral velocity to b

Sensitivity of Lateral Velocity to M vs Frequency, Longitudinal Velocity
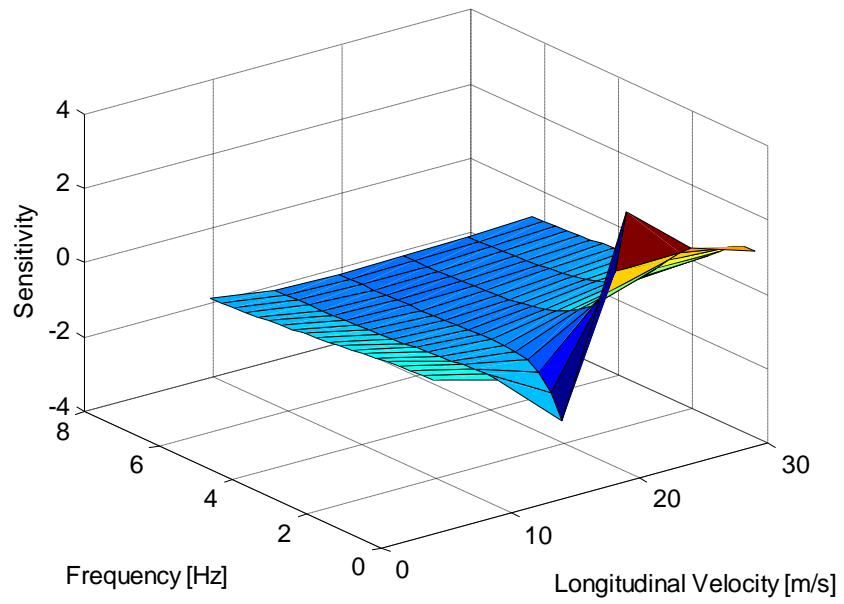
Figure A.3: Sensitivity of lateral velocity to M

Sensitivity of Lateral Velocity to U vs Frequency, Longitudinal Velocity
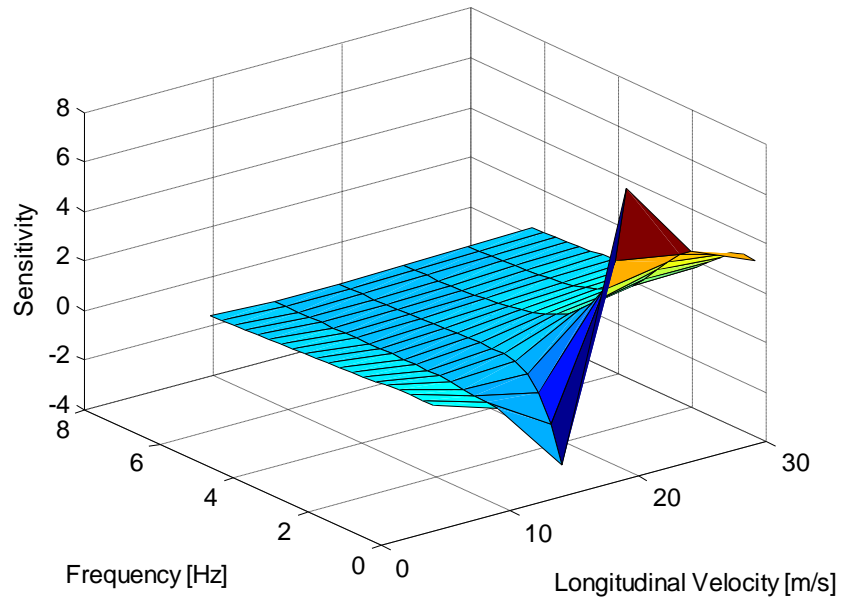
Figure A.4: Sensitivity of lateral velocity to U

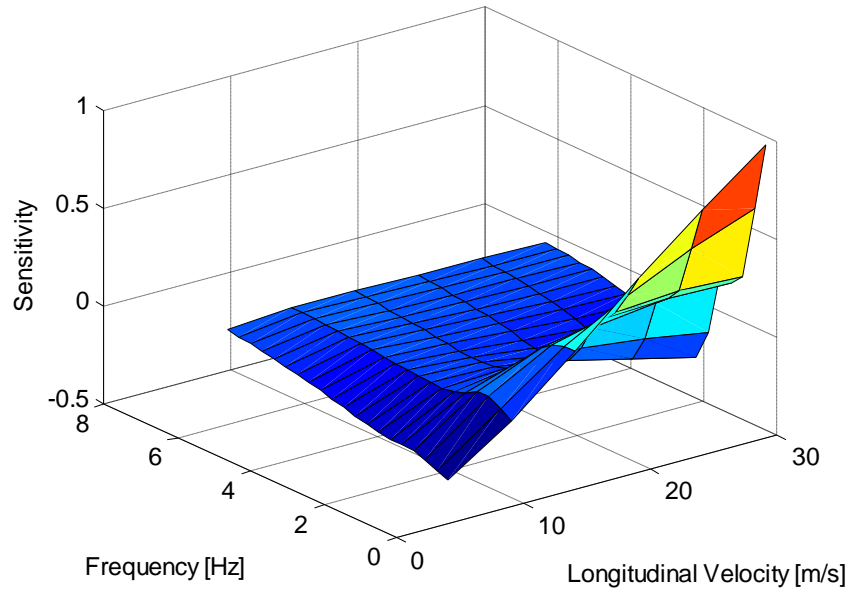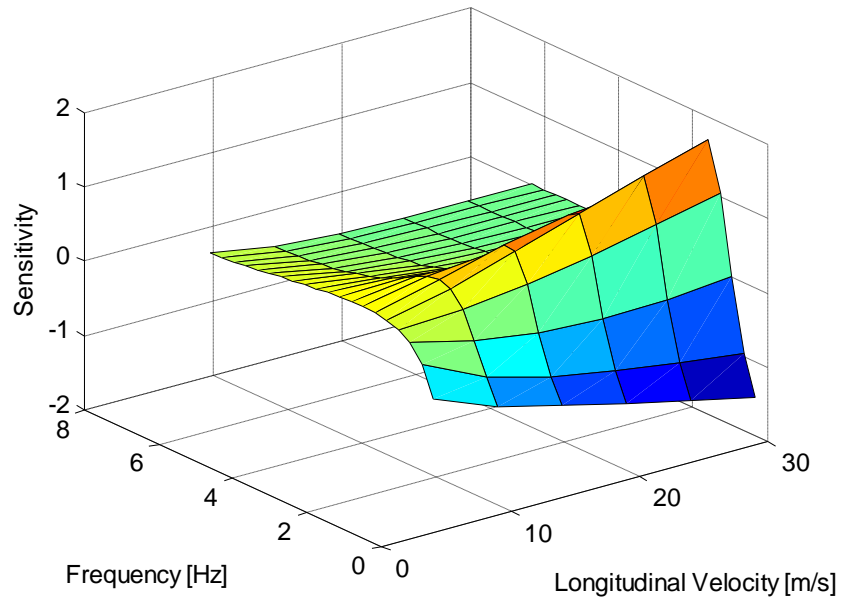Sensitivity of Yaw Velocity to a vs Frequency, Longitudinal Velocity
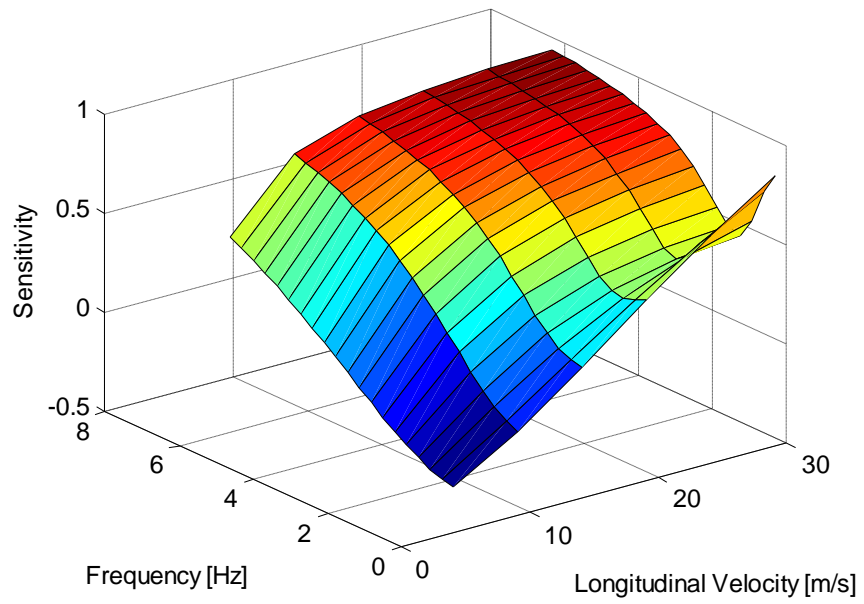
Figure A.5: Sensitivity of yaw velocity to a

Figure A.6: Sensitivity of yaw velocity to b
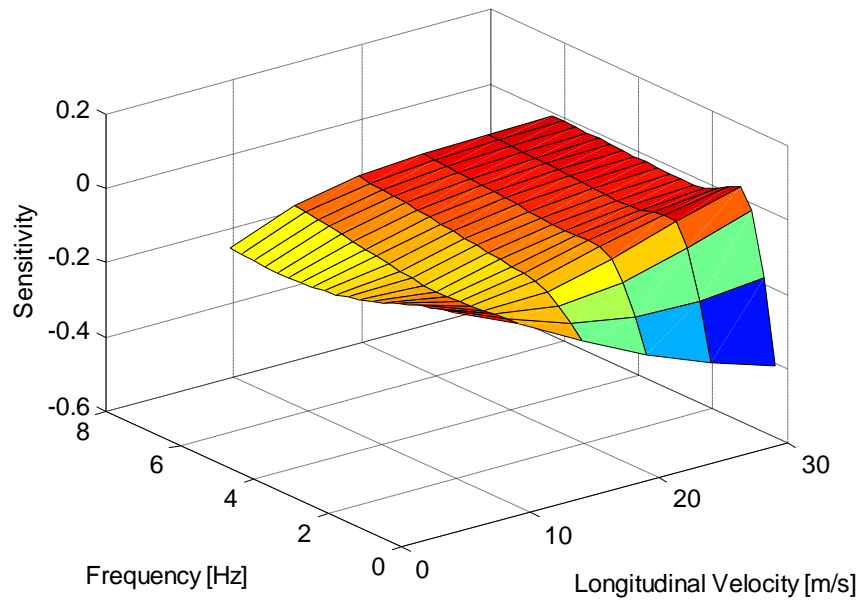
Figure A.7: Sensitivity of yaw velocity to M
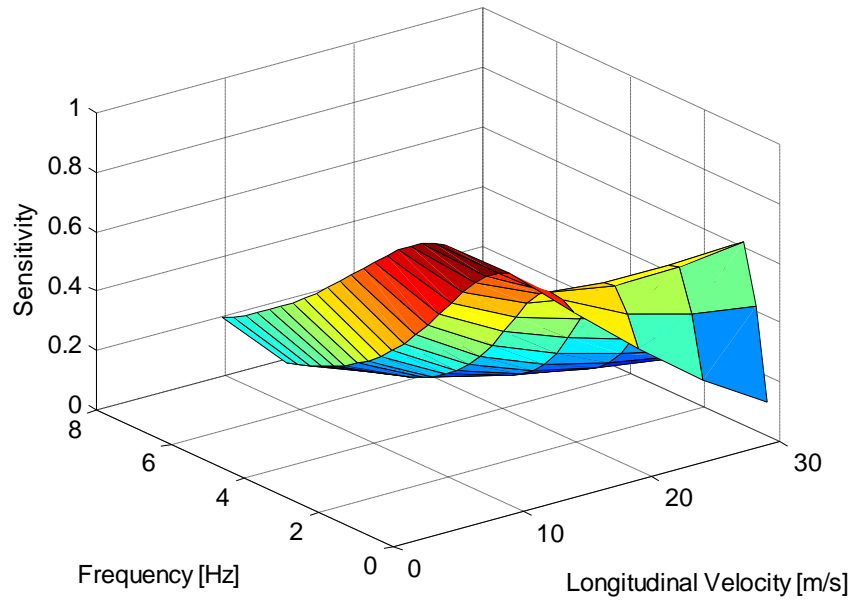
Figure A.8: Sensitivity of yaw velocity to U

A.2. ROLL MODEL SENSITIVITY ANALYSIS
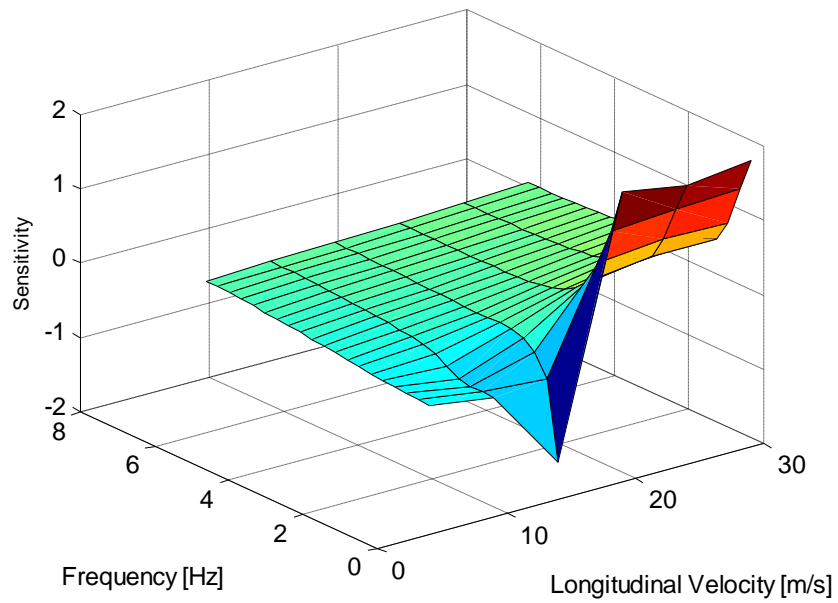
Figure A.9: Sensitivity of lateral velocity to a

Figure A.10: Sensitivity of lateral velocity to b

Figure A.11: Sensitivity of lateral velocity to M

185

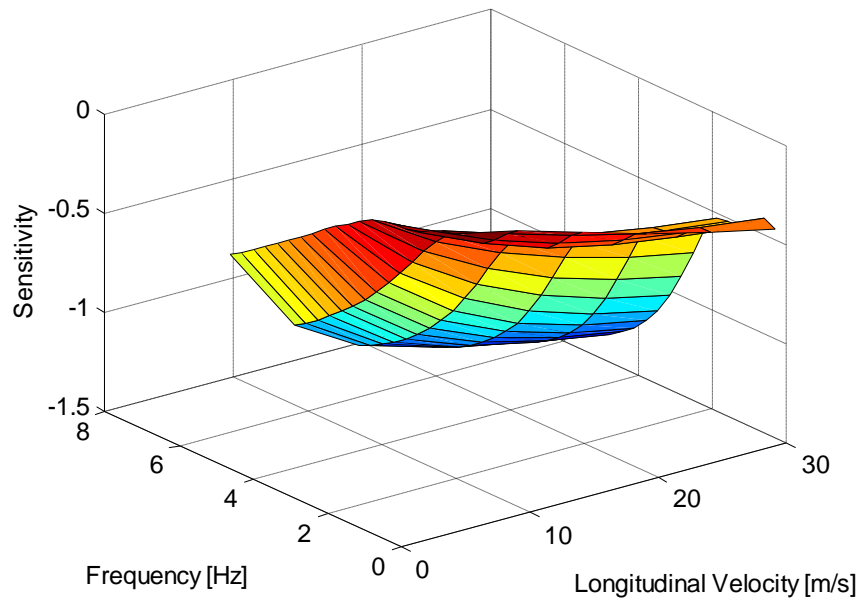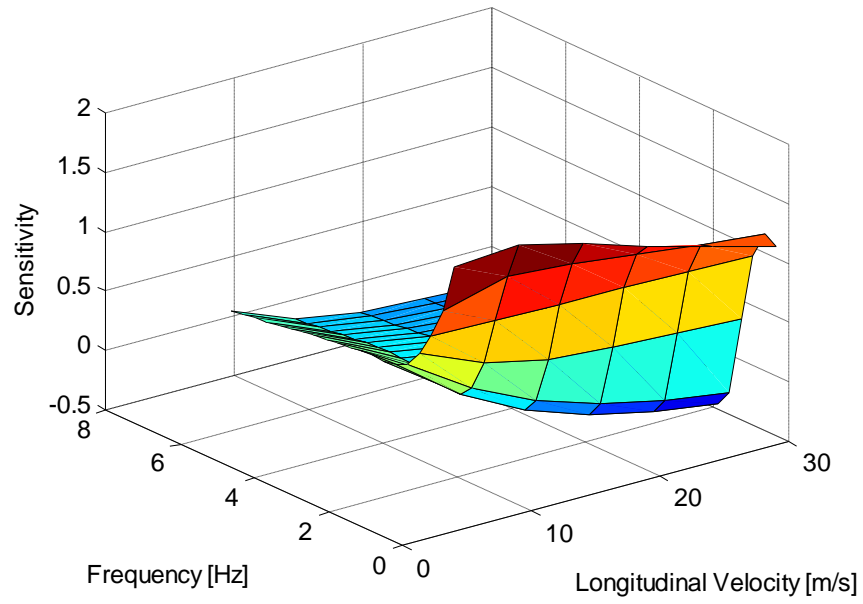**Figure A.12: Sensitivity of lateral velocity h_s**
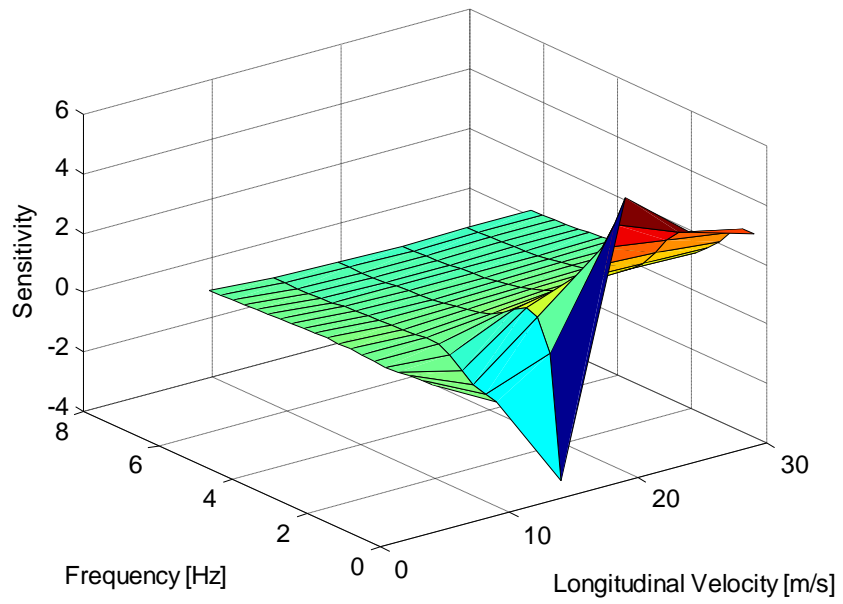
Figure A.13: Sensitivity of lateral velocity U

Sensitivity of Lateral Velocity to Ms vs Frequency, Longitudinal Velocity
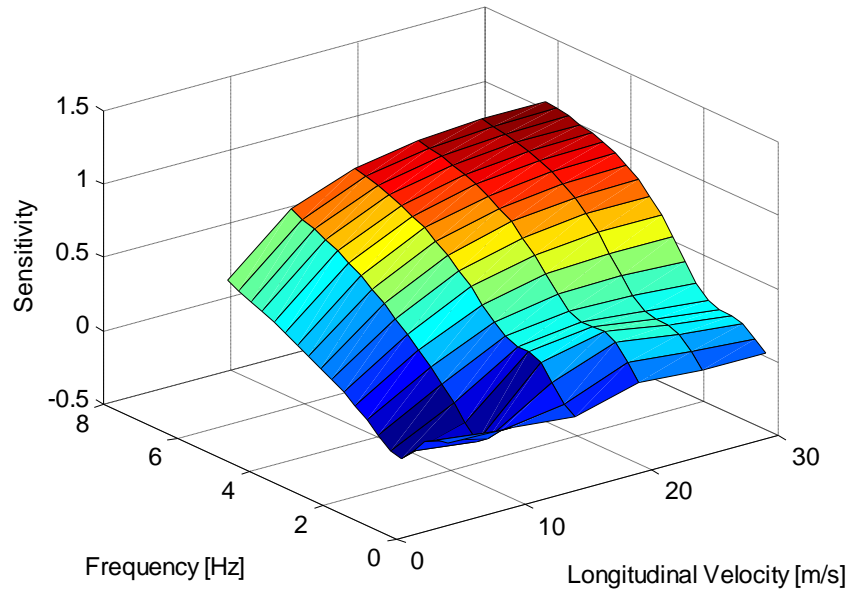
Figure A.14: Sensitivity of lateral velocity M_s

Sensitivity of Yaw Velocity to a vs Frequency, Longitudinal Velocity
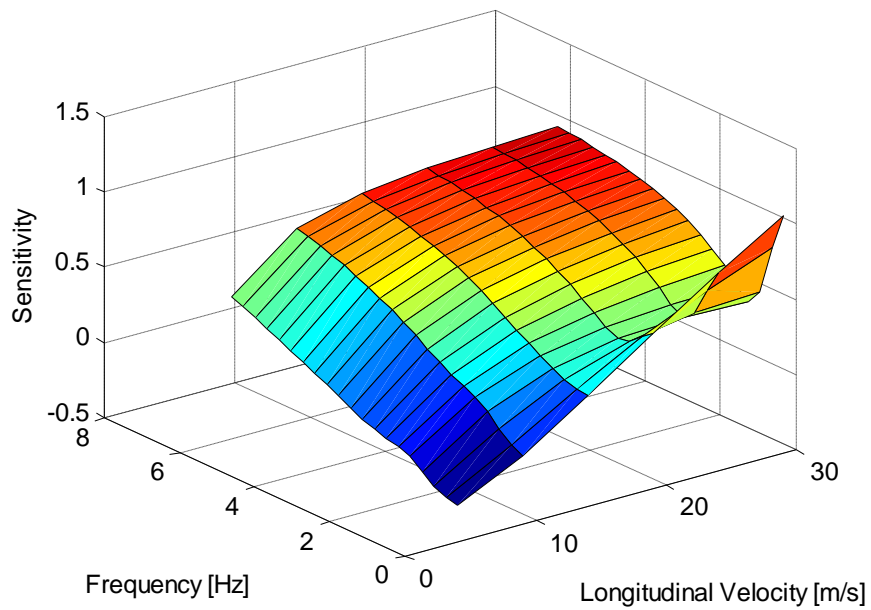
Figure A.15: Sensitivity of yaw velocity to a

Figure A.16: Sensitivity of yaw velocity to b

Figure A.17: Sensitivity of yaw velocity to M

Figure A.18: Sensitivity of yaw velocity to U

Figure A.19: Sensitivity of yaw velocity to h$_s$

Sensitivity of Yaw Velocity to Ms vs Frequency, Longitudinal Velocity
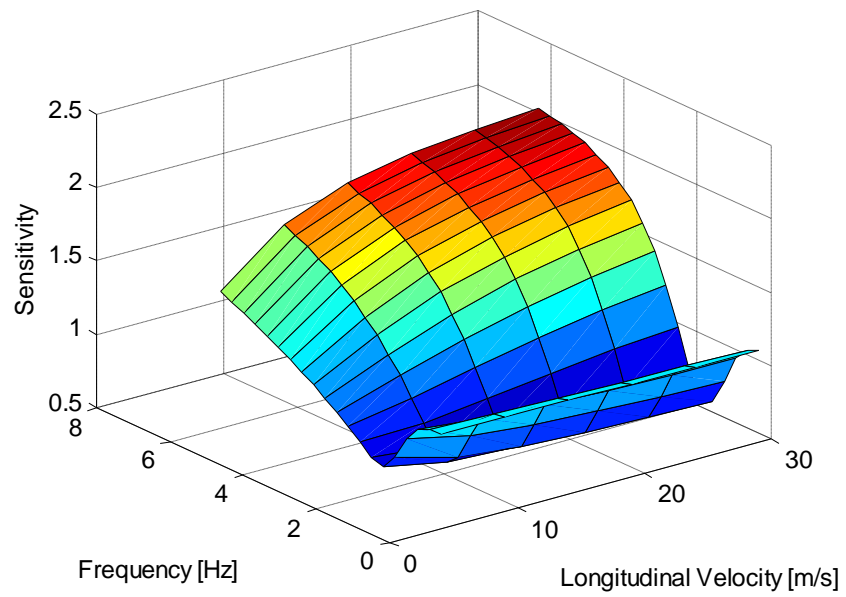
Figure A.20: Sensitivity of yaw velocity to M$_s$

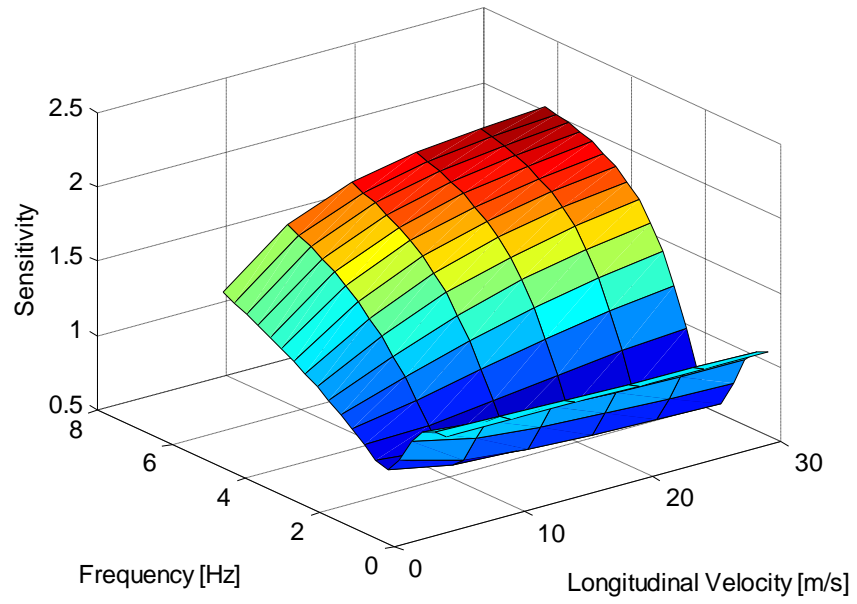Sensitivity of Roll Velocity to a vs Frequency, Longitudinal Velocity

Figure A.21: Sensitivity of roll velocity to a

190

Figure A.22: Sensitivity of roll velocity to b

Figure A.23: Sensitivity of roll velocity to M

191

Sensitivity of Roll Velocity to U vs Frequency, Longitudinal Velocity

Figure A.24: Sensitivity of roll velocity to U

Sensitivity of Roll Velocity to hs vs Frequency, Longitudinal Velocity

Figure A.25: Sensitivity of roll velocity to h_s

Sensitivity of Roll Velocity to Ms vs Frequency, Longitudinal Velocity

Figure A.26: Sensitivity of roll velocity to M_s

APPENDIX B

IDENTIFICATION OF BICYCLE MODEL WITH TRANSIENT TIRE MODEL

B.1. IDENTIFICATION WITH LATERAL VELOCITY

In this case, the bicycle model is identified from only lateral velocity. Estimation result is given in Table B.1.

Table B.1: Estimated and measured parameter values for the bicycle model with transient tire model using only lateral velocity

Estimated	C_f=119810 N/rad	C_r=74218 N/rad	J=1840kgm^2	τ=0.028 s
Actual:	C_f=82260 N/rad	C_r=65380 N/rad	J=1724 kgm^2	-
Error [%]	45.6	13.5	6.7	-

Estimated and measured responses are given in Figure B.1 and Figure B.2.
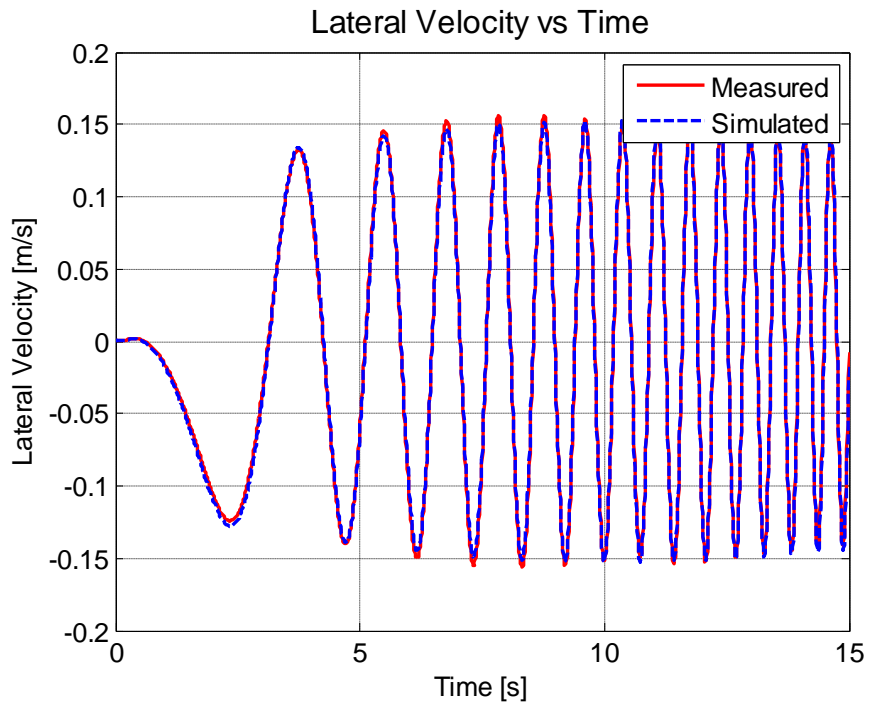
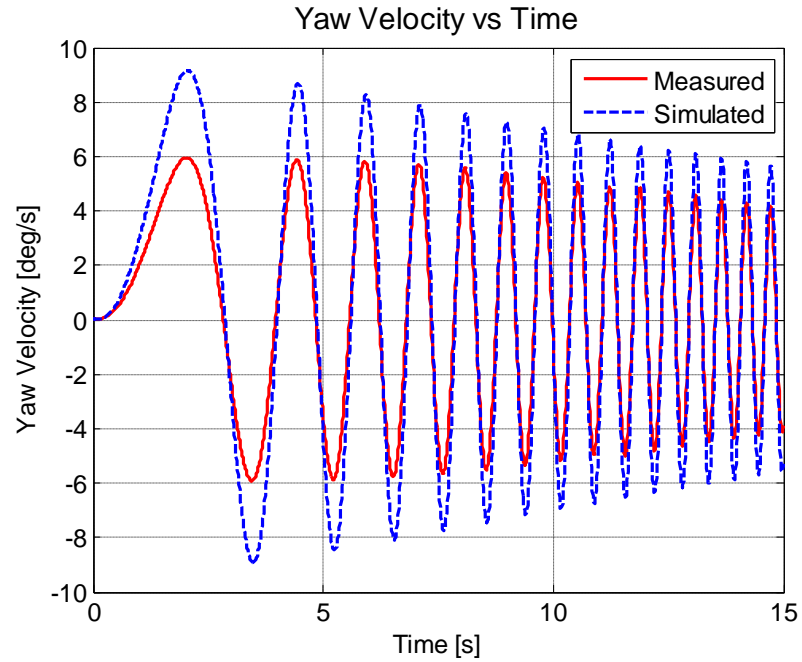**Figure B.1: Lateral velocity responses - estimated from lateral velocity data.**

Figure B.2: Yaw velocity responses estimated from lateral velocity.

195

Estimated and validated responses for model validation are given in Figure B.3 and Figure B.4.
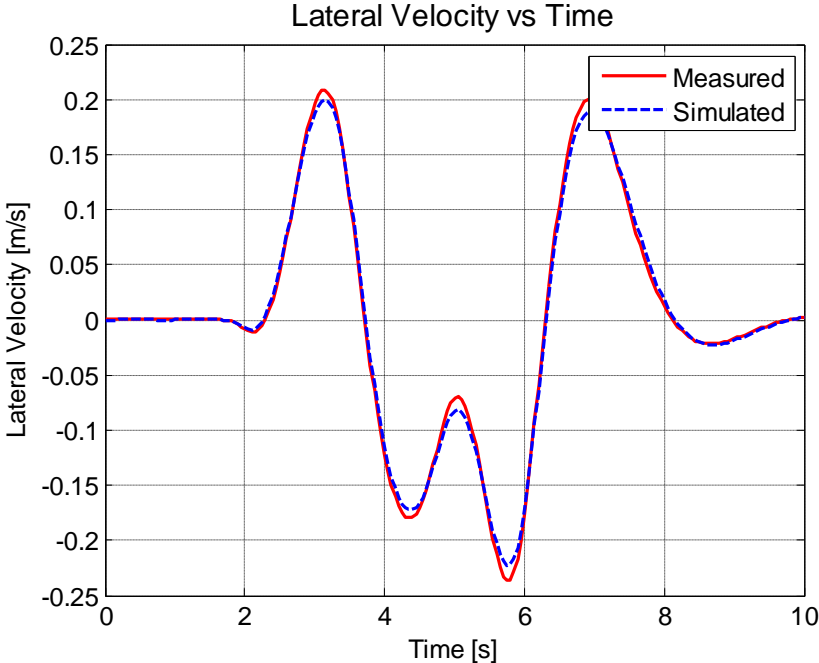

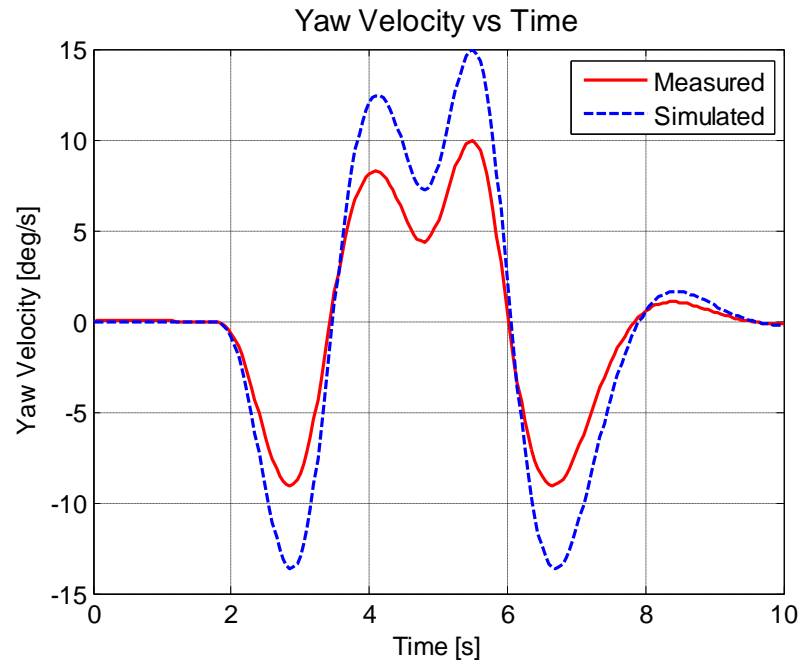**Figure B.3: Lateral velocity responses - estimated from lateral velocity for validation process.**

Figure B.4: Yaw velocity responses - estimated from lateral velocity for validation process.

B.2. IDENTIFICATION WITH YAW VELOCITY DATA

In this case bicycle model is identified by using only yaw velocity data, estimated parameters are given in Table B.2.

Table B.2: Estimated and measured parameter values for bicycle model with transient tire model using only yaw velocity

Estimated	C_f=71940 N/rad	C_r=74578 N/rad	J=1721 kgm^2	τ=0.017 s
Actual:	C_f=82260 N/rad	C_r=65380 N/rad	J=1724 kgm^2	-
Error [%]	-12.5	14	-0.2	-

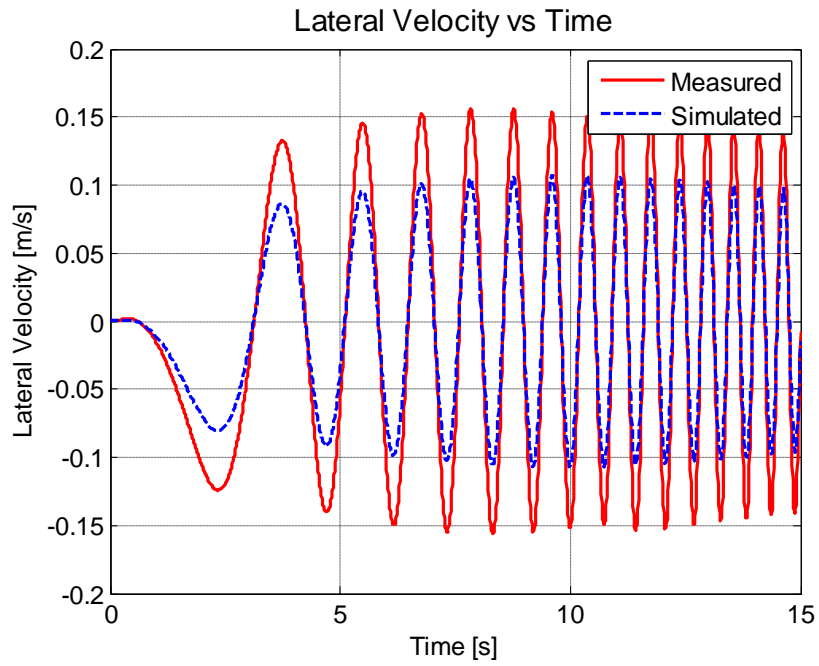Estimated and validated responses are given in Figure B.5 and Figure B.6.

Figure B.5: Lateral velocity responses - estimated from yaw velocity data.
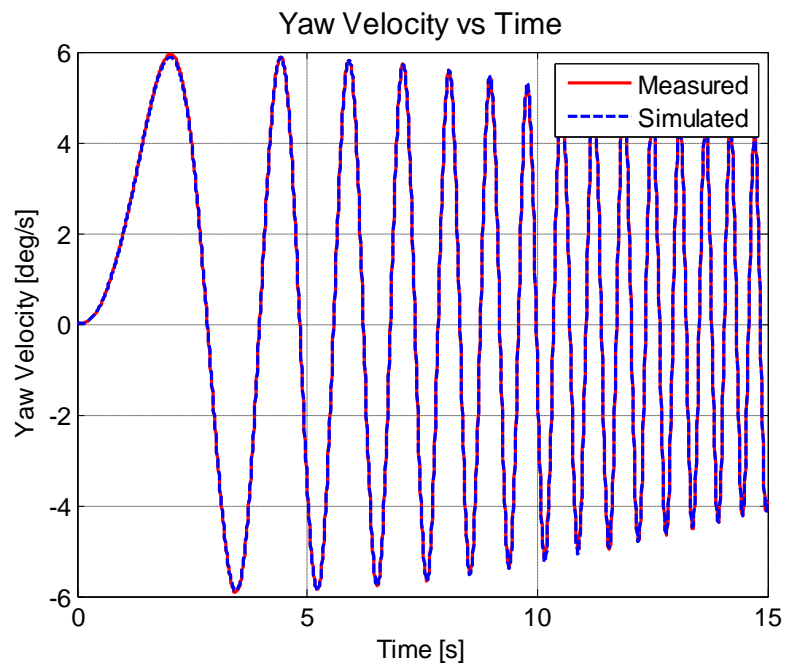

Figure B.6: Yaw velocity responses - estimated from yaw velocity data.

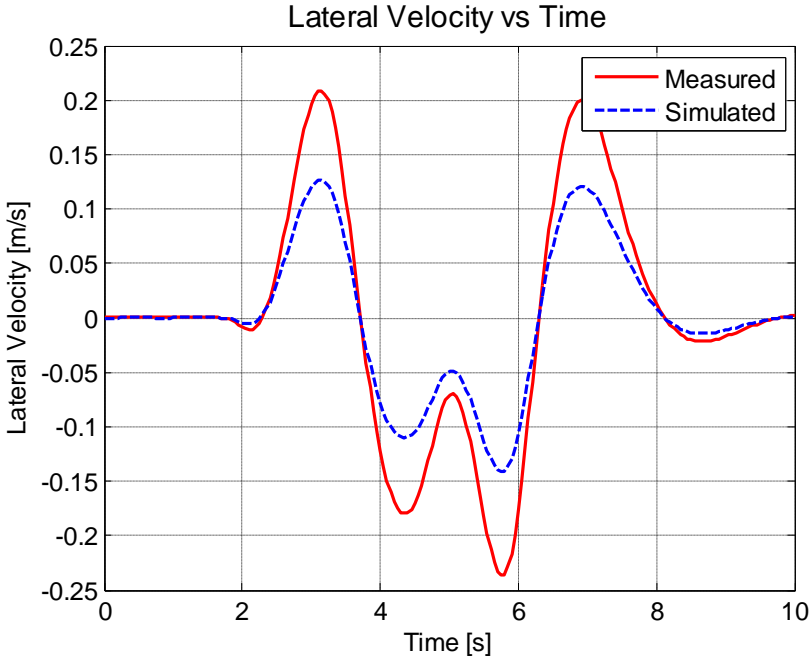Estimated and measured responses for model validation are given in Figure B.7 and Figure B.8.

Figure B.7: Lateral velocity responses - estimated from yaw velocity data for validation process.
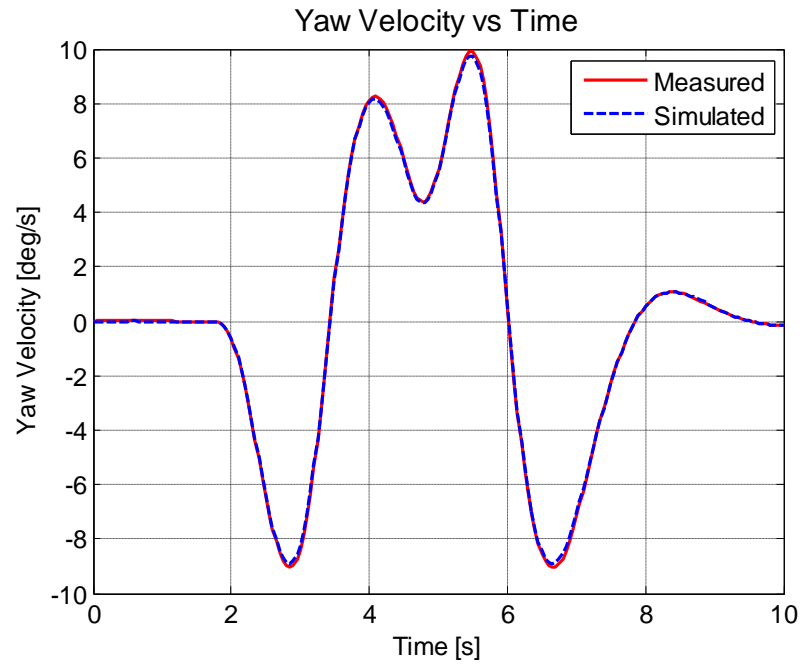
Figure B.8: Yaw velocity responses - estimated from yaw velocity data for validation process.